

CURRICULUM VITAE

STEPHANIE C. DEASEY

Email: scdeasey@gmail.com

EDUCATION

<u>Institution and Location</u>	<u>Degree</u>	<u>Year</u>	<u>Major</u>
University of Maryland School of Medicine Baltimore, MD	Ph.D.	2013	Biochemistry and Molecular Biology
Saint Joseph's University Philadelphia, PA	B.S.	2009	Chemistry

PROFESSIONAL EXPERIENCE

Graduate Research Assistant

University of Maryland School of Medicine (Fall 2009-Present)

- ❖ Presently conduct research on the *in vivo* role of enzyme transglutaminases in bone formation and regeneration in the zebrafish model organism

Undergraduate Honors Research

Saint Joseph's University

Advisor: Dr. Mark Forman (Summer 2007-Spring 2009)

- ❖ Investigation of synthetic pathways towards a highly strained bicyclic alkene

Teaching Assistant

Saint Joseph's University

Organic Chemistry Laboratory (Spring 2009)

- ❖ Supervised undergraduate students during Organic Chemistry Laboratory

General Chemistry Tutor

Saint Joseph's University, Athletics Department (Summer 2008-Spring 2009)

- ❖ Tutored student athletes in General Chemistry and Chemistry for the Consumer

Teaching Assistant

Saint Joseph's University

General Chemistry Laboratory (Spring 2007)

- ❖ Supervised undergraduate students during General Chemistry Laboratory
- ❖ Graded students pre-laboratory assignments

PEER-REVIEWED PUBLICATIONS

1. **Deasey S**, Nurminsky D, Shanmugasundaram S, Lima F, Nurminskaya M (2013) Transglutaminase 2 as a Novel Activator of LRP6/ β -Catenin Signaling. *Cellular Signaling* [In Press]
2. **Deasey S**, Shanmugasundaram S, Nurminskaya M (2011) Tissue-Specific Responses to Loss of Transglutaminase 2. *Amino Acids* 44(1):179-187.
3. **Deasey S**, Grichenko O, Du S, Nurminskaya M (2011) Characterization of the Transglutaminase Gene Family in Zebrafish and in vivo Analysis of Transglutaminase-Dependent Bone Mineralization. *Amino Acids* 42(2-3):1065-1075.
4. Beazley KE, Banyard D, Lima F, **Deasey SC**, Nurmisky DI, Konoplyannikov M, Nurminskaya MV (2013) Transglutaminase Inhibitors Attenuate Vascular Calcification in a Preclinical Model. *Arterioscler Thromb Vasc Biol* 33(1):43-52
5. Beazley KE, **Deasey S**, Lima F, Numinskaya M (2012) Transglutaminase 2-Mediated Activation of B-Catenin Signaling has a Critical Role in Warfarin-Induced Vascular Calcification. *Arterioscler Thromb Vasc Biol*, 32(1):123-130.
6. Nurminsky D, Shanmugasundaram S, **Deasey S**, Michaud C, Allen S, Hendig D, Dastjerdi A, Francis-West P, Nurminskaya M (2011) Transglutaminase 2 Regulates Early Chondrogenesis and Glycosaminoglycan Synthesis. *Mechanisms of Development*, 128(3-4):234-245.

PRESENTATIONS

Oral Presentations

1. Deasey S, Du S, Nurminskaya M
“Transglutaminase-Mediated Cross-Linking is Critical for Bone Regeneration in Zebrafish” **European Calcified Tissue Society**, May 2012

Poster Presentations

1. Deasey S, Du S, Nurminskaya M
“Transglutaminase-Mediated Cross-Linking is Critical for Bone Regeneration in Zebrafish” **Gordon Research Conference on Transglutaminases in Human Disease Processes**, July 2012

2. Deasey S, Du S, Grinchenko O, Nurminskaya M
“Regulation of Bone Mineralization by Transglutaminase-Mediated Cross-Linking in Zebrafish” **Extracellular Matrix in Health and Disease Symposium**, April 2011.
3. Deasey S, Du S, Grinchenko O, Nurminskaya M
“Regulation of Bone Mineralization by Transglutaminase-Mediated Cross-Linking in Zebrafish” **2011 Graduate Research Conference**, April 2011.
4. Deasey S, Nurminsky D, Weiner D, Nurminskaya M
“Serum Level and Activity of TG2 in Chronic Kidney Disease Patients” **Gordon Research Conference on Transglutaminases in Human Disease Processes**, July 2010.

AWARDS

- ECTS New Investigator Award for the ECTS 2012 39th Annual Congress in Stockholm.

ABSTRACT

Title of Dissertation: Transglutaminase-Mediated Bone Formation in Zebrafish

Stephanie Catherine Deasey, Doctor of Philosophy, 2013

Dissertation Directed by: Maria Nurminskaya, Associate Professor, Department of Biochemistry and Molecular Biology

The integrity of the human skeleton is maintained by a delicate balance of bone deposition and resorption. Disruption of this balance results in diseases such as sclerosteosis or osteoporosis, which are characterized by high or low bone mass respectively. Further, the skeleton is prone to injuries such as fractures and breaks throughout the human life-span. It has therefore become critical to understand the underlying mechanisms of bone formation and homeostasis in order to better target and treat such ailments. Two mammalian enzyme transglutaminases, TG2b and FXIIIa, which catalyze the formation of protein-protein cross-links, have been associated with bone mineralization *in vitro*. However, mouse single knockouts of these enzymes show no skeletal phenotype. In this study we demonstrate functional and transcriptional compensation for the loss of TG2 in various tissues of TG2 knockout mice; specifically, we demonstrate a compensation mechanism in the skeleton. To overcome this complication we utilize the zebrafish (*danio rerio*) model system to examine the role of transglutaminases *in vivo*. Zebrafish have become an invaluable model to the study of developmental processes due to several unique characteristics such as, transparency during early development, short gestation time and a remarkable regeneration capability. We characterized the zebrafish transglutaminase gene family and identified thirteen TG

genes. Of these thirteen genes, eleven were homologous to one of three mammalian transglutaminases, TG1, TG2, or FXIIIa, and two were specific to zebrafish. We show that transglutaminase activity promotes proper bone mineralization in both developing vertebrae and regenerating fin bones. Further, we show evidence for transglutaminases functioning in bone mineralization by promoting collagen type I deposition and activating canonical β -catenin signaling during bone regeneration. Importantly, these studies settled the previous discrepancy between *in vitro* studies and *in vivo* mouse studies on the role of TGs in osteo-chondrogenic differentiation by demonstrating a complex compensation mechanism in mammalian tissue. This identification of TGs in bone mineralization identifies a novel therapeutic target for various bone pathologies, such as bone-like tissue transformation in heterotopic ossification seen in musculoskeletal trauma, spinal cord injury and combat wounds.

Transglutaminase-Mediated Bone Formation in Zebrafish

by
Stephanie Deasey

Dissertation submitted to the Faculty of the Graduate School of the
University of Maryland, Baltimore in partial fulfillment
of the requirements for the degree of
Doctor of Philosophy
2013

© Copyright 2013 by Stephanie Deasey

All rights Reserved

DEDICATION

*To my family, Mom, Dad and Paul,
and friends who have supported me throughout.*

ACKNOWLEDGEMENTS

I would like to give a huge thanks to my family and friends without whom I would not have been able to achieve my goals. You have always encouraged me to continue with my work when I lacked the confidence, without your encouragement I would have never made it this far. I would also like to thank all the post-docs who have come through the lab Dr. Beatrice Milon, Dr. Corinne Niger, Dr. Derek Banyard, Dr. Florence Lima, Dr. Kelly Beazley, Dr. Mikal Konoplyannikov Dr. Olga Grinchenko, Dr. Saman Eghtesad, and Dr. Shobana Shanmugasundaram. Their guidance and support has been invaluable to my experience and learning. Additionally, I would like to thank Dr. Maria Nurminskaya for taking me into her lab and making my PhD experience all that it was. I would also like to thank Dr. Dmitry Nurminsky for all his additional advice and feedback during lab meetings. I also want to thank Dr. Shaojun Du for all of his counsel and guidance in our zebrafish studies.

Finally I thank my committee members, Dr. Richard Eckert, Dr. Dudley Strickland, Dr. Ian Thorpe, and Dr. Shaojun Du, for their considerable counsel over the years.

TABLE OF CONTENTS

DEDICATION.....	iii
ACKNOWLEDGEMENTS.....	iv
TABLE OF CONTENTS.....	v
LIST OF TABLES.....	x
LIST OF FIGURES.....	xi
LIST OF ABBREVIATIONS.....	xiii
CHAPTER 1: INTRODUCTION.....	1
A. PROJECT OVERVIEW.....	1
B. ENZYME TRANSGLUTAMINASES.....	2
1. GENERAL INTRODUCTION.....	2
2. TRANSGLUTAMINASE 2.....	4
3. FACTOR XIII A.....	5
C. ROLE OF ENZYME TGS IN BONE MINERALIZATION.....	6
1. BONE FORMATION.....	6
2. TGS IN BONE FORMATION.....	8
3. FXIII A AND TG2 MOUSE KNOCK-OUT MODELS.....	10
D. ZEBRAFISH AS A MODEL TO STUDY TGS IN BONE DEVELOPMENT.....	11
1. ZEBRAFISH AS A MODEL ORGANISM.....	11
2. ZEBRAFISH AS A MODEL ORGANISM OF BONE FORMATION.....	12
E. ZEBRAFISH CAUDAL FIN REGENERATION.....	14
1. REGENERATION.....	14
2. ZEBRAFISH CAUDAL FIN REGENERATION.....	14
F. CANONICAL β -CATENIN SIGNALING.....	17
1. CANONICAL β -CATENIN SIGNALING.....	17
2. CANONICAL β -CATENIN SIGNALING IN ZEBRAFISH FIN REGENERATION AND BONE FORMATION.....	19

CHAPTER 2: TISSUE SPECIFIC RESPONSES TO LOSS OF TRANSGLUTAMINASE 2.....	21
A. ABSTRACT.....	21
B. INTRODUCTION.....	22
C. MATERIALS AND METHODS.....	24
1. ANIMALS AND TISSUE DISSECTION.....	24
2. REAL-TIME PCR.....	24
3. TG ACTIVITY ASSAY.....	25
4. DATA AND STATISTICAL ANALYSIS.....	25
D. RESULTS.....	26
1. TISSUE-SPECIFIC EXPRESSION OF TG FAMILY.....	26
2. COMPENSATION FOR TG2 LOSS IN SKELETAL MUSCLE.....	30
3. COMPENSATION FOR TG2 LOSS IN LIVER.....	32
4. COMPENSATION FOR TG2 LOSS IN NON-HYPERTROPHIC CARTILAGE.....	33
5. COMPENSATION FOR TG2 LOSS IN JOINT/OSSIFYING CARTILAGE.....	35
6. COMPENSATION FOR TG2 LOSS IN CARDIOVASCULAR TISSUES.....	36
6.1 AORTA.....	36
6.2 HEART.....	38
7. COMPENSATION FOR TG2 LOSS IN THE KIDNEY.....	40
E. DISCUSSION.....	41
CHAPTER 3: CHARACTERIZATION OF THE TRANSGLUTAMINASE GENE FAMILY IN ZEBRAFISH AND <i>IN VIVO</i> ANALYSIS OF TRANSGLUTAMINASE- DEPENDENT BONE MINERALIZATION.....	44
A. ABSTRACT.....	44
B. INTRODUCTION.....	45
C. MATERIALS AND METHODS.....	47

1. BLAST SEARCH, SEQUENCE ALIGNMENTS AND PHYLOGENETIC ANALYSIS.....	47
2. EMBRYO GENERATION AND MAINTENANCE.....	47
3. <i>EX VIVO</i> IDENTIFICATION OF TG CROSS-LINKING ACTIVITY IN ZEBRAFISH.....	48
4. WHOLE-MOUNT <i>IN SITU</i> HYBRIDIZATION.....	48
5. REAL-TIME PCR.....	49
6. TG ACTIVITY ASSAY.....	49
7. CALCEIN STAINING OF MINERALIZED VERTEBRAE.....	50
8. DATA AND STATISTICAL ANALYSIS.....	50
D. RESULTS.....	50
1. IDENTIFICATION OF ZEBRAFISH TG GENES.....	50
2. EXPRESSION AND ACTIVITY OF TGS IN ZEBRAFISH.....	56
3. LOCALIZATION OF ZTGS EXPRESSION BY <i>IN SITU</i> HYBRIDIZATION.....	58
4. KCC-009 IS A POTENT INHIBITOR OF ZTG CROSS-LINKING ACTIVITY IN ZEBRAFISH TISSUES.....	61
5. <i>IN VIVO</i> INHIBITION OF TG ACTIVITY WITH KCC-009 HINDERS BONE FORMATION.....	63
E. DISCUSSION.....	65
 CHAPTER 4: TRANSGLUTAMINASE ACTIVITY IN THE REGENERATIVE BLASTEMA CONTRIBUTES TO BONE REGENERATION IN THE ZEBRAFISH CAUDAL FIN.....	 68
A. ABSTRACT.....	68
B. INTRODUCTION.....	69
C. MATERIALS AND METHODS.....	71
1. ZEBRAFISH CAUDAL FIN AMPUTATION.....	71
2. REAL-TIME PCR.....	72
3. <i>IN SITU</i> HYBRIDIZATION.....	72

4. <i>IN VIVO</i> DETECTION OF TG CROSS-LINKING ACTIVITY IN ZEBRAFISH.....	73
5. HISTOLOGICAL ANALYSIS.....	74
6. IMMUNOCYTOCHEMISTRY.....	74
7. DATA AND STATISTICAL ANALYSIS.....	75
D. RESULTS.....	75
1. ZTG EXPRESSION DURING FIN REGENERATION.....	75
2. LOCALIZATION OF ZFXIII A-87 AND ZTG2B MRNA IN MATURE AND REGENERATING CAUDAL FINS.....	79
3. <i>IN VIVO</i> ZTG ACTIVITY IN THE REGENERATING CAUDAL FIN.....	82
4. CYSTAMINE TREATMENT INMPEDES BONE REGENERATION.....	83
5. ZTG INHIBITION EFFECTS CANONICAL β -CATENIN SIGNALING IN REGENERATING FINS.....	88
E. DISCUSSION.....	91
CHAPTER 5: TRANSGLUTAMINASE 2 AS A NOVEL ACTIVATOR OF LRP6/ β -CATENIN SIGNALING.....	95
A. ABSTRACT.....	95
B. INTRODUCTION.....	96
C. MATERIALS AND METHODS.....	98
1. CELL CULTURE, PLASMID CONSTRUCTS, DNA TRANSFECTION AND LUCIFERASE ASSAY.....	98
2. WESTERN BLOT ANALYSIS AND IMMUNOPRECIPITATION.....	99
3. TG2 OVER-EXPRESSION IN ZEBRAFISH LARVAE.....	100
4. TG ACTIVITY ASSAY.....	100
5. DATA AND STATISTICAL ANAYSIS.....	101
D. RESULTS.....	101
1. EXTRACELLULAR TG2 ACTIVATES β -CATENIN SIGNALING IN COS-7 CELLS.....	101
2. TG2-INDUCED ACTIVATION OF β -CATENIN IS MEDIATED BY LRP6.....	103

3. TG2 OVER-EXPRESSION MIRRORS β -CATENIN OVER-ACTIVATION PHENOTYPE IN ZEBRAFISH.....	104
4. TG2 BINDS TO THE EXTRACELLULAR DOMAIN OF LRP6 <i>IN VITRO</i>	107
5. EXTRACELLULAR DOMAIN OF LRP6 IS CROSS-LINKED BY TG2.....	108
E. DISCUSSION.....	109
CHAPTER 6: CONCLUSIONS AND FUTURE DIRECTIONS.....	113
A. CONCLUSIONS.....	113
1. TG COMPENSATION MECHANISM IN THE MOUSE MODEL.....	113
2. ZEBRAFISH TRANSGLUTAMINASES.....	114
3. TGS IN BONE FORMATION/REGENERATION.....	115
4. TG2 AS A REGULATOR OF β -CATENIN SIGNALING.....	115
B. FUTURE DIRECTIONS.....	116
APPENDIX.....	119
A. EXPANDED MATERIALS AND METHODS.....	119
1. RNA ISOLATION.....	119
2. RNA DNASE DIGESTION AND CLEAN-UP.....	119
3. REVERSE TRANSCRIPTION.....	120
4. REAL-TIME PCR.....	120
5. TOTAL PROTEIN ISOLATION.....	121
6. WHOLE-MOUNT <i>IN SITU</i> HYBRIDIZATION.....	121
7. DIG-RNA PROBE PREPARATION.....	122
8. REAL-TIME PCR.....	123
9. TISSUE SECTION <i>IN SITU</i> HYBRIDIZATION.....	123
B. SUPPLEMENTARY TABLES.....	125
1. PRIMER SEQUENCES FOR MOUSE GENES.....	125
2. PRIMER SEQUENCES FOR ZEBRAFISH GENES.....	125
REFERENCES.....	126

LIST OF TABLES

Table 2.1: Transamidating Activity and Percent Inhibition by TG2 Inhibitor KCC-009.....	31
Table 3.1: Abbreviations for each of the zTGs in zebrafish.....	54
Table 4.1: zTG Expressions at 1dpa Compared to a No Amputation Control.....	77
Table 4.2: Cystamine has No Effect on Hedgehog Activation.....	89
Table B.1: Primer Sequences for Mouse Genes Analyzed by Real-Time PCR.....	125
Table B.2: Primer Sequences for Zebrafish Genes Analyzed by Real-Time PCR.....	125

LIST OF FIGURES

Figure 1.1: Schematic of Cross-Linking Reaction Catalyzed by TGs.....	3
Figure 1.2: Endochondral vs. Intramembranous Ossification.....	7
Figure 1.3: Diagram of the Zebrafish Axial Skeleton.....	13
Figure 1.4: Diagram of Longitudinal Section of Lepidotrichia.....	13
Figure 1.5: Schematic of Phases of Fin Regeneration.....	16
Figure 1.6: Schematic of β -Catenin Activation.....	18
Figure 2.1: Tissue-Specific Expression of FXIIIa in WT Mice.....	27
Figure 2.2: Tissue-Specific Expression of TG1 and TG3 in WT Mice.....	28
Figure 2.3: Tissue-Specific Expression of TG2 and TG5 in WT Mice.....	29
Figure 2.4: Tissue-Specific Expression of TG6 in WT Mice.....	30
Figure 2.5: TG Expression and Activity in Mouse Skeletal Muscle.....	31
Figure 2.6: TG Expression and Activity in Mouse Liver Tissue.....	33
Figure 2.7: TG Expression and Activity in Mouse Non-Hypertrophic Cartilage.....	34
Figure 2.8: TG Expression and Activity in Mouse Joint/Ossifying Cartilage.....	36
Figure 2.9: TG Expression and Activity in Mouse Aorta.....	38
Figure 2.10: TG Expression and Activity in Mouse Heart Tissue.....	39
Figure 2.11: TG Expression and Activity in Mouse Kidney Tissue.....	41
Figure 3.1: Phylogenic Analysis of Zebrafish TGs.....	53
Figure 3.2: Analysis of Genomic Organization of zTGs.....	56
Figure 3.3: Expression Patterns of zTGs During Zebrafish Development.....	58
Figure 3.4: Tissue Specific Expression of zTGs in 2-3dpf Zebrafish.....	60
Figure 3.5: zTG Catalytic Activity in Zebrafish Larvae.....	61

Figure 3.6: KCC-009 Inhibits Total TG Activity in Zebrafish.....	62
Figure 3.7: KCC-009 Shows No Toxicity in Zebrafish.....	63
Figure 3.8: Inhibition of TGs Reduces Vertebrae Mineralization.....	64
Figure 4.1: zTG Expression Pattern During Zebrafish Fin Regeneration.....	78
Figure 4.2: Expression of zFXIIIa-87 and zTG2b Localizes to the Regenerative Blastema in Zebrafish Fins.....	80
Figure 4.3: Expression of zFXIIIa-87 and zTG2b Localizes to the Regenerative Blastema in Zebrafish Fins.....	81
Figure 4.4: zTG Activity in Regenerating Zebrafish Fins.....	83
Figure 4.5: Cystamine Treatment Impedes Bone Formation in Regenerating Fins.....	85
Figure 4.6: Cystamine Treatment Impedes Bone Formation and Type-I Collagen Deposition in Regenerating Caudal Fins.....	87
Figure 4.7: Cystamine Treatment Affects Activation of Canonical β -Catenin Signaling in Regenerating Caudal Fins.....	88
Figure 4.8: Cystamine Treatment Affects Activation of Canonical β -Catenin Signaling in Regenerating Caudal Fins.....	90
Figure 5.1: Extracellular TG2 Activates β -Catenin Signaling in Cos-7 Cells.....	102
Figure 5.2: Extracellular TG2 Stimulates LRP6 Phosphorylation in Cos-7 Cells.....	102
Figure 5.3: TG2-Induced Activation of β -Catenin is Mediated by LRP6.....	104
Figure 5.4: TG2 Over-Expression Mirrors β -Catenin Over-Activation Phenotype in Zebrafish.....	106
Figure 5.5: TG2 Binds to the Extracellular Domain of LRP6 <i>In Vitro</i>	108
Figure 5.6: Extracellular Domain of LRP6 is Cross-Linked by TG2.....	109

LIST OF ABBREVIATIONS

AEC: Apical ectodermal cap
APC: Adenomatosis Polyposis Coli
BSA: Bovine Serum Albumin
Col I: Type I Collagen
dpa: Days post-amputation
dpf: Days post-fertilization
EtOH: Ethanol
ECM: Extracellular Matrix
FXIIIa: Factor XIIIa
Fz: Frizzled
gpITG2: Guinea pig liver transglutaminase 2
GSK3: Glycogen synthase kinase 3
LRP5/6: Low-density lipoprotein receptor 5 or 6
hpa: Hours post-amputation
hTGs: Human Transglutaminases
RT: Room temperature
SL: Standard Length
TGs: Transglutaminases
TG2: Transglutaminase 2
TG2^{-/-}: Transglutaminase 2 null
VSMCs: Vascular smooth muscle cells
WT: Wild type
zTGs: Zebrafish transglutaminases

CHAPTER 1: INTRODUCTION

A. PROJECT OVERVIEW

The integrity of the human skeleton is maintained by a delicate homeostatic balance, with any perturbation of this balance resulting in detrimental skeletal defects. Specifically, homeostatic deregulation can lead to diseases resulting in either low or high bone mass such as osteoporosis or sclerosteosis respectively (Baron et al., 2006). Further, the skeleton is a tissue that is prone to injuries throughout an average human life-span such as fractures and breaks. Additionally, the bones of the human skeleton not only function for structural support but also in maintaining the human immunity. These diverse roles of the human skeleton make it crucial to have a comprehensive understanding of its regulating factors.

In vitro studies have identified two mammalian enzyme transglutaminases (TGs) as regulators of the process of bone mineralization (Borge et al., 1996; Demignot et al., 1995; Nurminskaya et al., 2002; Al-Jallad et al., 2006; Thomazy and Davies, 1999). However, single knock-out mice of these TGs show no obvious skeletal phenotype, likely due to a compensation mechanism (Koseki-Kuno et al., 2003; Nanda et al., 2001; Lauer et al., 2002). This discrepancy between *in vitro* and *in vivo* studies has led to a gap in the understanding of the role of TGs in bone formation. It is therefore essential to identify an *in vivo* model in which the molecular mechanisms behind TGs in bone formation and maintenance can be uncovered to allow for the identification of novel targets to treat bone pathologies.

The zebrafish model organism has become invaluable to the investigation of developmental processes and various pathologies. Numerous unique characteristics such as early transparency, easy access for both pharmacologic and genetic approaches, and regenerative capability make this model of particular interest for examination of the mechanisms behind bone formation.

B. ENZYME TRANSGLUTAMINASES

1. General Introduction

Transglutaminases (TGs) are a family of calcium (Ca^{2+}) dependent enzymes that catalyze multiple biological reactions. The mammalian family of TGs is composed of nine proteins, TG 1-7, FXIIIa and Band Protein 4.2. Eight of these nine TGs, TG1-7 and FXIIIa, have enzymatic activities while Band Protein 4.2 lacks enzymatic activity and functions as a structural protein. Reactions catalyzed by TGs have been linked to a plethora of biological reactions, including but not limited to, blood coagulation, skin formation, cellular apoptosis and extracellular matrix assembly. Interestingly, two of the nine enzyme TGs, TG2 and FXIIIa, have been identified with bone mineralization by previous *in vitro* studies (discussed in section C.2).

TGs catalyze three major reaction types: Transamidation, Esterification and Hydrolysis (Iismaa et al., 2009; Lorand and Graham, 2003). Each reaction is initiated by the binding of a substrate containing a glutamine acceptor residue leading to the formation of an acylenzyme intermediate; at which point the three reactions diverge. Transamidation (also known as cross-linking) is the most thoroughly studied reaction catalyzed by TGs and results in either addition of a small biological amine to a glutamine

acceptor, acylation of a glutamine residue or formation of an isopeptide bridge. This covalently formed isopeptide bridge is formed both intra- and extra-cellularly between the γ -carbon of a glutamine residue and the ϵ -amine of a lysine residue and is extremely resistant to chemical and physical cleavage (Fig. 1.1). Interestingly, TGs show a high specificity for the glutamine residue, while there is considerable flexibility for the donor ϵ -amine group (Aeschlimann et al., 1993). The lesser-studied esterification reaction utilizes an alcohol as the donor group and results in the formation of an ester. Lastly, the hydrolysis reaction utilizes a water to result in either deamidation or isopeptide cleavage of the acceptor glutamine substrate. The main focus of our studies is on the cross-linking/transamidation reaction catalyzed by TGs.

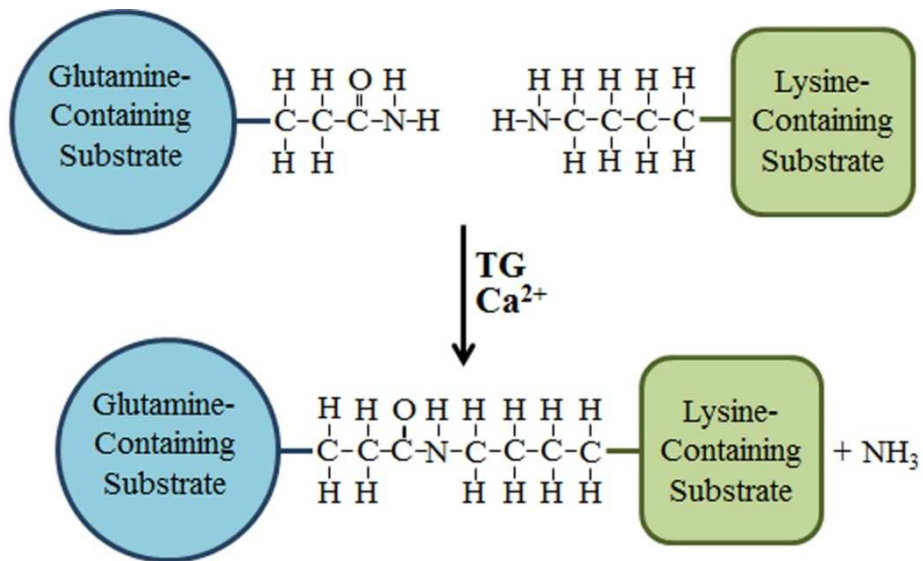


Figure 1.1 Schematic of Cross-Linking Reaction Catalyzed by TGs. Reaction occurs between the glutamine residue one substrate and the lysine residue of a second substrate. This reaction results in the formation of an isopeptide linkage between these two residues.

2. Transglutaminase 2 (TG2)

TG2 is the most thoroughly studied TG due to its ubiquitous expression as compared to the other eight mammalian TGs, in which expression and function are tissue specific. TG2 has been observed in various cell types that are present throughout the body such as endothelial cells and smooth muscle cells (Thomazy and Davies, 1999), in addition to being identified in organ specific cells, such as cardiac striated muscle cells, arterial myointimal cells and glomerular mesangial cells (Thomazy and Davies, 1999).

TG2 catalyzes the traditionally associated transamidation, hydrolysis and esterification reactions; interestingly TG2 is also able to function as a G protein in the liver (Nakaoka et al., 1994). The roles of TG2 as a G protein and as a transamidating enzyme are reciprocally regulated, due to an allosteric inhibition of transamidating activity by GTP binding. Binding of GTP causes a conformational change in TG2 to a more compact form whereas Ca^{2+} binding results in TG2 adopting a more open conformation that favors the transamidation reaction (Begg et al., 2006; Achyuthan and Greenberg, 1987). This allosteric regulation results in low intracellular and high extracellular transamidating activity under normal conditions, due to high GTP and low Ca^{2+} concentrations inside the cell and vice versa outside the cell (Gundemir et al., 2012). TG2 has also been identified as a regulator of numerous signaling pathways. Studies have shown that this multi-functional enzyme is able to activate numerous pathways *in vitro* including the canonical β -catenin signaling (Condello et al., 2013; Faverman et al., 2008), hedgehog signaling (Dierker et al., 2009) and cAMP-dependent protein kinase (PKA) (Nurminskaya et al., 2003). The ability of TG2 to activate canonical β -catenin signaling is of particular interest to this project and is further described in Section F.1.

Due to the wide range of roles for TG2 in biological processes, it is no surprise that aberrant activity results in a number of pathologies. Among the various pathologies that have been associated with TG2 are Celiac's disease, Osteoarthritis, Cancer and Alzheimer's disease (Iismaa et al., 2009).

3. Factor XIIIa (FXIIIa)

FXIIIa shows a more selective expression pattern in comparison to TG2. This TG is largely expressed in blood plasma (Iismaa et al., 2009), but is also found in cells that originate from the bone marrow (Muszbek et al., 2011), such as platelets (Jayo et al., 2009a), megakaryocytes (Kiesselbach and Wagner, 1972), monocytes (Jayo et al., 2009b; Muszbek et al., 1985), macrophages (Komaromi et al., 2011), chondrocytes (Nurminskaya and Linsenmayer, 1996) and osteoblasts (Al-Jallad et al., 2006).

FXIIIa is synthesized as an inactive zymogen with a NH₂-terminal activation peptide, which must be cleaved to be activated. In the plasma, FXIII circulates as a heterotetramer composed of two inactive FXIIIa subunits and two FXIIIb subunits. FXIIIb is not a transglutaminase and serves as a carrier for FXIIIa in the plasma to protect FXIIIa subunits from degradation. The most thoroughly studied function of FXIIIa is stabilization of the fibrin matrix by forming covalent bridges (transamidation reaction) between fibrin monomers of a blood clot in the last step of the coagulation cascade (Iismaa et al., 2009). Activation of FXIIIa in the plasma requires cleavage of the NH₂-terminal activation peptide by thrombin; this cleavage is followed by Ca²⁺ binding which allows for the release of the FXIIIb subunits (Iismaa et al., 2009). Cellular FXIIIa, however, does not bind to FXIIIb, likely due to a reduced need for protection from degradation, instead cellular FXIIIa exists as a homodimer. Interestingly, thrombin is not

present inside the cell preventing cleavage of the NH₂ activation peptide. Under high cellular Ca²⁺ concentrations FXIIIa is able to bind Ca²⁺ which results in its activation. These high cellular Ca²⁺ concentrations occur during Ca²⁺ fluxes as a result of a cellular stimuli and it is under these conditions that cellular FXIIIa is able to be activated without activation peptide cleavage (Kristiansen and Andersen, 2011).

In humans, aberrant FXIIIa activity is most commonly associated with pathologies resulting in a blood clotting defect, increased miscarriage during pregnancy and impaired wound healing have also been observed (reviewed in Iismaa *et al.*, 2009).

C. ROLE OF ENZYME TGS IN BONE MINERALIZATION

1. Bone Formation

The mammalian skeleton is formed and maintained via a delicate homeostasis, which relies on a balance of bone deposition and resorption. This homeostasis is maintained by three cell types: osteoblasts, osteocytes and osteoclasts. Each of these has a specific role in preserving the homeostatic balance of deposition and resorption. Osteoblasts lay down new bone matrix, thereby mediating bone deposition, whereas osteoclasts mediate bone resorption by taking up bone matrix. Osteocytes are matured osteoblasts that have become embedded into the bone matrix and are relatively inactive cells with their main function being to serve as sensory cells in the bone.

Bones of the adult skeleton are formed via two mechanisms: endochondral and intramembranous ossification (Fig. 1.2). These two ossification processes form different bone types in the mammalian skeleton, with endochondral ossification forming the

majority of bones, such as long bones and vertebrae, whereas intramembranous ossification is utilized for formation of “flat” bones such as the skull. The most obvious difference between these two processes of ossification is that endochondral ossification occurs via a cartilaginous intermediate, while intramembranous ossification forms bones without a cartilaginous precursor.

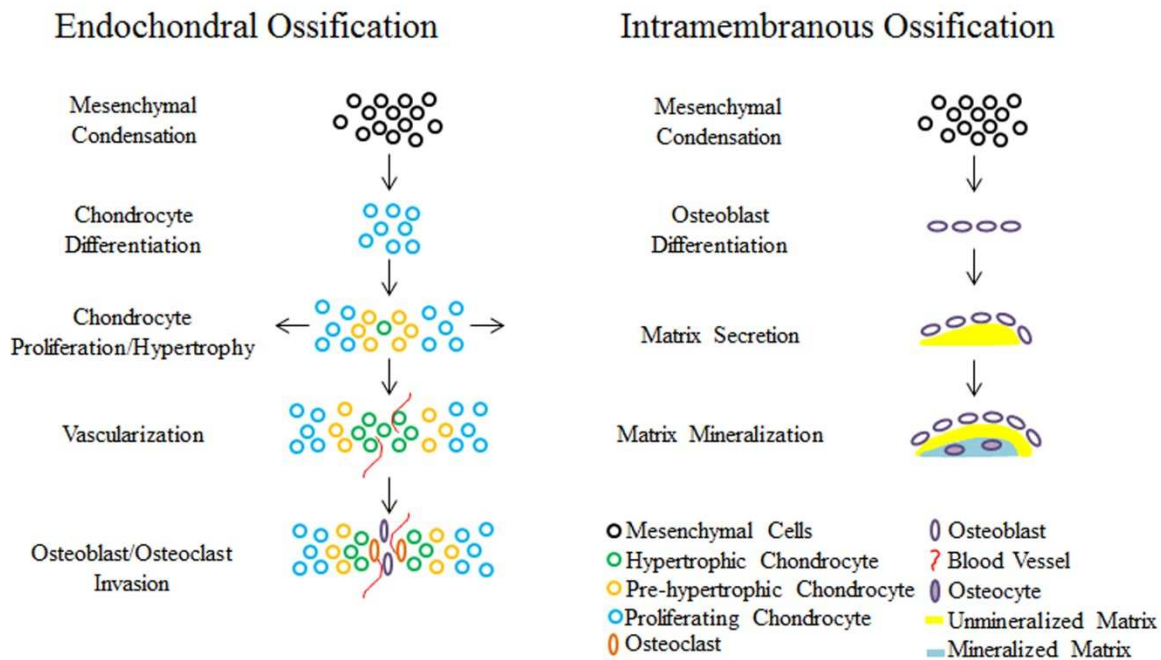


Figure 1.2 Endochondral vs. Intramembranous Ossification. A schematic of the two mechanisms of bone mineralization. Both begin with the condensation of mesenchymal precursors after which endochondral ossification forms bone through a cartilaginous intermediate, while intramembranous bone forms through direct mineralization of the matrix.

Condensation of mesenchymal precursors initiates these two processes of ossification; at which point they diverge to result in their respective types of bone. During endochondral ossification mesenchymal cells differentiate into chondrocytes, which then proliferate and hypertrophy. These hypertrophic chondrocytes serve to calcify the extracellular matrix and promote vascularization before they ultimately

undergo apoptosis. Osteoblasts and osteoclasts, which differentiate from the same mesenchymal precursors, enter the matrix through the newly formed vasculature and begin degradation of the cartilaginous matrix left behind by hypertrophic chondrocytes and laying down of the new bone matrix.

Intramembranous ossification also begins with the condensation of mesenchymal precursor cells, which instead differentiate into osteo-progenitor cells. These osteo-progenitor cells then mature into osteoblasts, which begin secreting bone matrix. As matrix secretion progresses, some osteoblasts become trapped in the matrix where they further mature and become osteocytes.

2. TGs in Bone Formation

As previously stated, TGs are associated with numerous biological processes, among which is bone mineralization. TGs have been identified with intramembranous and endochondral ossification through *in vitro* studies by examination of osteoblasts and hypertrophic chondrocytes in culture and by *ex vivo* examination of bones arising from each type of ossification. TGs were first associated with the process of endochondral ossification, but as studies accumulated evidence arose for their role in intramembranous ossification. TG2 was the first transglutaminase to be identified with bone mineralization by immunohistochemical analysis of three different endochondral bones: the tibia, tarsal and metatarsal bones of rats. This showed that intracellular TG2 was expressed by hypertrophic chondrocytes in each of these bones (Aeschlimann et al., 1993). While this only examined the expression of TG2 in hypertrophic chondrocytes, a later study by Nurminskaya *et al.*, 1996 identified FXIIIa as the major TG isoform in hypertrophic chondrocytes by subtractive hybridization. It is now widely accepted that chondrocytes

express two TGs (Demignot et al., 1995), TG2 and FXIIIa; in addition to supporting that FXIIIa and not TG2 is the major form of TGs in these cells (Nurminskaya and Linsenmayer, 1996; Nurminskaya et al., 1998; Nurminskaya et al., 2002; Thomazy and Davies, 1999).

In addition to the numerous studies showing evidence for the role of TGs in chondrocytes, studies have also identified a role for TGs in osteoblasts during endochondral ossification. Utilization of a co-culture system of hypertrophic chondrocytes and pre-osteoblast cells demonstrated a role for TGs in osteoblasts during *in vitro* endochondral ossification. This showed that TG2 and FXIIIa are secreted by hypertrophic chondrocytes and that their secretion and activity are necessary for differentiating osteoblasts to mineralize the bone matrix (Nurminskaya et al., 2003).

These results demonstrated a role for TGs in formation of endochondral bones and specifically their expression by chondrocytes *in vitro*. Interestingly, studies have also examined TGs in osteoblast cultures lacking chondrocytes (mirroring intramembranous ossification) and found that TGs are also expressed by osteoblasts. Examination of human osteosarcoma cell lines revealed expression of extracellular TG2 and upon inhibition of transamidation activity by one of two broad-spectrum inhibitors, Putrescine or Cystamine, reduced matrix mineralization was observed (Heath et al., 2001; Yin et al., 2012). Additionally, the immortalized mouse MC3T3-E1 pre-osteoblast cell line showed expression of both FXIIIa and TG2 in osteoblasts during differentiation. In correlation with the results observed for chondrocytes, FXIIIa was identified as the major transglutaminase regulating osteoblast differentiation and matrix mineralization (Al-Jallad et al., 2011).

Together, these results show an *in vitro* role for TG2 and FXIIIa in bone mineralization and suggest FXIIIa as the main contributing TG. While many mechanisms have been suggested for TGs mode of action in bone formation, it still remains largely unknown. It has been suggested that TGs promote bone mineralization by cross-linking matrix proteins (Heath et al., 2001; Aeschlimann et al., 1993; Al-Jallad et al., 2006), by aiding in the secretion of matrix proteins through microtubule stabilization (Al-Jallad et al., 2011) or through activation of various signaling pathways (Nurminskaya et al., 2002; Yin et al., 2012). Despite *in vitro* evidence for each of these mechanisms, the *in vivo* mechanism remains unclear, thereby creating a requirement for further studies to better pinpoint the mechanism(s).

3. FXIIIa and TG2 Mouse Knock-Out Models

Strong *in vitro* evidence supports a role of TGs in bone formation; therefore the next logical step was to investigate their role *in vivo*. To this purpose, a genetic approach was adopted and single knock-out mice for both TG2 and FXIIIa were developed. Neither of these mouse knock-out lines showed a lethal phenotype (Koseki-Kuno et al., 2003; Nanda et al., 2001; Lauer et al., 2002). Surprisingly, these single knock-out mice did not present any significant skeletal phenotype, in contrast to the growing *in vitro* evidence for TGs in bone formation. This discrepancy between *in vitro* and *in vivo* results was proposed to be due to a compensation mechanism occurring between the two TG isoforms. *In vitro* data has shown that the roles of FXIIIa and TG2 in mineralization are redundant and therefore in the absence of one the other can perform the same function, indicating a possible compensation mechanism. Specifically, in TG2 knock-out mice it was suggested that either the expression or activation level of FXIIIa (as it is

produced as a zymogen) was being increased due to the loss of TG2 or vice versa that TG2 expression was increasing in response to the loss of FXIIIa in FXIIIa knock-out mice. However, further examination is necessary to determine whether this compensation mechanism is occurring. This potential compensation effect complicated the process of examining TGs in bone mineralization *in vivo* and created the need for an alternative model.

D. ZEBRAFISH AS A MODEL TO STUDY TGs IN BONE DEVELOPMENT

1. Zebrafish as a Model Organism

The zebrafish (*danio rerio*) model system has become central to the study of numerous biological systems, as can be demonstrated by the drastic increase in publications over the past two decades (Lieschke and Currie, 2007). Several key characteristics of this model organism have made them invaluable for studies of biological systems, among these are: transparency during early development, regeneration capacity, easy maintenance and short gestation time.

Numerous groups have taken advantage of these unique characteristics to study various developmental mechanisms. This model is especially appropriate for the study of developmental processes as a single zebrafish breeding pair can yield up to a couple hundred embryos per week. These embryos then develop quickly and by 3 days post-fertilization (dpf) have hatched from their eggs and are able to swim; allowing for a high throughput analysis of developmental processes. Further, the presence of established genetic approaches makes this model even more appropriate for developmental studies.

Specifically, zebrafish have been used to study the development of tissues such as the heart, muscle, eye and skeletal system.

2. Zebrafish as a Model Organism of Bone Formation

The use of zebrafish to study the process of bone development was of particular interest to our project. This model system has become very useful for the study of bone development, especially as zebrafish and humans share many aspects of bone formation (Brittijn et al., 2009). Early transparency is a unique characteristic that makes this model ideal by permitting *in vivo* imaging and analysis of bone by stains such as calcein. *In vivo* analysis allows for the preservation of valuable transgenic animals in addition to monitoring bone formation throughout development and not just at one end time-point. Additionally, by 21dpf axial skeletal elements have undergone mineralization, as detected by calcein staining, allowing for rapid examination of skeleton formation and mineralization (Du et al., 2001).

The zebrafish axial skeleton is composed of the vertebral column and unpaired fins. The vertebral column contains 31 vertebrae, which are divided into three classes: Weberian (the anterior vertebrae), precaudal (middle vertebrae) and caudal (the posterior vertebrae) (Bird and Mabee, 2003) (Fig. 1.3). The vertebrae are visible via calcein staining by 7dpf (Du et al., 2001) and form via endochondral ossification. Vertebrae mineralization proceeds from the anterior to the posterior of the body with the exception of the 2nd and 3rd vertebrae, which mineralize after the 4th vertebrae (Du et al., 2001). The unpaired fins also make up the skeletal system in zebrafish and include the dorsal, anal and caudal fins. Each of these fins is composed of multiple bony fin rays, termed lepidotrichia, that form via intramembranous ossification. Within these lepidotrichia are

blood vessels, nerves, pigment cells and mesenchymal-like cells (Fig. 1.4) (Poss et al., 2003). All three of the fins also maintain a regenerative capability which is described in Section E.2.

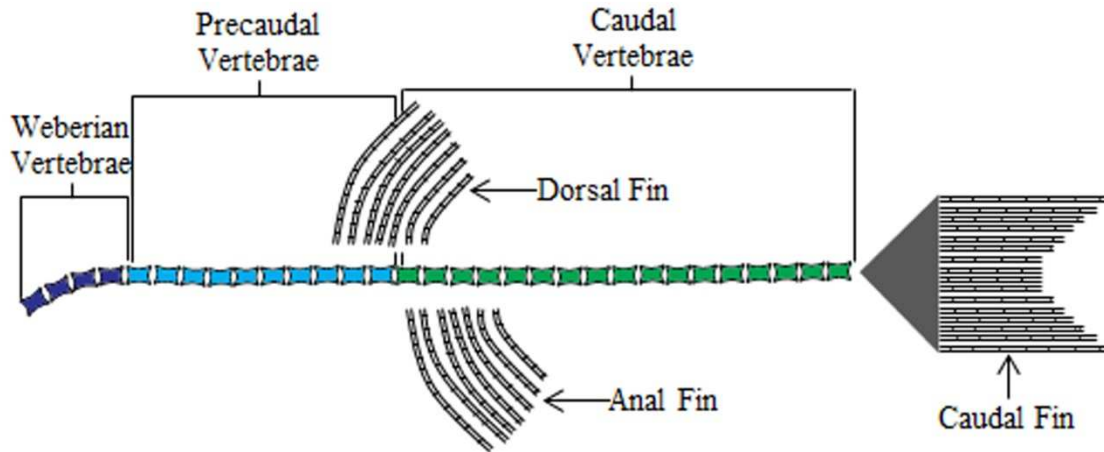


Figure 1.3 Diagram of the Zebrafish Axial Skeleton. The major elements of the axial skeleton are composed of the fins and vertebral column which is divided into three types of vertebrae: Weberian Vertebrae (Purple), Precaudal Vertebrae (Blue) and Caudal Vertebrae (Green). Additionally, it contains three fin types: the dorsal, anal and caudal fin.

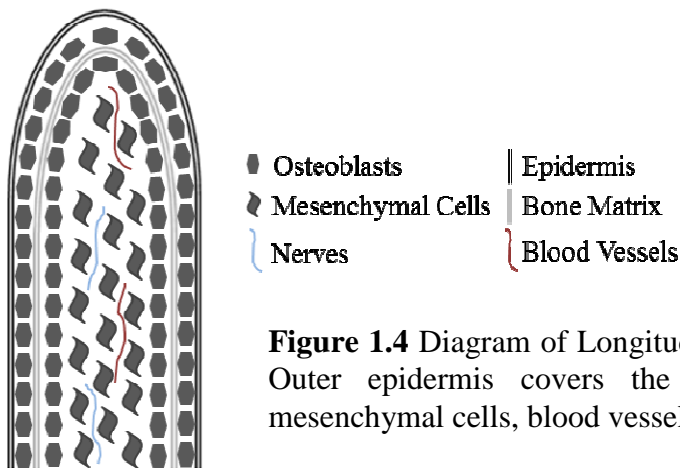


Figure 1.4 Diagram of Longitudinal Section of Lepidotrichia. Outer epidermis covers the bony ray, which contains mesenchymal cells, blood vessels and nerves.

E. ZEBRAFISH CAUDAL FIN REGENERATION

1. Regeneration

Upon injury, tissues are able to heal via two mechanisms: repair or regeneration. Tissues healed via repair form permanent scars, whereas tissues healed by regeneration result in an almost identical tissue (Poss et al., 2003). It is tissue scarring that makes repair a less-than-ideal mechanism of tissue healing when compared to the no-scarring mechanism of regeneration. The ability to regenerate tissues is a fairly common trait that can be seen from species to species; however the regenerative capacity (i.e. the number of tissues able to regenerate or the required amount of starting tissue to allow for regeneration) varies largely between species (Sanchez, 2000). Unfortunately, the majority of higher vertebrates has a very limited regeneration capability and heals tissues mostly by repair. However, due to the obvious benefits of regeneration, many studies have begun examining the processes of regeneration in lower vertebrates in hopes of gaining a better understanding of the mechanisms and factors controlling this process to allow for application to regenerative medicine.

2. Zebrafish Caudal Fin Regeneration

Zebrafish have the remarkable ability to regenerate numerous tissues, such as the optic nerve, scales, heart, spinal cord and fins (Poss et al., 2003). Among these regenerative tissues, the caudal fin is the most commonly studied, due to its easy access for amputation, symmetrical shape, simple structure and amputation having little to no effect on survival. The process of caudal fin regeneration is commonly divided into three different phases: Wound Healing, Blastema Formation, and Regenerative Outgrowth (Fig. 1.5). During wound healing, which occurs from approximately 0-12hours post-

amputation (hpa), the wound is covered with a layer of epidermis termed the apical ectodermal cap (AEC). The second phase of regeneration, blastema formation, occurs from approximately 12hpa-2 days post amputation (dpa) and can be divided into two separate phases: mesenchymal disorganization and migration and blastema formation. Mesenchymal disorganization and migration occurs from approximately 12hpa-1dpa and consists of tissue disorganization and cell migration towards the amputation plane to provide for the cellular population of the blastema which then forms from approximately 1-2dpa. Once the blastema has formed the last phase of fin regeneration, regenerative outgrowth, begins. This phase of regeneration lasts from approximately 2dpa until completion of regeneration around 10dpa and is when the amputated tissues are regenerated. It is the regenerative outgrowth phase of regeneration that this study is particularly interested in as this is when tissue regeneration and in particular bone regeneration is occurring.

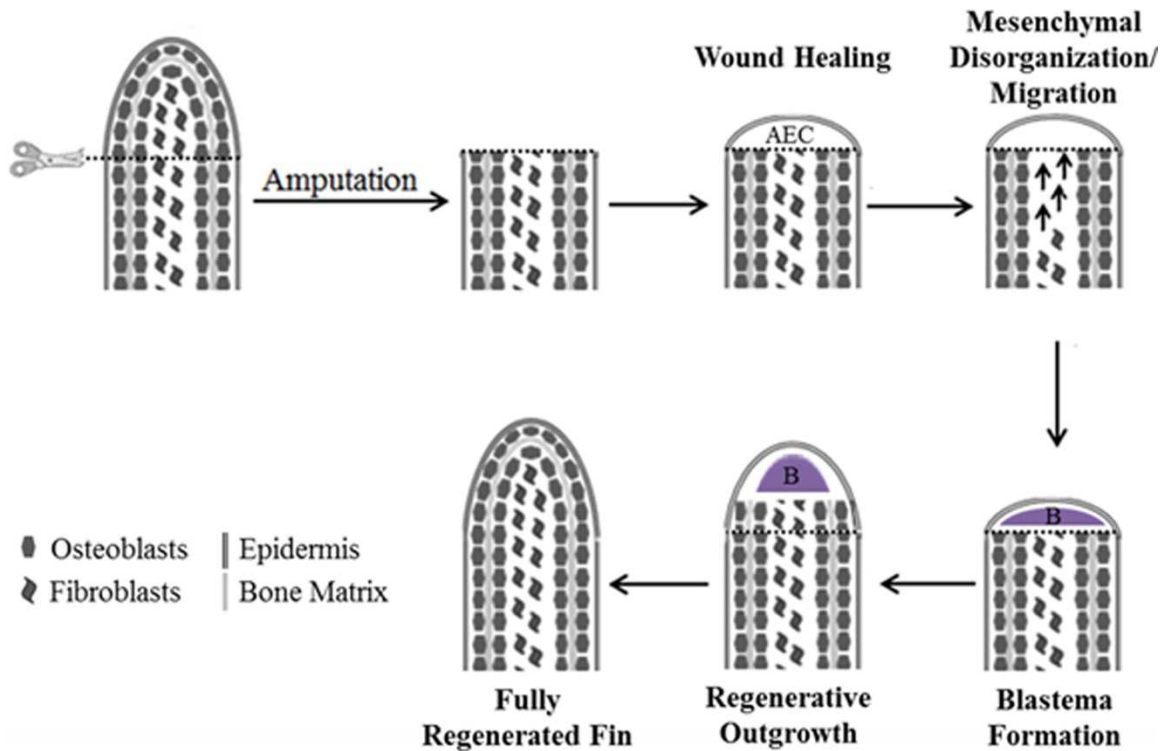


Figure 1.5. Schematic of Phases of Fin Regeneration. Dashed line indicating the plane of amputation. After amputation regeneration begins with wound healing which results in the formation of the AEC by 12hpa. This is followed by mesenchymal disorganization and migration and blastema formation (Marked by B) lasting from 12hpa-2dpa. Lastly, regenerative outgrowth begins and continues until ~10dpa at which point a fully regenerated fin has been formed.

The blastema, a mass of proliferative undifferentiated cells, serves as the progenitor cell population for newly regenerated tissues. This cellular mass and its origins during regeneration has become of great interest as an understanding of these cells and the factors that promotes their differentiation is invaluable for the development of regenerative medicine. Of particular interest to our studies are the osteo-progenitor cells which differentiate into osteoblasts and form newly regenerated bones. However, the origin of these osteo-progenitor cells remains unclear and two prevailing theories have been proposed: (1) intra-ray mesenchymal-like cells re-enter the cell cycle and migrate towards the regeneration area upon amputation or (2) differentiated osteoblasts of

the mature bone de-differentiate and migrate to the amputation site. Both differentiated osteoblasts of the mature bone and intra-ray mesenchymal-like cells have been found to migrate towards the regeneration site post-amputation (Poleo et al., 2001). Further, differentiated osteoblasts have been found to de-differentiate and migrate to the blastema post amputation, indicating a role for differentiated osteoblasts in bone regeneration (Knopf et al., 2011; Sousa et al., 2011). However, when differentiated osteoblasts were deleted from caudal fins prior-to amputation, regeneration was unaffected and the blastema was formed instead by intra-ray mesenchymal-like cells (Singh et al., 2012). Thus indicating a role for both differentiated osteoblasts and intra-ray mesenchymal-like cells in bone regeneration; however it remains unclear to what degree each population participates in this process.

F. CANONICAL β -CATENIN SIGNALING

1. Canonical β -Catenin Signaling

β -catenin is a multifunctional protein that has been associated with both maintenance of adherent junctions and signal transduction pathways (Xu and Kimelman, 2007). Despite the majority of β -catenin molecules in the cell being allocated to adherent junctions, its role in signal transduction is essential to multiple developmental processes and diseases (Xu and Kimelman, 2007).

In the absence of an activation signal, β -catenin binds a destruction complex composed of four proteins: Axin, Adenomatosis Polyposis Coli (APC) and two kinases, casein kinase 1 and glycogen synthase kinase 3 (GSK3). These kinases phosphorylate β -

catenin, thereby targeting it for ubiquitination and ultimately resulting in degradation. Signal transduction is initiated by the binding of an activating ligand to the extracellular domain of two receptors, Frizzled (Fz) and low-density lipoprotein receptor 5 or 6 (LRP5/6), resulting in the formation of a complex between these two proteins. The intracellular domain of this complex then recruits axin, preventing formation of the destruction complex, resulting in β -catenin no longer being phosphorylated and targeted for degradation. Instead β -catenin accumulates in the cytosol resulting in its nuclear translocation. Once in the nucleus β -catenin mediates/activates gene expression by interacting with the Tcf/Lef transcription factors (Fig. 1.6) (Huang and He, 2008).

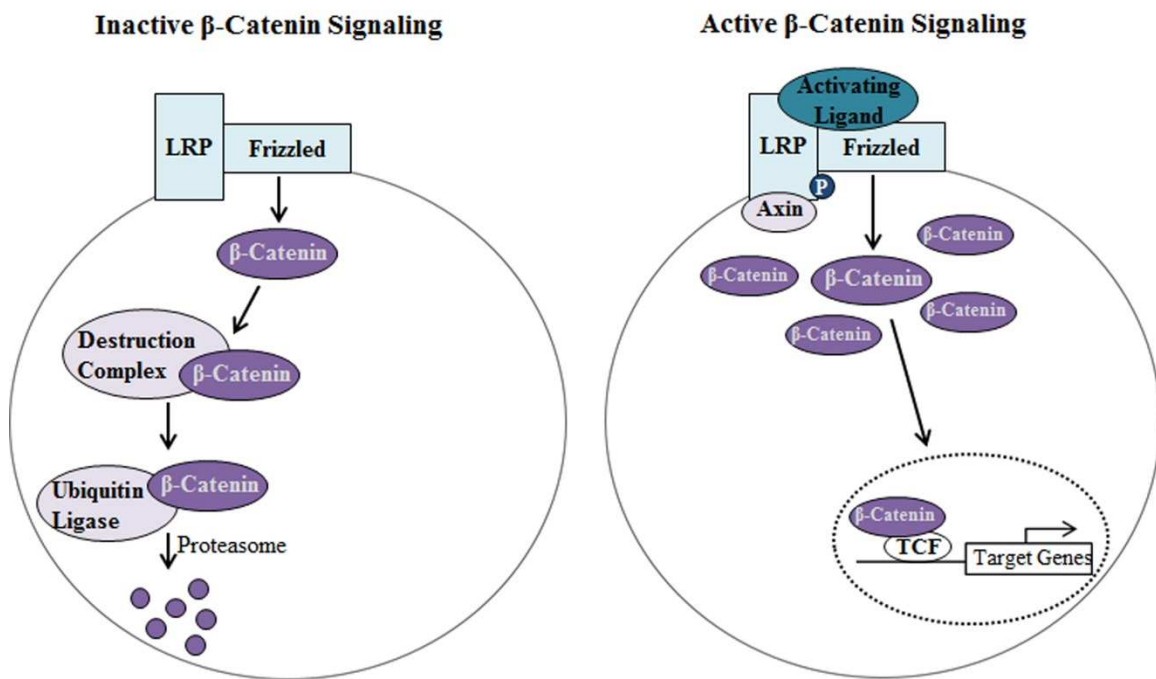


Figure 1.6 Schematic of Canonical β -Catenin Activation. Without ligand binding (Left panel) β -Catenin binds to the destruction complex resulting in phosphorylation and targeting to proteasomal degradation. Upon ligand binding, signaling is activated (Right panel) and axin is recruited to the LRP receptor, thereby preventing formation of the destruction complex. β -Catenin is no longer targeted for degradation, thereby allowing for accumulation in the cytosol and resulting in nuclear translocation. In the nucleus β -Catenin interacts with transcription factors resulting in transcription of target genes.

The principle activating ligands associated with canonical β -catenin signaling are Wnt glycoproteins. However, studies have shown that various other extracellular proteins are able to interact with this crucial signaling pathway. This pathway can be inhibited by the binding of proteins, such as, Dkk1 (Boudin et al., 2013), SOST (Ellies et al., 2006; Li et al., 2005) and WISE (Itasaki et al., 2003) to the LRP receptor which inhibits interaction with the activating ligand. Further, extracellular proteins un-related to Wnts are able to activate this crucial signaling pathway. These proteins include but are not limited to R-spondins (Han et al., 2011), Norrin (Xu et al., 2004a) and importantly TG2 (Beazley et al., 2012b; Faverman et al., 2008; Condello et al., 2013).

2. Canonical β -Catenin Signaling in Zebrafish Fin Regeneration and Bone Formation

Interestingly, the canonical β -catenin signaling pathway has been identified to be crucial to both zebrafish fin regeneration and bone formation. During each of the three stages of fin regeneration, wound healing, blastema formation and regenerative outgrowth, β -catenin protein is up-regulated, thereby indicating a role in fin regeneration (Stoick-Cooper et al., 2007). While traditionally associated Wnt ligands have been identified as activators of β -catenin signaling for wound healing, the activating ligand for the next two steps, blastema formation and regenerative outgrowth has yet to be identified (Stoick-Cooper et al., 2007; Poss et al., 2003).

β -catenin has also been found to be a key component for both initiating bone development and repair in numerous systems (Westendorf et al., 2004). It has been found that β -catenin is active in proliferating chondrocytes and osteoblasts during bone fracture repair and regeneration (Chen et al., 2007; Kim et al., 2007). Aberrant signaling of the canonical β -catenin signaling pathway has also been associated with numerous

diseases resulting in an abnormal skeleton such as: Sclerosteosis, Van Buchem disease, Osteoporosis, Pagets disease and multiple myeloma (Boudin et al., 2013).

This project identifies TGs with bone formation and regeneration *in vivo*, specifically with the deposition of the type I collagen matrix. It further identifies canonical β -catenin as a potential mechanism through which TGs promote bone mineralization. This identification can be further used to better treat diseases and injuries involving the skeletal system.

CHAPTER II: TISSUE SPECIFIC RESPONSES TO LOSS OF TRANSGLUTAMINASE 2¹

A. ABSTRACT

Of the eight catalytic TGs, TG2 is the most comprehensively studied due to its ubiquitous expression in multiple cell types. Despite the critical role for this enzyme in multiple biological processes *in vitro*, TG2 knock-out mouse models have shown no severe developmental phenotypes, suggesting compensation by other TGs. To begin characterization of the compensating mechanisms, we analyzed total transamidating activity and expression patterns of all catalytically active TGs in seven different tissues/organs from wild-type and TG2 knock-out mice. Inhibitory analysis with the TG2-specific inhibitor KCC-009 suggests that the relative contribution of TG2 to total transamidating activity differs in various tissues. Accordingly, our data indicate tissue-specific mechanisms of compensation for the loss of TG2, including transcriptional compensation in heart and liver versus functional compensation in aorta, kidney and skeletal/cartilaginous tissues. On the contrary, no compensation has been detected in skeletal muscle, suggesting a limited role for TG2-mediated transamidation in normal development of this tissue.

¹ CITATION: Deasey S.D., Shanmugasundaram S., Nurminskaya M.N. *Amino Acids* 2013 Jan 44(1):179-187

B. INTRODUCTION

The mammalian TG protein family consists of nine proteins with eight zymogens/enzymes, designated TG1-7 and FXIIIa in addition to a structural protein, protein 4.2, which lacks catalytic activity. TG-mediated reactions are essential for multiple biological processes ranging from blood coagulation to skin barrier formation and extracellular matrix assembly (Griffin et al., 2002; Lorand and Graham, 2003). These enzymes function in a wide range of biological processes by catalyzing three types of posttranslational modifications: transamidation, esterification, and hydrolysis (Iismaa et al., 2009). In addition, TG2, TG4 and TG5 can bind to and hydrolyze GTP, which inhibits their transamidase catalytic activity (Iismaa et al., 2009; Spina et al., 1999; Candi et al., 2004). Interestingly, while these distinct enzymes are able to recognize the same protein substrate, they generally exhibit remarkable substrate specificity *in vivo*.

TG2 is the most comprehensively studied of this diverse enzyme family. It is constitutively expressed in many cell types, including but not limited to, endothelial cells, vascular smooth muscle cells and fibroblasts (Thomazy and Fesus, 1989). Further, its expression correlates with cell differentiation in some cell lineages, such as the osteochondrogenic lineage (Aeschlimann et al., 1993; Nurminsky et al., 2011; Thomazy and Fesus, 1989). In addition to traditional TG activities, TG2 has been reported to act as a protein kinase (Mishra and Murphy, 2004) and a protein disulfide isomerase (Hasegawa et al., 2003), as well as to facilitate cell-matrix interaction independently from its enzymatic activity (Akimov et al., 2000; Xu et al., 2006; Dardik and Inbal, 2006). TG2 is localized to both the extracellular matrix and multiple cellular compartments, with ample

in vitro studies showing a wide range of TG2 functions from cell adhesion to cell death (Iismaa et al., 2009;Griffin et al., 2002;Fesus and Szondy, 2005;Nadalutti et al., 2011).

Two mouse knockout models for TG2 were developed simultaneously by different groups to evaluate its *in vivo* function (De, V and Melino, 2001;Nanda et al., 2001). These models were based on disrupting mouse *Tgm2* gene around exon 5 (which encodes part of the catalytic core domain) and both showed absence of TG2 protein in homozygote progeny. However, no obvious developmental phenotype was observed in either of these mouse models despite the previously demonstrated *in vitro* role for TG2 in multiple developmental processes. These phenotypes suggest the common biological phenomenon of backup compensation, which occurs when functionally overlapping proteins compensate for the loss of each other. For example, rescuing/compensation mechanisms have been described for the family of small leucine-rich proteoglycans (Ameys and Young, 2002). Further, in TG2 null ($TG2^{-/-}$) chondrocytes compensatory activation of FXIIIa has been observed, resulting in an unchanged level of total transamidase activity (Nurminskaya and Kaartinen, 2006;Tanaka et al., 2007).

In this study, we analyzed the relative contribution of TG2-mediated catalytic activity in seven different wild-type (WT) mouse tissues. Next we examined enzymatic activity in $TG2^{-/-}$ tissues and analyzed expression of the eight TGs in the $TG2^{-/-}$ versus WT tissues to identify possible tissue-specific compensation mechanisms supporting the $TG2^{-/-}$ phenotype.

C. MATERIALS AND METHODS

1. Animals and tissue dissection

Animals used were CB57/B6 and TG2^{-/-} mice (a kind gift from Robert Graham, Victor Chang Cardiovascular Institute, New South Wales, Australia). All procedures were approved by the institutional animal care and use committee at the University Of Maryland School Of Medicine and were conducted in compliance with NIH guidelines for the care and use of laboratory animals. Two 3-4 week old mice of each genotype were used to dissect sternum (designated as non-hypertrophic cartilage), knee joint (designated as ossifying cartilage), skeletal muscle from the limb, aorta, heart, kidney, and liver. Tissues from both animals were pooled together and total RNA was isolated by Trizol (Invitrogen) (Detailed description of RNA isolation in Appendix A.1). Resulting RNA was DNase digested and cleaned-up with the RNeasy mini kit (Qiagen) (Detailed description of DNase digest and RNA clean-up in Appendix A.2)

2. Real-Time PCR

Primers for TGs were designed using NCBI primer design software (List of primers in Appendix B.1). Real-time PCR was run using first-strand synthesized cDNA (Detailed description of reverse transcription in Appendix A.3) as a template on a BIORAD CFX96 Real-Time System. Real-time PCR was run following the manufactures instructions for heat activation, amplification and melting curves for 45 cycles (Detailed description of real-time PCR in Appendix A.4). Expression levels were normalized to RLP-19 mRNA with anything showing expression after 35 cycles being disregarded for analysis.

3. TG Activity Assay

Total TG cross-linking activity in mouse tissue was assayed by incorporation of the biotinylated pentylamine Ez-link Pentylamine-Biotin (Pierce) into *N,N'*-Dimethylcasein (Sigma-Aldrich) in an ELISA-like assay as previously described (Trigwell et al., 2004). 96-well microtiter plates (Maxisorp NUNC) were incubated overnight with 250 μ L of 1mg/mL *N,N'*-Dimethylcasein (Sigma-Aldrich) in 5mM Sodium Carbonate (pH 9.8), and blocked with 200 μ L of 0.1% bovine serum albumin (BSA) (HyClone) in 5mM Sodium Carbonate (pH 9.8) for one hour at 37°C. Mouse tissue was lysed and centrifuged and TG-containing supernatant was used for further assays (Detailed description of protein extraction in Appendix A.5). Purified guinea pig liver transglutaminase 2 (gpLTG2) (Sigma-Aldrich) was used as a standard for activity tests. For inhibitory studies, mouse lysates (20 μ g total protein) or purified gpLTG2 (75ng purified protein) were pre-incubated with 30 μ M inhibitors for one hour at 37°C. Reaction was carried out in 100mM Tris-HCl pH 8.5, 6.7mM CaCl₂, 13.3mM DTT and 2.5mM Ez-link Pentylamine-Biotin (Pierce) for one hour at 37°C. Incorporated Ez-link Pentylamine-Biotin was detected with 1:5000 ExtrAvidin-Peroxidase (Sigma) and Super AquaBlue ELISA Substrate (eBioscience) followed by reading the absorbance at 405nm on a Polarstar Optima plate reader.

4. Data and Statistical Analysis

Statistical significance was calculated by the student's T-test (*P \leq 0.05; **P \leq 0.005) and error bars demonstrate the standard error mean.

D. RESULTS

1. Tissue-specific expression of TG family

The expression pattern of all catalytic TG enzymes was analyzed in WT mouse tissues that were chosen based on previously implicated roles for TG2 in development and pathology. Earlier studies reported expression of these proteins in various cell types and tissues; however, to our knowledge comparative analysis of their expression in various tissues has been limited. To examine the relative expression of each TG in the various tissues, we compared expression in each tissue to the average expression of that TG in all tissues analyzed. We were unable to detect expression of TG7 and TG4 in any of the tissues, in agreement with previous studies identifying restricted expression of TG4 protein to the prostate (Ho et al., 1992). Expression of FXIIIa varies between the analyzed tissues, with lowest expression of FXIIIa observed in the liver and kidney where the regulatory/carrier B subunit of the heterotetrameric plasma coagulation Factor XIII is expressed. Despite FXIIIa's historical identification as a "plasma" transglutaminase, our results combined with previous reports (www.ncbi.nlm.nih.gov/UniGene) demonstrate its expression in a vast variety of tissues (Fig. 2.1).

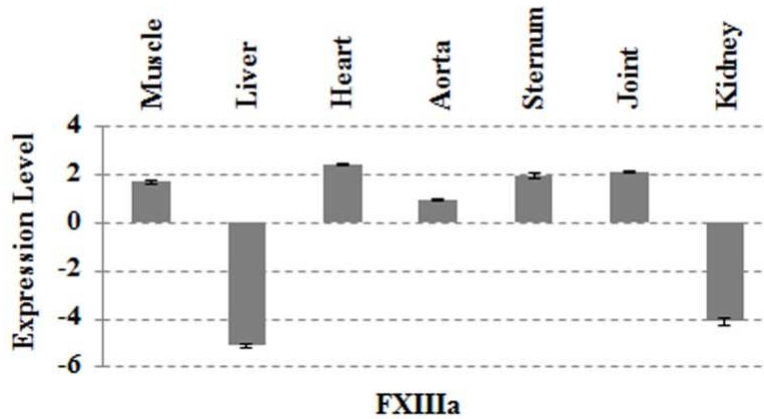


Figure 2.1 Tissue-Specific Expression of FXIIIa in WT Mice. Real-time PCR revealed expression in muscle, heart, aorta, sternum and joint. Levels of expression for each enzyme were compared to its average expression in all analyzed tissues.

TG1 and TG3 have both been identified in skin and are known to be required for stabilization of the cornified cell envelope in skin (Kuramoto et al., 2002;Candi et al., 2002). We, however, also identified expression of these enzymes in skinless-internal tissues. TG1 was identified in the liver, aorta and kidney of mice (Fig 2.2A) and may be functioning in these tissues to stabilize adherent junctions, similar to its previously proposed role in the lung epithelium, liver, kidney and endothelium of the myocardial microvasculature (Hiragi et al., 1999;Baumgartner et al., 2004). TG3 was identified in the aorta, sternum and kidney (Fig 2.2B); however, the biological role of TG3 in these skinless tissues remains largely unknown.

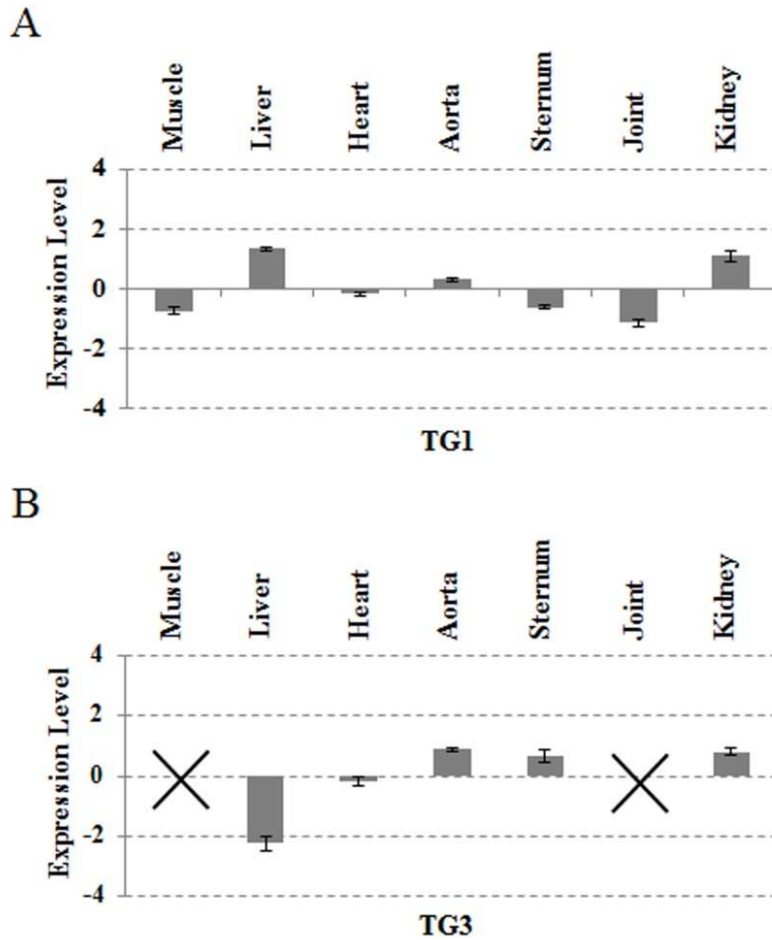


Figure 2.2 Tissue-Specific Expression of TG1 and TG3 in WT Mice. Real-time PCR analysis revealed that TG1 was expressed in the liver, aorta and kidney (A), while TG3 was identified in the liver, aorta, sternum and kidney (B). Both of these enzymes have been correlated with skin maintenance and function. Levels of expression for each enzyme were compared to its average expression in all analyzed tissues. X's indicating no detected expression in respective tissue.

The highest level of TG2 expression was detected in the aorta (Fig. 2.3A), correlating with its previously proposed role in vascular remodeling (Bakker et al., 2008). Similarly, the highest expression of TG5 was also detected in aorta (Fig. 2.3B). Expression of both TG2 and TG5 in the liver was significantly lower than that of the other analyzed tissues, while in skeletal muscle and joint, expression of TG5 was undetectable (Fig. 2.3B). The tissue-specific expression pattern of TG3 was found to be

similar to that of TG2, possibly implicating a common long-range regulatory mechanism for these genes localized on the same chromosome (Grenard et al., 2001).

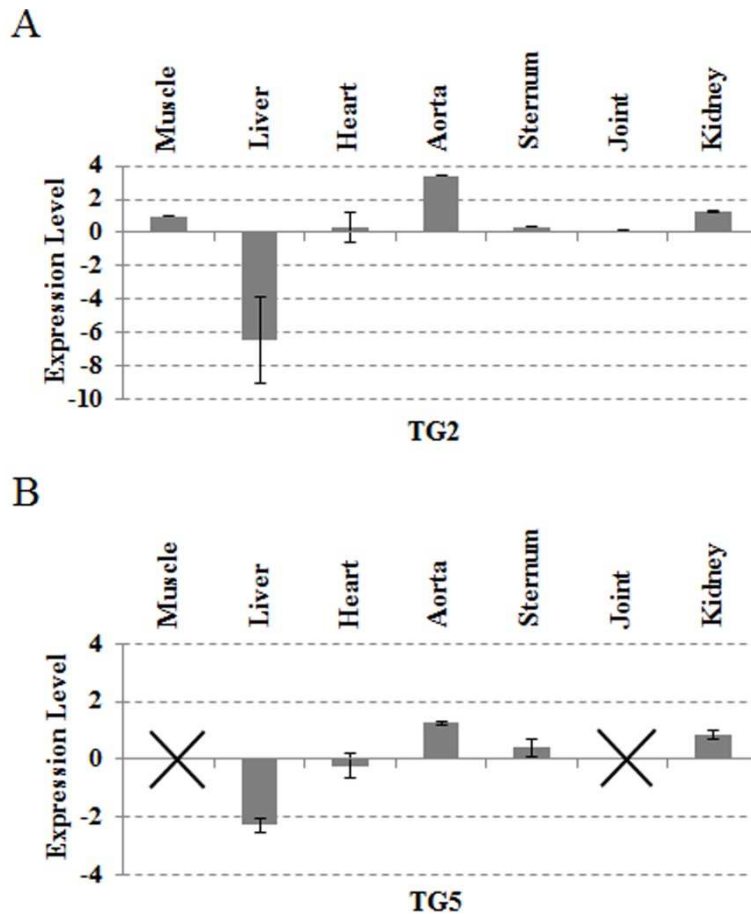


Figure 2.3 Tissue-Specific Expression of TG2 and TG5 in WT Mice. Real-time PCR analysis identified TG2 in the muscle, heart, aorta, sternum, joint and kidney (A), while TG5 was identified by the same means in the aorta, sternum and kidney (B). Both these enzymes showed their highest level of expression in the aorta. Levels of expression for each enzyme were compared to its average expression in all analyzed tissues. X's indicating no detected expression in respective tissue.

Expression of TG6 was detected in the cardiovascular tissues, heart and aorta, and also in the kidney, but absent from skeletal muscle and joint (Fig 2.4), adding new sites of expression to the previously described skin, eyes and neurons (www.ncbi.nlm.nih.gov/UniGene; Hadjivassiliou *et al.*, 2008). Thus, TG6 seems to be an isoform with a wider distribution than previously believed.

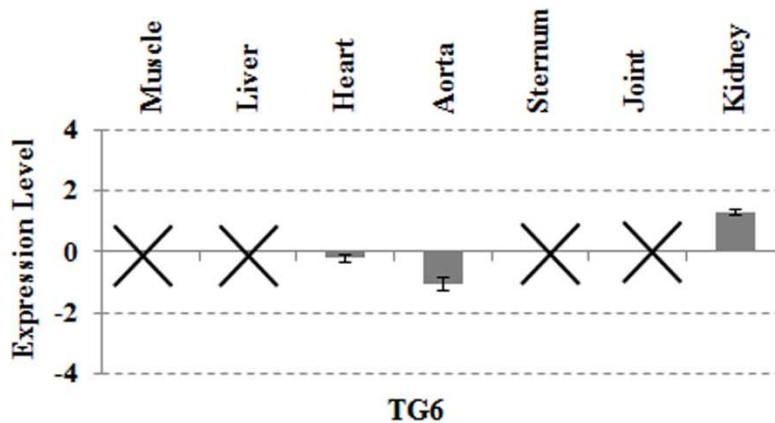


Figure 2.4 Tissue-Specific Expression of TG6 in WT Mice. Real-time PCR revealed expression in heart, aorta and kidney. Levels of expression were compared to its average expression in all analyzed tissues. X's indicating no detected expression in respective tissue.

2. Compensation for TG2 loss in skeletal muscle

Expression of three TGs was identified in the WT skeletal muscle – with TG2 and FXIIIa expressed at relatively high levels and TG1 at much lower levels (Fig. 2.5A). The TG2-specific inhibitor KCC-009 inhibited approximately 60% of the total transamidating activity (Table 2.1), attributing 60% of the transamidating activity in the skeletal muscle to TG2. Accordingly, genetic ablation of TG2 resulted in a 60% reduction of total transamidating activity in the skeletal muscle (Fig. 2.5B), corresponding to the portion of transamidating activity attributed to endogenous TG2. In agreement with this lack of transamidation compensation, expression of TG1 did not change significantly and expression of FXIIIa was significantly reduced in the TG2^{-/-} versus WT muscle (Fig. 2.5C). This lack of compensation for the loss of TG2-mediated transamidating activity by other TGs suggests that TG2-mediated transamidation activity is not crucial for muscle formation and function.

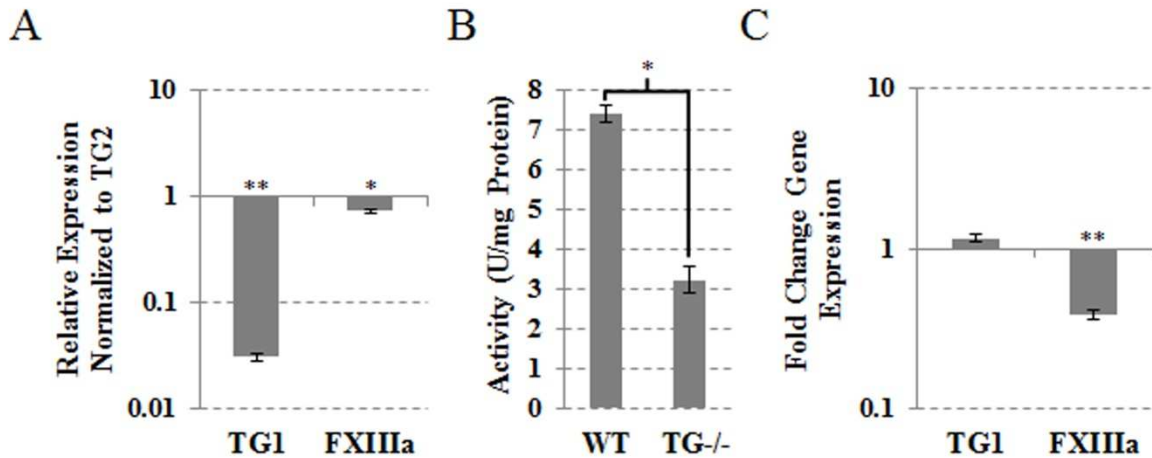


Figure 2.5 TG Expression and Activity in Mouse Skeletal Muscle. (A) Real-time PCR analysis showing expression of TGs compared to TG2 expression in WT mouse skeletal muscle. (B) TG cross-linking activity assayed by pentylamine-biotin incorporation into *N,N'*-dimethylcasein. Total protein lysates from WT and TG2^{-/-} mouse skeletal muscle were used. (C) Real-time PCR analysis showing expression of TGs in TG2^{-/-} mouse skeletal muscle compared to WT tissue. (*P ≤ 0.05; **P ≤ 0.005)

Organ/Tissue	Activity (U/mg Protein)	Activity (U/mg Protein) with 30μM KCC-009 Treatment	Percent Inhibition with KCC-009
Skeletal Muscle	7.39 ± 0.34	2.85 ± 0.60	61.37%
Liver	46.74 ± 0.19	10.05 ± 0.84	78.50%
Heart	29.00 ± 2.52	12.74 ± 0.70	56.06%
Aorta	8.11 ± N.A.	6.16 ± N.A.	23.94%
Sternum	4.53 ± 1.07	Not Detectable	100%
Joint/Ossifying Cartilage	19.80 ± 0.87	7.33 ± 0.55	62.98%
Kidney	20.99 ± 1.46	11.80 ± 0.78	43.78%

Table 2.1 Transamidating Activity and Percent Inhibition by TG2 Inhibitor KCC-009. Transamidating activity was measured in tissues ±KCC-009 to determine the contribution of TG2 to total transamidating activity.

3. Compensation for TG2 loss in liver

Similar to muscle, TG1, FXIIIa and TG2, were expressed in the liver (Fig. 2.6A). Approximately 80% of total transamidating activity was attributed to TG2 (Table 2.1), however the total transamidating activity in the TG2^{-/-} liver was reduced to 42% (Fig. 2.6B), indicating a possible compensation effect by other TGs. Expression analysis of the TG2^{-/-} liver revealed a 2-fold increase in FXIIIa expression (SEM 0.157, p<0.05) and a 1.6-fold increase in TG1 expression (SEM 0.076, p<0.005) (Fig. 2.6C). No other TGs were induced in the TG2^{-/-} liver tissue, suggesting transcriptional compensation for the loss of TG2 via increased expression of TG1 and FXIIIa, which are expressed in the WT tissue. Interestingly, the combined activity of TG1 and FXIIIa in the liver constitutes approximately 20% of the total transamidating activity, in contrast to their approximately 40% contribution in skeletal muscle (Table 2.1). This is accompanied by high levels of TG1 expression in the liver (compared to TG2) while FXIIIa expression is comparable in these tissues (Figs. 2.5, 2.6). Two possible explanations can be proposed: (1) TG1 and/or FXIIIa, both requiring proteolytic activation, are activated to a higher extent in the muscle than the liver or (2) TG2 in the muscle maybe less active than in the liver, possibly due to regulation via the Ca²⁺/GTP binding balance. The significantly lower level of total transamidating activity in the muscle (Table 2.1) favors the latter explanation.

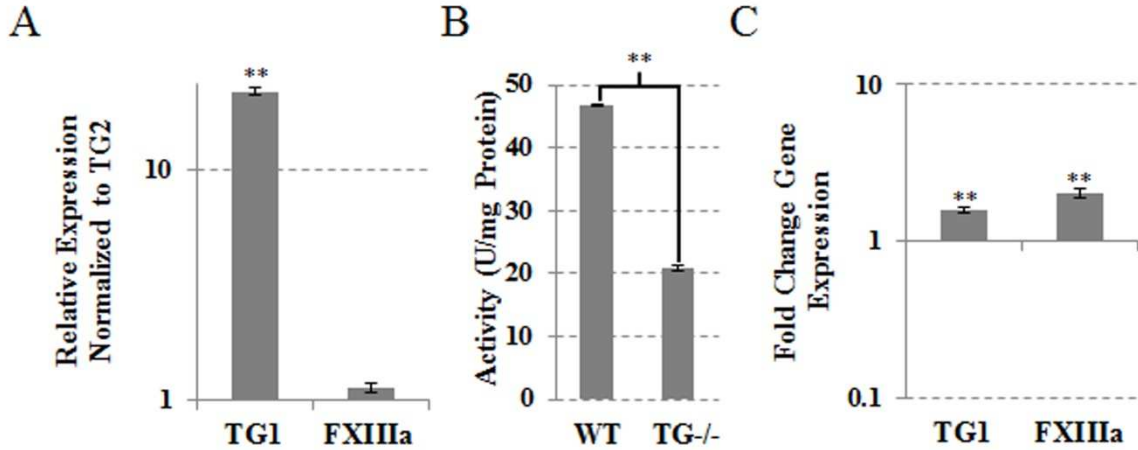


Figure 2.6 TG Expression and Activity in Mouse Liver Tissue. (A) Real-time PCR analysis showing expression of TGs compared to TG2 expression in WT mouse liver. (B) TG cross-linking activity assayed by pentylamine-biotin incorporation into *N,N'*-dimethylcasein. Total protein lysates from WT and TG2^{-/-} mouse liver were used. (C) Real-time PCR analysis showing expression of TGs in TG2^{-/-} mouse liver compared to WT liver tissue. (*P ≤ 0.05; **P ≤ 0.005)

4. Compensation for TG2 loss in non-hypertrophic cartilage

In our previous studies, TG2 was shown to regulate the early stages of chondrogenic differentiation in mesenchymal cells (Nurminsky et al., 2011). However, cartilaginous tissues in TG2^{-/-} mice have been found to be phenotypically normal, suggesting a compensation mechanism by other TGs. We, therefore, analyzed expression of the eight TG enzymes in the sternum cartilage, which is composed of mostly non-hypertrophic chondrocytes and identified four TGs: TG2, FXIIIa, TG1, and TG3. Relative to TG2 expression, FXIIIa was expressed at comparable levels, while TG1 and TG3 were expressed at lower levels (Fig. 2.7A). The TG2 inhibitor KCC-009 dramatically decreased total transamidating activity in the WT sternum (Table 2.1), suggesting that TG2 is the major active enzyme in this tissue. Unexpectedly, genetic ablation of TG2 resulted in a significant 3-fold increase in total TG activity (SEM 0.6, p<0.005) (Fig. 2.7B). However, there was no significant change in FXIIIa expression, a

slight down-regulation of TG1 (Fig. 2.7C) and expression of TG3 is reduced to almost undetectable levels (data not shown). These results implicate catalytic rather than transcriptional activation of FXIIIa, TG1 and/or TG3 in the TG2^{-/-} cartilage, and present an example of functional in contrast to the transcriptional compensation that was proposed for liver.

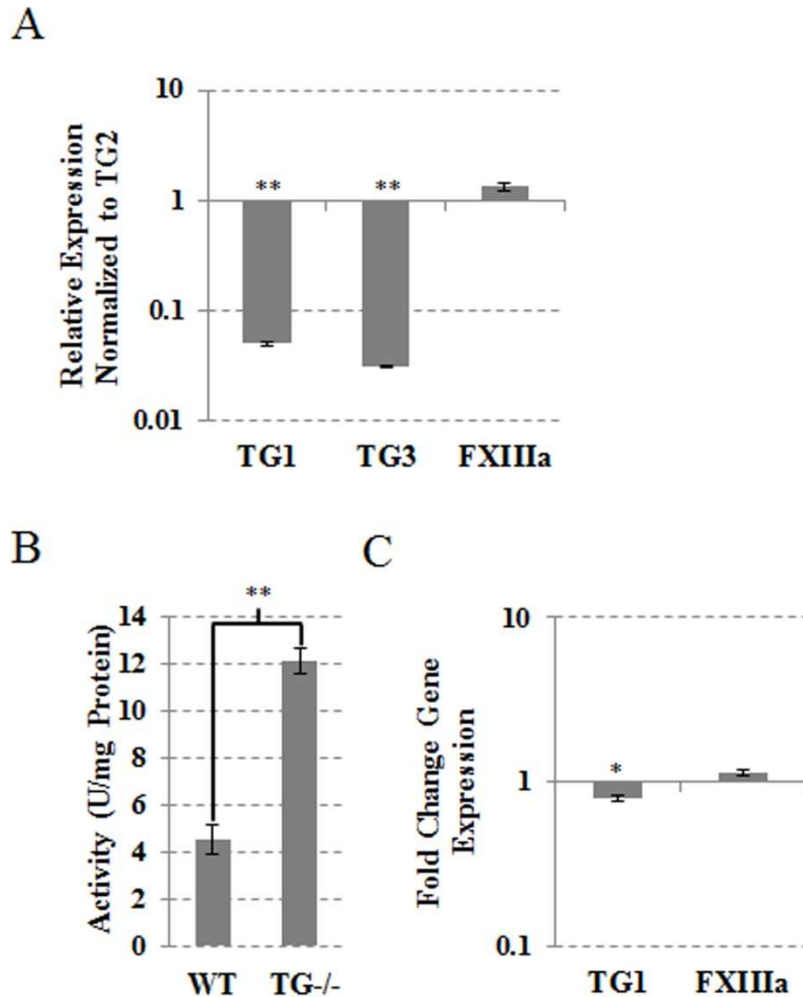


Figure 2.7 TG Expression and Activity in Mouse Non-Hypertrophic Cartilage. (A) Real-time PCR analysis showing expression of TGs compared to TG2 expression in WT mouse non-hypertrophic cartilage. (B) TG cross-linking activity assayed by pentylamine-biotin incorporation into *N,N'*-dimethylcasein. Total protein lysates from WT and TG2^{-/-} mouse non-hypertrophic cartilage were used. (C) Real-time PCR analysis showing expression of TGs in TG2^{-/-} mouse non-hypertrophic cartilage compared to WT tissue. (*P ≤ 0.05; **P ≤ 0.005)

5. Compensation for TG2 loss in joint/ossifying cartilage

Differentiating chondrocytes of the growth plate have been shown to express both TG2 and FXIIIa (Aeschlimann et al., 1993; Nurminskaya and Linsenmayer, 1996). Here, we analyzed expression of eight TGs in the whole joint, which includes the cartilaginous growth plate, articular cartilage, periosteum and secondary ossification center. All soft tissues, including tendon, muscle, ligament, bursa and synovial sac, were carefully removed at dissection. In addition to the previously described expression of TG2 and FXIIIa, TG1 was expressed in the joint tissues although at much lower levels (Fig. 2.8A). Specific inhibition of TG2 with KCC-009 significantly inhibited (approximately 60% inhibition) the transamidase activity in the WT joint tissue (Table 2.1). However, genetic ablation of TG2 had only minor effects on the transamidase activity (Fig. 2.8B), indicating that enzymes other than TG2 can support the transamidase activity in the skeletal tissues, in agreement with earlier studies (Nurminskaya et al., 1998; Nurminskaya and Kaartinen, 2006; Tanaka et al., 2007). A novel observation of this study was the up-regulation of TG1 and induction of TG3 expression in the TG2^{-/-} joint (Fig. 2.8C). In addition to the previously demonstrated proteolytic activation of the FXIIIa proenzyme (Nurminskaya et al., 1998; Tanaka et al., 2007), TG1 and TG3 may also compensate for the loss of TG2 in skeletal tissue. This finding suggests that even a double TG2/FXIIIa knock-out model may be insufficient to delineate the role of the TG-mediated protein modifications in skeletal formation.

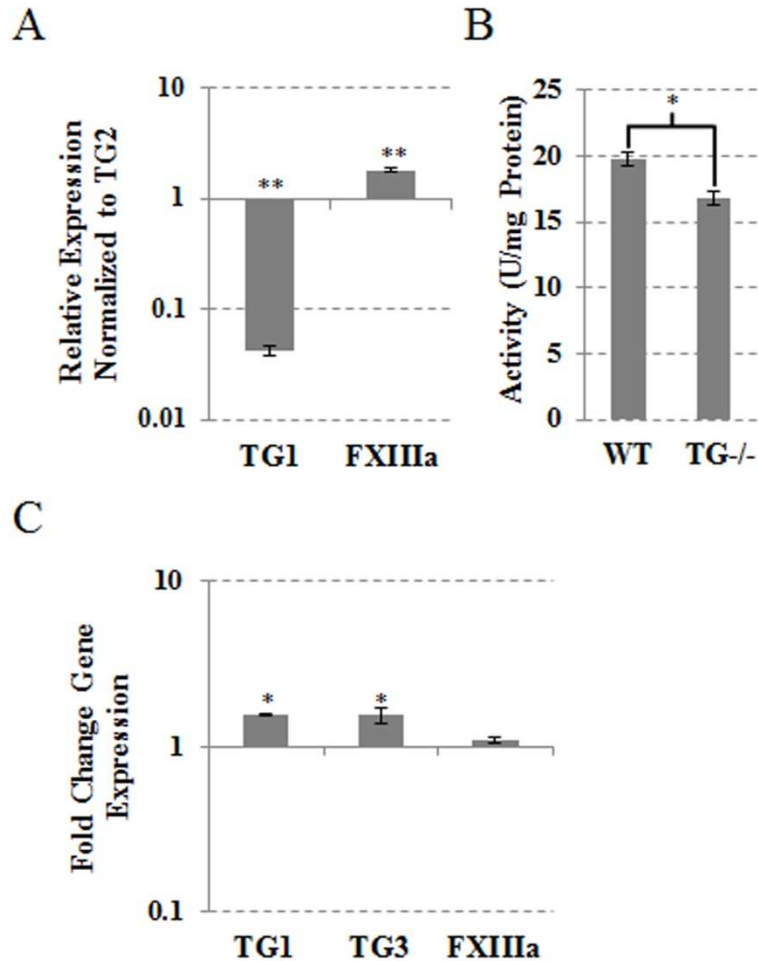


Figure 2.8 TG Expression and Activity in Mouse Joint/Ossifying Cartilage. (A) Real-time PCR analysis showing expression of TGs compared to TG2 expression in WT mouse joint/ossifying cartilage. (B) TG cross-linking activity assayed by pentylamine-biotin incorporation into *N,N'*-dimethylcasein. Total protein lysates from WT and TG2^{-/-} mouse joint/ossifying cartilage were used. (C) Real-time PCR analysis showing expression of TGs in TG2^{-/-} mouse joint/ossifying cartilage compared to WT tissue. (*P ≤ 0.05; **P ≤ 0.005)

6. Compensation for TG2 loss in cardiovascular tissues

6.1 Aorta

High levels of TG2 expression have been detected in the aortic tissues, where different cell types express TG2 including endothelial cells, vascular smooth muscle cells and fibroblasts of the adventitia (Greenberg et al., 1991). Additionally, a significant role

for TG2 has been implicated in vascular pathologies such as vascular inward remodeling (Bakker et al., 2008;Pistea et al., 2008), and medial calcification (Johnson et al., 2008;Beazley et al., 2012a). Nevertheless, no phenotypic abnormalities have been reported in the developing vasculature of TG2^{-/-} mice. Endogenous transamidating activity in WT aortic tissue was much lower than in any of the other analyzed tissues (Table 2.1), and expression analysis revealed dominant expression of TG2, although several other TGs were expressed at low levels as well (Fig. 2.9A). Surprisingly, total transamidating activity in the aortic tissue was only slightly inhibited by KCC-009 (Table 2.1), suggesting that TG2 is mostly present in an inactive (maybe GTP-bound) form in the aorta. However, genetic ablation of TG2 resulted in enhanced total transamidating activity (Fig. 2.9B) despite no induction in TG expression (Fig. 2.9C). Proteolytic activation of the pro-enzymes expressed in the TG2^{-/-} aortic tissue offers a credible explanation for this observation, but further analysis is needed to elucidate the molecular regulation of this effect. Of note, we did not detect up-regulation of TG5 expression in the fresh TG2^{-/-} aortic tissue which has been previously reported in the passaged TG2^{-/-} VSMCs and maybe an artifact of cell culture (Johnson et al., 2008).

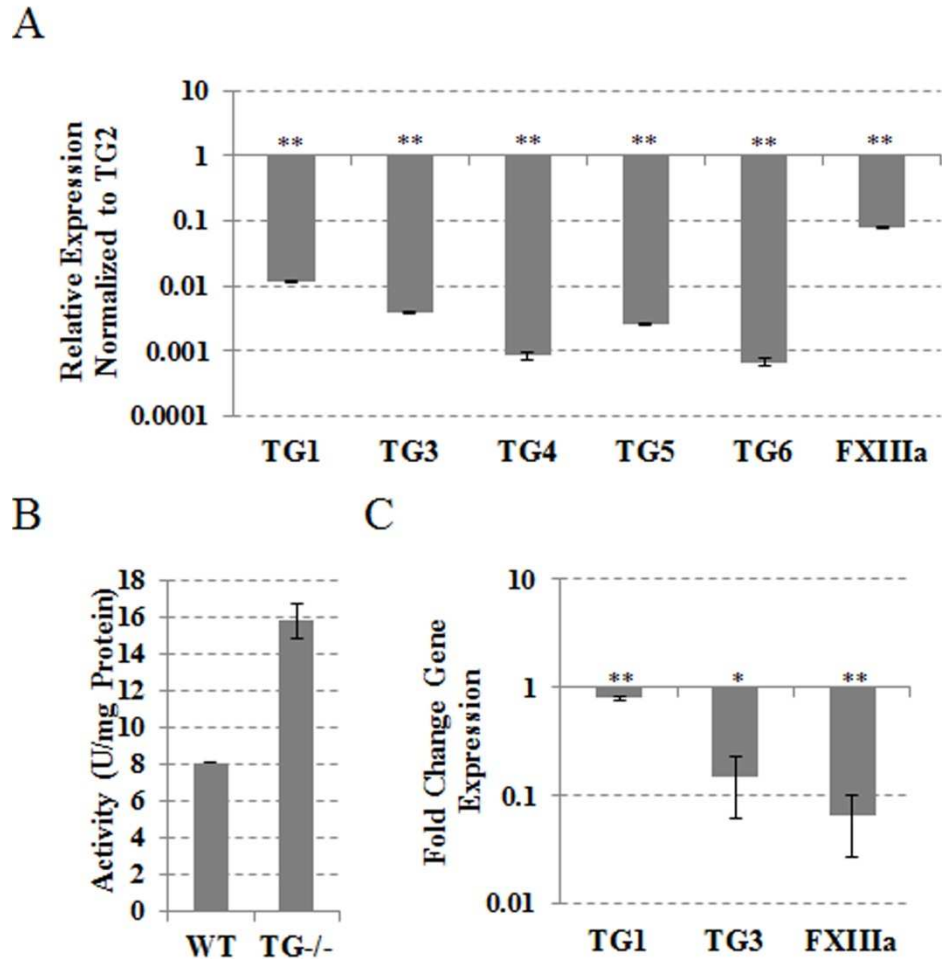


Figure 2.9 TG Expression and Activity in Mouse Aorta. (A) Real-time PCR analysis showing expression of TGs compared to TG2 expression in WT mouse aorta. (B) TG cross-linking activity assayed by pentylamine-biotin incorporation into *N,N'*-dimethylcasein. Total protein lysates from WT and TG2^{-/-} mouse aorta were used. (C) Real-time PCR analysis showing expression of TGs in TG2^{-/-} mouse aorta compared to WT tissue. (*P ≤ 0.05; **P ≤ 0.005)

6.2 Heart

A role for TG2 in heart biology has been suggested by the finding that its activity is down-regulated in cardiac failure (Hwang et al., 1996) and by TG2-induced ventricular remodeling caused by cardiomyocyte-specific transgenic overexpression of TG2 (Small et al., 1999). In addition to TG2, heart tissue expresses FXIIIa at a level similar to TG2 along with lower levels of TG1 and TG3 (Fig. 2.10A). TG2-mediated transamidation

contributes to almost 60% of total transamidation activity as determined by KCC-009 inhibition (Table 2.1). Nevertheless, in TG2^{-/-} heart tissue total transamidating activity remains practically unchanged suggesting compensation by other TGs (Fig. 2.10B). In this tissue, transcriptional compensation by TG3, TG5 and TG6 is suggested by real-time PCR analysis (Fig. 2.10C). Further studies are needed to identify the cellular origin of elevated TG3, TG5 and TG6 expression in the TG2^{-/-} hearts.

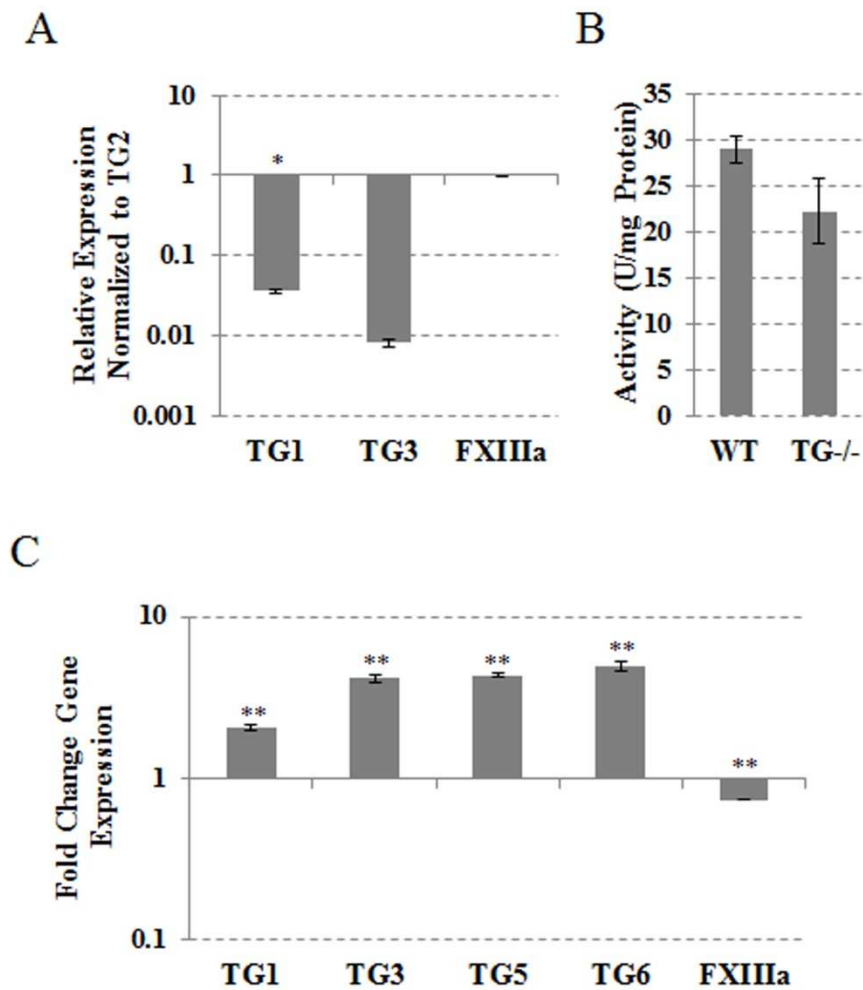


Figure 2.10 TG Expression and Activity in Mouse Heart Tissue. (A) Real-time PCR analysis showing expression of TGs compared to TG2 expression in WT mouse heart. (B) TG cross-linking activity assayed by pentylamine-biotin incorporation into *N,N'*-dimethylcasein. Total protein lysates from WT and TG2^{-/-} mouse heart were used. (C) Real-time PCR analysis showing expression of TGs in TG2^{-/-} mouse heart compared to expression in the WT tissue. (* $P \leq 0.05$; ** $P \leq 0.005$)

7. Compensation for TG2 loss in the kidney

TG2 has previously been shown to contribute to extracellular matrix accumulation by accelerating matrix deposition of collagens in kidneys (Fisher et al., 2009). In our studies we found TG2 to be the most abundantly expressed TG in the WT kidney followed by TG1 and low levels of TG3, TG5, TG6, and FXIIIa (Fig. 2.11A). In the kidney, TG2 contributed to approximately 44% of the transamidase activity as shown by KCC-009 inhibition (Table 2.1), with only a 25% reduction in transamidase activity in the TG2^{-/-} kidney (Fig. 2.11B). When examining expression of seven other enzymatic TGs we found that TG1 and FXIIIa were significantly up-regulated while TG6 was down-regulated (Fig. 2.11C), indicating that TG1 and FXIIIa could be functioning to compensate for the decreased transamidating activity in the TG2^{-/-} mice. However, further analysis is required to determine whether compensation is supported by an increase in transcription or proteolytic activation of TG1 and FXIIIa.

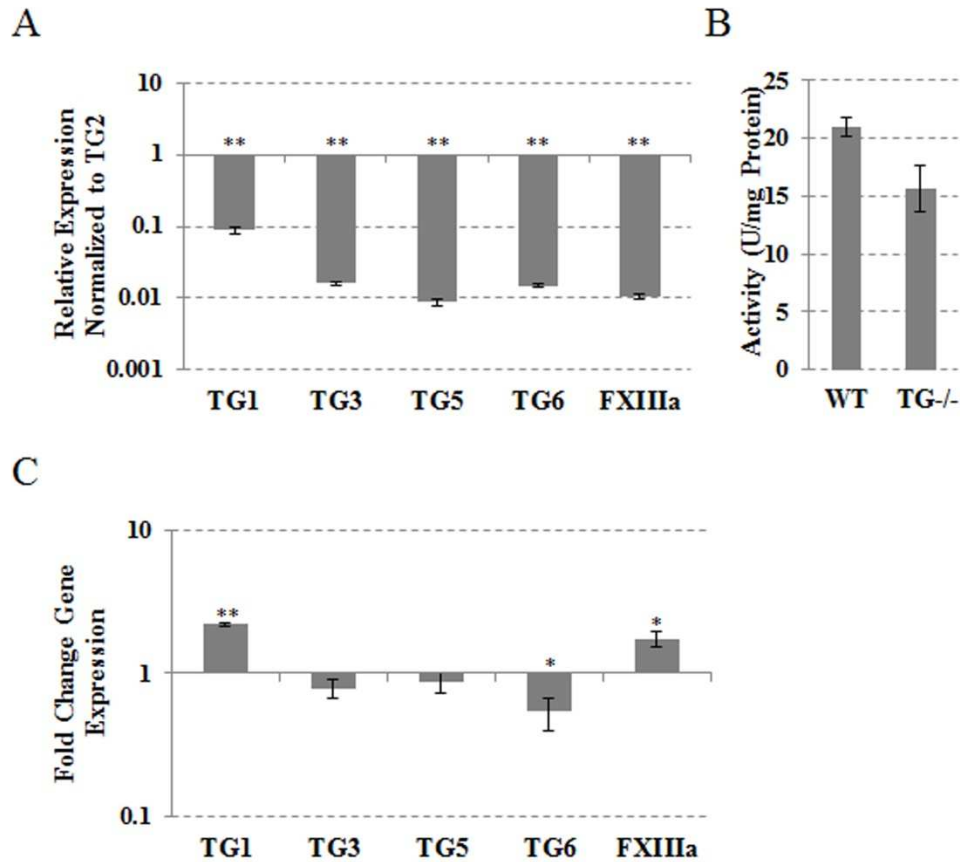


Figure 2.11 TG Expression and Activity in Mouse Kidney Tissue. (A) Real-time PCR analysis showing expression of TGs compared to TG2 expression in WT mouse kidney. (B) TG cross-linking activity assayed by pentylamine-biotin incorporation into *N,N'*-dimethylcasein. Total protein lysates from WT and TG2^{-/-} mouse kidney were used. (C) Real-time PCR analysis showing expression of TGs in TG2^{-/-} mouse kidney compared to expression in the WT tissue. (* $P \leq 0.05$; ** $P \leq 0.005$)

E. DISCUSSION

Of the eight catalytically active TGs, TG2 has been the most thoroughly studied due to its ubiquitous expression and association with numerous biological processes. Further, aberrant activation of TG2 has been associated with multiple pathologies such as Alzheimer's disease (Johnson et al., 1997), Celiacs Disease (Stenberg et al., 2008) and Cancer (Chhabra et al., 2009). This association of TG2 with both normal and pathological biological processes makes it critical to understand its underlying

mechanisms. To better understand the role of this enzyme, TG2 mouse knockout models were developed. Interestingly, despite TG2's association with numerous biological and pathological processes, TG2^{-/-} mice showed no severe developmental phenotype. This lack of phenotype in TG2^{-/-} mice was proposed to be due to a compensation mechanism between TGs.

In this study we performed a comparative expression analysis of TGs in several tissues from WT and TG2^{-/-} mice to better understand the potential of a compensation mechanism. We determined the total transamidating activity in each tissue and the level of contribution by TG2 to the activity and identified the presence of tissue-specific compensations mechanisms for the genetic ablation of TG2. Specifically, we observed transcriptional compensation in the liver, heart and kidney and functional compensation in the non-hypertrophic cartilage and aorta. Further, we proposed the presence of both transcriptional compensation by TG1 and TG3 and functional compensation by FXIIIa in the joint/ossifying cartilage. Lastly, we did not observe any significant compensation for loss of TG2 in the skeletal muscle, suggesting that TG2 is not enzymatically active in this tissue. This preliminary analysis of TG2^{-/-} mice identified potential transcriptional and functional compensation; however, further studies are required to better understand the underlying mechanisms of compensation.

In conclusion, our data reveal wide and varying patterns of expression and compensation for TGs, implicating an additional level of complexity in the biological functions of TGs. This additional complexity hinders the examination of the *in vivo* role of TG2 in several biological processes, specifically, for our studies on the role of TGs in bone formation, a tissue in which transamidating activity was unaffected by genetic

ablation of TG2. Therefore, to examine TGs *in vivo* role in bone and circumvent this complexity an alternative *in vivo* model needed to be adopted.

CHAPTER III: CHARACTERIZATION OF THE TRANSGLUATMINASE GENE FAMILY IN ZEBRAFISH AND *IN* *VIVO* ANALYSIS OF TRANSGLUTAMIANSE-DEPENDENT BONE MINERALIZATION²

A. ABSTACT

In this study we characterized protein cross-linking enzyme TG genes in zebrafish, *Danio rerio*, based on analysis of their genomic organization and phylogenetics. We identified thirteen zebrafish TG genes (zTGs), eleven of which showed high homology to only three mammalian enzymes - TG1, TG2 and FXIIIa. No zebrafish homologues were identified for mammalian TGs 3-7. Real-time PCR analysis demonstrated distinct temporal expression profiles for zTGs in larvae and adult fish. Further, analysis by *in situ* hybridization revealed restricted expression of zTG2b and zFXIIIa-87 to skeletal elements, similarly to the observed expression of their mammalian homologues in osteo-chondrogenic cells. Two mammalian TGs, TG2 and FXIIIa, have previously been implicated in osteoblast differentiation and bone mineralization *in vitro*, however mouse models lacking either gene show no skeletal phenotype likely due to a compensation effect. Here we examined the *in vivo* role of zTGs in bone development and show that mineralization of newly formed vertebrae is significantly reduced in fish grown for 5 days in the presence of TG-specific inhibitor KCC-009. This treatment

² CITATION: Deasey SC, Grichenko O, Du S, Nurminskaya M *Amino Acids* 2011
March 42:1065-1075

reduced average vertebrae mineralization by 30%, with complete inhibition in some fish, and had no effect on overall growth and vertebrae number. This is the first *in vivo* demonstration of the crucial requirement for the TG-catalyzed cross-linking activity in bone mineralization.

B. INTRODUCTION

The comprehensive identification and understanding of both systemic and local bone anabolic factors is essential for the development of new therapeutic targets to treat bone diseases and fractures. Previous *in vitro* studies from ours and other groups have demonstrated that enzyme TGs promote osteoblast differentiation and enhance deposition of mineralized matrix (Aeschlimann et al., 1993; Nurminskaya et al., 2003). TGs (R-glutamylpeptide: amine γ -glutamyl transferases, EC 2.3.2.13) are multifunctional Ca^{2+} dependent proteins that are crucial for the formation of ϵ -(γ -glutamyl)-lysine-protein cross-links (Lorand and Graham, 2003).

Two mammalian TGs, TG2 and FXIIIa, have been reported to be up-regulated in the osteo-chondrogenic lineage (Aeschlimann et al., 1993; Nurminskaya and Linsenmayer, 1996; Borge et al., 1996; Rosenthal et al., 1997; Nurminskaya and Linsenmayer, 1996; Summey, Jr. et al., 2002; Al-Jallad et al., 2006). Both enzymes are expressed in pre-hypertrophic and hypertrophic chondrocytes of the growth plate and in the “borderline chondrocytes” that are localized to the lateral edges of the growth plate (Nurminskaya and Kaartinen, 2006). These “borderline chondrocytes” are thought to regulate the formation of the bony collar (Bianco et al., 1998), suggesting that extracellular chondrocyte-derived TGs may mediate the coordination of osteoblast and chondrocyte differentiation - a key event in proper bone formation (Karsenty and

Wagner, 2002). This hypothesis has been confirmed *in vitro* by the ability of TG2 and FXIIIa to promote osteoblast differentiation (Nurminskaya et al., 2003;Becker et al., 2008) and osteoblast-like transformation in vascular smooth muscle cells (Faverman et al., 2008). Despite strong *in vitro* evidence, genetic ablation of either enzyme shows no skeletal phenotype in mouse models (Nanda et al., 2001;Lauer et al., 2002;Koseki-Kuno et al., 2003). A plausible explanation for the discrepancy between *in vitro* and *in vivo* studies takes into account the functional redundancy between TGs due to a high similarity in substrate specificity (Achyuthan et al., 1996), and as a result, there is a compensation for loss of each isoform by other TGs in embryonic development. Our studies have shown maintenance of transamidating activity in skeletal tissue of TG2^{-/-} mice demonstrating the presence of a compensation mechanism in this tissue (Deasey et al., 2013b).

To overcome complications associated with this compensation mechanism in the genetic loss-of-function mammalian models and to obtain insight into the role of TG-mediated cross-linking in bone formation *in vivo*, we employed the zebrafish, *Danio rerio*, model for analysis of bone development. Several physiologic features, such as early transparency, short maturation period, and high reproductive capacity, make this model ideal for studying developmental processes (Brittijn et al., 2009). Additionally, numerous zebrafish developmental mechanisms, including bone development, share common factors with mammalian systems. Furthermore, the presence of orthologues for genes commonly seen in human diseases makes zebrafish especially useful for preliminary *in vivo* drug studies (Brittijn et al., 2009). However, transglutaminase enzymes in zebrafish have not been studied on either a genetic or functional level.

In the present study, we analyzed the zebrafish genome for zTG genes, and identified thirteen isoforms, eleven of which are highly similar to one of the three human TGs (hTGs) - hFXIIIa, hTG2 and hTG1. Taking into consideration that two of these mammalian homologues have been implicated in the regulation of mammal tissue calcification, we analyzed regulation of bone formation in zebrafish in which total transamidating activity was inhibited during vertebrae mineralization. Our study demonstrates a crucial role for TG-mediated cross-linking in bone calcification *in vivo*.

C. MATERIALS AND METHODS

1. BLAST Search, Sequence Alignments and Phylogenetic Analysis

NCBI database of *Danio rerio* protein sequences was searched with the blastp algorithm using the NCBI Blast server. We aligned the sequences with CLUSTAL-W (<http://www.ebi.ac.uk/Tools/clustalw2>) and constructed a phylogenetic tree using maximum parsimony algorithm with protpars tool in the PHYLIP 3.5 package (<http://www.es.embnnet.org>). We also aligned sequences and constructed a phylogenetic tree using the COBALT tool at NCBI (<http://www.ncbi.nlm.nih.gov/tools/cobalt>). Further, we used the phylogeny.fr package (<http://www.phylogeny.fr/version2.cgi/index.cgi>) for alignment and phylogenetic analyses.

2. Embryo Generation and Maintenance

WT zebrafish were maintained at the zebrafish facility of the Aquaculture Research Center, Center of Marine Biotechnology University of Maryland, as previously described (Du et al., 2001). Embryos were obtained from natural mating, staged according to morphology or by days post fertilization (dpf), and kept at 28.5°C on a 14 hour light 10 hour dark cycle. During inhibitor treatment zebrafish larvae were kept in 6-well plates

with 5 fish in 5mL of water per well. Inhibitors were dissolved to a stock concentration of 10mM in 100% Dimethyl Sulfoxide (DMSO) (Sigma) and added directly to the fish water to a final concentration of 30 μ M. Fish water, supplemented with paramisol and inhibitor, was changed once per day.

3. *Ex vivo* Identification of TG Cross-Linking Activity in Zebrafish

Transglutaminase cross-linking activity in zebrafish was visualized *ex vivo* by incubation with 5mM rhodamine-conjugated synthetic substrate Pro-Val-Lys-Gly (SY2011) (Kim et al., 1997) in PBS for 4 hours at 28°C. Zebrafish were then washed with PBS and left overnight, to allow all unincorporated substrate to diffuse out, at room temperature (RT) in PBS. Zebrafish then were fixed in 4% PFA at RT for 2 hours. Images were acquired by a Leica DMIL FLUO microscope equipped with a SPOT RT slider real-time CCD camera (Diagnostic Instruments, Inc.).

4. Whole Mount *In Situ* Hybridization

A detailed description of the whole mount *in situ* hybridization protocol is provided in Appendix A.6. Embryos were fixed in 4% PFA and bleached with 3% Hydrogen Peroxide in 0.5% Potassium Hydroxide in PBS-T for 15 minutes. This was followed by Proteinase K (Novagen) digestion (10 μ g/mL) for 30 minutes, second fixation in 4% PFA and acetone treatment for 8 minutes at -20°C. The DIG-labeled antisense RNA probes (Detailed description DIG-RNA probe preparation in Appendix A.7) were used at 2ng/ μ L concentration in hybridization buffer. Hybridized DIG-RNA probes were detected with an anti-DIG fab fragments antibody fused to alkaline phosphatase (Roche) at a 1:4000 dilution followed by colorimetric assay with NBT/BCIP solution (Roche) in the dark for

24-72 hours until color developed. Staining progression was monitored with Nikon AZ100 microscope and analyzed with Nikon Elements software.

5. Real-Time PCR

Total RNA was isolated from unfertilized eggs, 4dpf, 13dpf and torso of adult zebrafish with Trizol reagent (Invitrogen) (Detailed description of RNA isolation in Appendix A.1) and used for first-strand cDNA synthesis (Detailed description of first strand cDNA synthesis in Appendix A.3). Primers for zTGs were designed using NCBI primer design software (Table of primers in Appendix B.2). Real-time PCR was run on a Roche LightCycler 480 II following the manufactures instructions for heat activation, amplification and melting curves for 45 cycles (Detailed description of real-time PCR in Appendix A.8). Expression levels were normalized to β -actin mRNA.

6. TG Activity Assay

Total TG cross-linking activity in whole fish lysates was assayed by incorporation of the biotinylated pentylamine Ez-link Pentylamine-Biotin (Pierce) into *N,N'*-Dimethylcasein (Sigma-Aldrich) in the ELISA-like assay as previously described (Trigwell et al., 2004). 96-well microtiter plates (Maxisorp NUNC) were incubated overnight with 250 μ l of 1mg/mL *N,N'*-Dimethylcasein (Sigma-Aldrich) in 5mM Sodium Carbonate (pH 9.8), and blocked with 200 μ L of 0.1% bovine serum albumin (BSA) (HyClone) in 5mM Sodium Carbonate (pH 9.8) for one hour at 37°C. Whole 14dpf zebrafish mated larvae were lysed (Detailed description of protein lysis in Appendix A.5) centrifuged and TG-containing supernatant was used for further assays. Purified gpITG2 (Sigma-Aldrich) was used as a standard for activity tests. For inhibitory studies, zebrafish lysates (20ng total protein) or purified gpITG2 (75ng purified protein) were pre-incubated with 100 μ M

inhibitors for one hour at 28°C. Reaction was carried out in 100mM Tris-HCl pH 8.5, 6.7mM CaCl₂, 13.3mM DTT and 2.5mM Ez-link Pentylamine-Biotin (Pierce) for one hour at 37°C. Incorporated Ez-link Pentylamine-Biotin was detected with 1:5000 ExtrAvidin-Peroxidase (Sigma) and Super AquaBlue ELISA Substrate (eBioscience) followed by reading the absorbance at 405nm on a Polarstar Optima plate reader.

7. Calcein Staining of Mineralized Vertebrae

Protocol was adapted from Du *et al.*, 2001. Zebrafish were transferred from fish water to 0.03% Calcein Stain (Sigma) in water, pH 7, and incubated in the dark for 10 minutes at RT. Fish were washed in fish water (0.3g/L aquarium salt) and then transferred into fish water and incubated for 10 minutes in the dark at RT. After incubation zebrafish were euthanized with 150mg/L Tricaine (Sigma) and mounted in 3% methyl-cellulose. Images of the fluorescently stained vertebrae were taken 5 minutes after staining to avoid bleaching. Photos were taken with a Leica DMIL FLUO microscope equipped with a SPOT RT slider real-time CCD camera (Diagnostic Instruments, Inc.). Intensity of the calcein staining was analyzed for each vertebra with Photoshop.

8. Data and Statistical Analysis

Data was collected and analyzed by both Microsoft Excel and Photoshop. Statistical significance was calculated by the student's T-test and the error bars demonstrate the standard error mean.

D. RESULTS

1. Identification of Zebrafish TG Genes

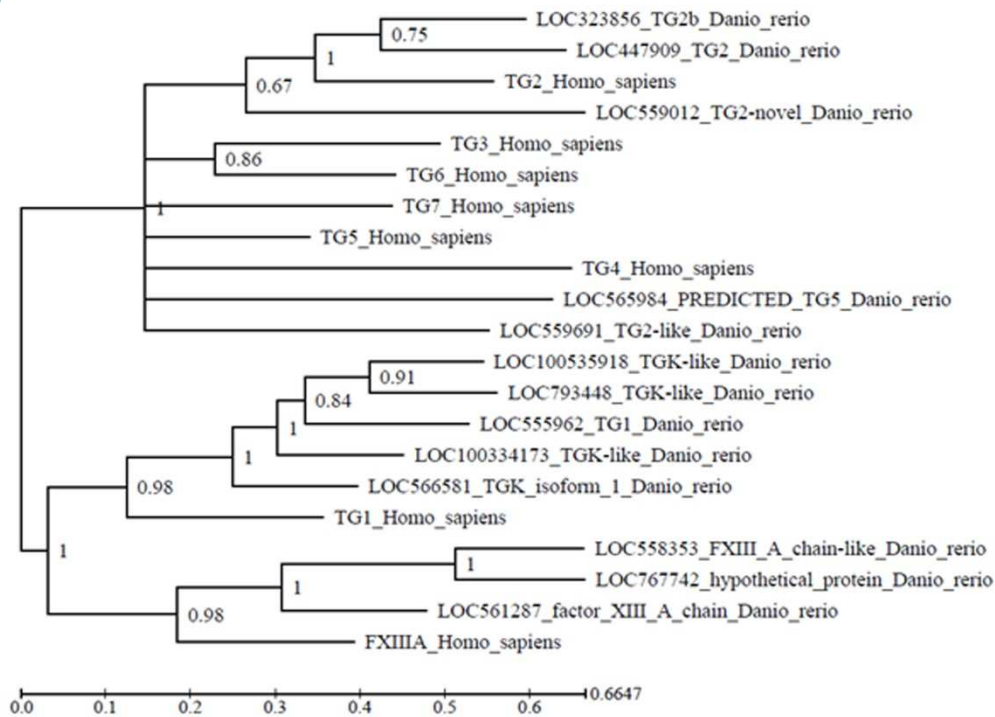
To identify zTG genes we analyzed the current version of the NCBI zebrafish proteome database by blastp searches. By using hTG1, hTG2, hTG4, and hFXIIIa

protein sequences as queries, we found the same set of fourteen homologous zebrafish proteins. Among these, one protein and corresponding gene LOC793095 initially described as a partial TG-homologous sequence was removed from the genome assembly as not supported by sufficient evidence. Consistent with this, we did not detect expression of this gene throughout zebrafish development by real-time PCR. Therefore, our analysis identified thirteen zTGs.

To further clarify phylogenetic relationship between the identified zTGs and human TGs (hTGs), we performed multiple alignments of protein sequences and constructed phylogenetic trees using the following approaches: (1) TG sequences were aligned with CLUSTAL-W and a phylogenetic tree was constructed using maximum parsimony algorithm with protpars tool in the PHYLIP 3.5 package, (2) sequence alignment and phylogenetic tree construction were done using the COBALT tool at NCBI and (3) phylogeny.fr package was used to align the sequences using the MUSCLE tool and to employ the maximum likelihood or neighbor-joining algorithm to construct the trees and analyze them with bootstrapping (1,000 iterations), or alternatively to use the Bayesian tree building algorithm with 1,000 iterations and burnin parameter of 50. All of these approaches resulted in the same tree configuration (a representative Bayesian tree is shown in Fig. 3.1A). We found that five zTGs (LOC's 793448, 100535918, 555962, 100334173, and 566581) are strikingly close to each other and hTG1 and probably originated by gene amplification after divergence of their common ancestor from hTG1. Also, three zTGs (LOC's 558353, 767742, and 561287) are similar to each other and hFXIIIa, this group of zTGs also originated by a relatively recent gene amplification after their common ancestor diverged from hFXIIIa. Further, three zTGs are similar to hTG2.

Among these, two genes (LOC's 323856 and 447909) originated after their common ancestor split from hTG2, and the third (LOC559012) is more ancient. Finally, two zTGs have been annotated as zTG2-like (LOC559691) and zTG5 (LOC565984) (Fig. 3.1A). However, these zebrafish proteins are similarly distant from all hTGs based on pair wise comparisons (Fig. 3.1B) and their association with hTG2 and hTG5 as suggested by annotations, or with other hTGs, is not supported by phylogenetic analysis. Therefore, based on this sequence analysis these two zTGs should be considered novel TG isoforms, and we refer to these henceforth as zTG-91 and zTG-84. A list of gene names and gene abbreviations is supplied in Table 3.1.

A



B

Percent Similarity Between Human and Zebrafish TGs								
	hTG1	hTG2	hTG3	hTG4	hTG5	hTG6	hTG7	hFXIII
LOC559691 TG2-like	53	57	56	54	55	58	54	52
LOC565984 TG5	52	54	54	51	57	54	52	52

Figure 3.1 Phylogenetic Analysis of Zebrafish TGs. (A) Phylogenetic tree depicting the evolutionary relationships among TG genes of *Danio rerio* and human origin as established by the Bayesian tree building algorithm. Only three out of nine mammalian TGs have an overt zebrafish homologue, including *TG2*, *FXIIIa* and *TG1*. (B) Table showing the similarity between the two novel zTGs, LOC559691 TG2-like and LOC565984 TG5, and human TGs.

Gene Name	Gene Abbreviation
LOC555962 TG1	zTG1-62
LOC793448 TGK-like	zTG1-48
LOC100535918 TGK-like	zTG1-18
LOC566581 TGK isoform 1	zTG1-81
LOC100334173	zTG1-73
LOC323856 TG2b	zTG2b
LOC559012 TG2-novel	zTG2-12
LOC447909 TG2	zTG2c
LOC767742 hypothetical protein	zFXIIIa-42
LOC558353 FXIIIa chain-like	zFXIIIa-53
LOC561287 FXIIIa chain	zFXIIIa-87

Table 3.1 Abbreviations for each of the zTGs in zebrafish.

The chromosomal arrangement of zTG genes (Fig. 3.2A; schematic diagram of the chromosomal arrangements of TG genes in human and zebrafish genomes is shown in Fig 3.2B) is dramatically different from TGs gene clustering pattern in humans (Grenard et al., 2001) where hTG2, hTG3 and hTG6 form a cluster on chromosome 20, hTG5 and hTG7 are clustered on chromosome 15, and hTG1, hTG4 and hFXIIIa are present on different chromosomes. In zebrafish, the TG1-like TG genes are located on two chromosomes. The most ancient gene zTG1-81 (LOC566581) is located on chromosome 2, and the other four genes are located on chromosome 23. Among these, the two most recently diverged genes zTG1-18 (LOC100535918) and zTG1-48 (LOC793448) are separated by 1 Mb, and the others are located more distantly (Fig. 3.2A-B). A similar arrangement exists for the FXIIIa-like transglutaminases, where the most ancient gene zFXIIIa-87 (LOC561287) is located on chromosome 7 and the two recently diverged

genes zFXIIIa-like (LOC558353) and zFXIIIa-42 (LOC767742) are both located on chromosome 24 separated by a mere 7 kb. In contrast, all three zTG2 genes are located on different chromosomes with the most ancient zTG2 gene zTG2-12 (LOC559012) being located on chromosome 18, and zTG2b (LOC323856) on chromosome 6 versus zTG2c (LOC447909) on chromosome 23 despite their recent divergence. The remaining zTG genes that are not closely related to other hTGs, zTG-84 and zTG-91 (LOC565984 and LOC559691), are located on the opposite ends of chromosome 6. All zTG genes have introns and hence are not likely the products of retrotranspositions. Thus, the expansion of the TG2-like subfamily and initial expansions of the TG1-like and FXIIIa-like subfamilies in zebrafish may be associated with gene duplications and inter-chromosomal rearrangements, while further amplification of the FXIIIa-like and TG1-like genes probably occurred by local gene duplications which in the case of TG1-like genes were followed with intra-chromosomal rearrangements. These findings, and the absence of overt *TG3*, *TG4*, *TG5*, *TG6* and *TG7* homologues in zebrafish, raise a possibility that amplification of hTG genes occurred after the evolutionary split between these species. Accordingly, it appears that the expansion of the TG1-like, TG2-like, and FXIIIa-like gene families in zebrafish occurred independently during the same time period.

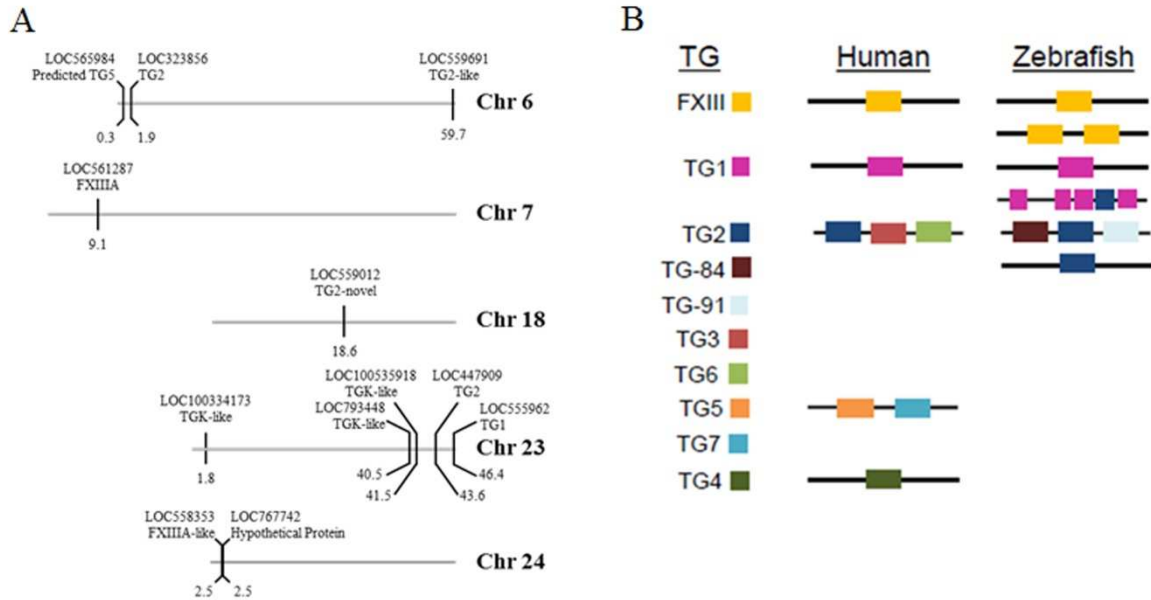


Figure 3.2 Analysis of Genomic Organization of zTGs. (A) Chromosomal arrangement of zebrafish TG genes. (B) Color-coded schematic of chromosomal clustering of TGs in both human and zebrafish.

2. Expression and Activity of TGs in Zebrafish

The expression profiles for all identified zTG genes were analyzed by real-time PCR in embryonic and adult fish. Since our study aimed to determine the role of zTGs in bone calcification which begins around 5 days post fertilization (dpf) and by 16dpf calcification of all vertebrae can be visualized with vital calcein staining (Du et al., 2001), we analyzed expression of zTGs in 4dpf larvae just before the initiation of vertebral calcification, and in 13dpf larvae when most vertebrae have already been calcified. In addition, expression levels for zTG genes were analyzed in adult torso representing homeostatic bone. Expression of each zTG was normalized to the housekeeping β -actin gene and compared to unfertilized eggs. This analysis identified five zTGs (zFXIIIa-87, zTG2c, zTG2-12, zTG1-81, and zTG1-73) induced in larvae as compared to non-fertilized eggs, but almost completely silenced in adulthood (Fig 3.3A),

implicating their involvement in developmental processes. In contrast, zFXIIIa-53 and zFXIIIa-42 are both up-regulated in adult tissue (Fig. 3.3B), suggesting a putative role for these enzymes in body homeostasis rather than in growth and development. A minor role in fish growth and development is also suggested for two zTG1 genes - zTG1-62 and zTG1-18 - based on their dramatic down-regulation after fertilization (Fig 3.3A). No expression was detected by real-time PCR analysis for zTG1-48 at any stage (data not shown), implicating that this locus maybe a silent pseudogene, however more detailed studies are required to test this further. Conversely, novel genes zTG-84 and zTG-91, in addition to zTG2b, are almost ubiquitously expressed in zebrafish tissues at all analyzed stages (Fig. 3.3B, zTG-84 is not included in the figure because all data in this figure is normalized to non-fertilized eggs in which zTG-84 is not expressed), resembling the ubiquitous expression of mammalian TG2 enzyme. The most noticeable distinction between these three ubiquitous zTGs is the complete absence of zTG-84 transcript in the non-fertilized eggs, suggesting a minimal role in early embryogenesis.

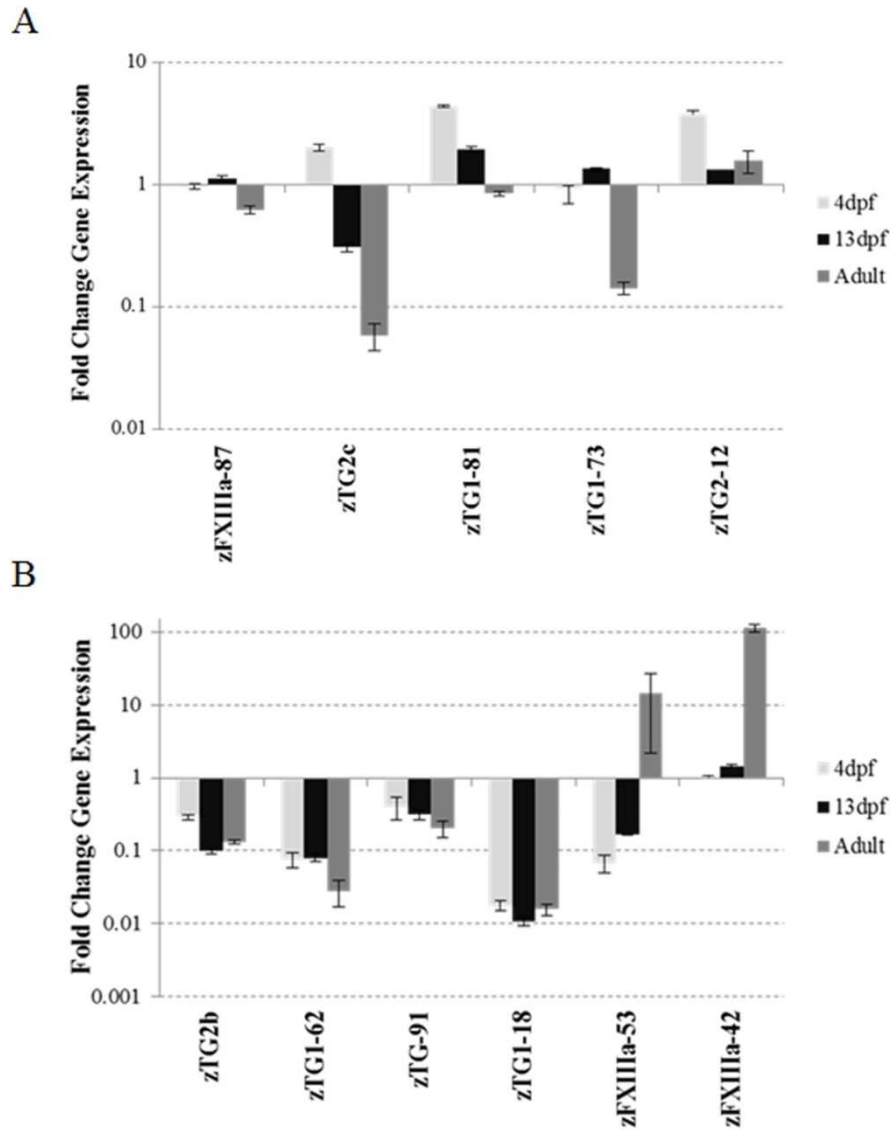


Figure 3.3 Expression Patterns of zTGs During Zebrafish Development. Real-time PCR analysis was used to determine zTGs expression pattern. Whole bodies were used for analysis at 4dpf, 13dpf and the torso from adult zebrafish. Data was normalized to β -actin and compared to unfertilized eggs. (A) Real-time PCR showing zTG up-regulated genes during development (in 4 and 13dpf zebrafish). (B) Real-time PCR analysis showing the zTG genes that have either little change in expression during development or significant up-regulation in adult fish.

3. Localization of zTG Expression by *In Situ* Hybridization

The expression data from the real-time PCR analysis was expanded by *in situ* hybridization studies on 2-3dpf zebrafish. Although many zTGs were not detectable at

these stages by *in situ* hybridization indicating relatively low levels of expression, expression of several genes was observed in a tissue-specific pattern (Fig. 3.4 top panel). zTG2c expression was restricted to muscles while zTG1-81 was expressed in the muscle and, likely, in the notochord. Expression of zTG2b was restricted to notochord and zFXIIIa-87 was detected in the pectoral fin. Sense RNA probes were used as negative controls (Fig. 3.4 bottom panel). The identified muscle-specific expression of zTG1-81 and zTG2c in 2-3dpf fish suggests a role for these enzymes in muscle development. While zTG2c has been detected in the muscle even earlier, at 1 dpf fish (ZFIN (<http://zfin.org/cgi-bin/webdriver?Mlval=aa-xpatsselect.apg>), further analysis is needed to investigate in more detail the stage-specific and muscle-type specific expression of zTG1-81. A novel finding of our study is the notochord-specific expression of zTG2b in 2-3 dpf fish. Earlier in development, at 1dpf, this gene is ubiquitously expressed throughout the embryo (ZFIN (<http://zfin.org/cgi-bin/webdriver?Mlval=aa-xpatsselect.apg>), suggesting that it may be expressed in the progenitor cells which give rise to the osteo-chondrogenic lineage. This pattern of expression corresponds to that seen for the TG2 gene in avian mesenchymal limb bud cells (Nurminsky et al., 2011) and suggests a role for this enzyme in skeletal formation. In addition, expression of zFXIIIa-87 was detected in the developing fins, which are enriched with skeletal elements, implicating this enzyme in bone formation.

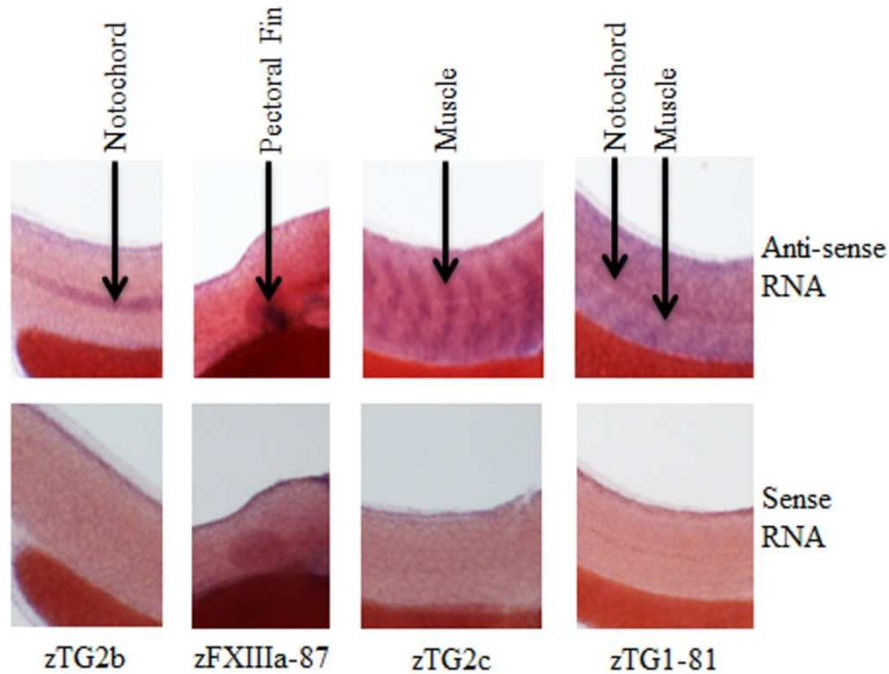


Figure 3.4 Tissue Specific Expression of zTGs in 2-3dpf Zebrafish. Representative images from whole mount *in situ* hybridization for zTG2b, zFXIIIa-87, zTG2c, and zTG1-81 showing the tissue-specific expression patterns for zTGs (top) and the negative control with sense probes (bottom).

To determine whether zTGs expressed in the skeletal and muscle tissue are enzymatically active, we employed a rhodamine-labeled peptide Pro-Val-Lys-Gly, SY2011, which is a substrate for TGs (Kim et al., 1997). Decapitated fish were incubated with 5mM SY2011 for *ex vivo* incorporation through TG-mediated cross-linking. Incorporated peptide was visualized by rhodamine fluorescence to detect tissue with active zTGs. In agreement with the results of *in situ* hybridization, SY2011 was cross-linked into striated muscles of the torso, into periosteal bone of the vertebrae and in the in large blood vessels (Fig 3.5). Together, these results demonstrate the presence of enzymatically active zTGs in the developing skeleton of zebrafish justifying this organism as a good model to analyze the role of TGs in bone formation.

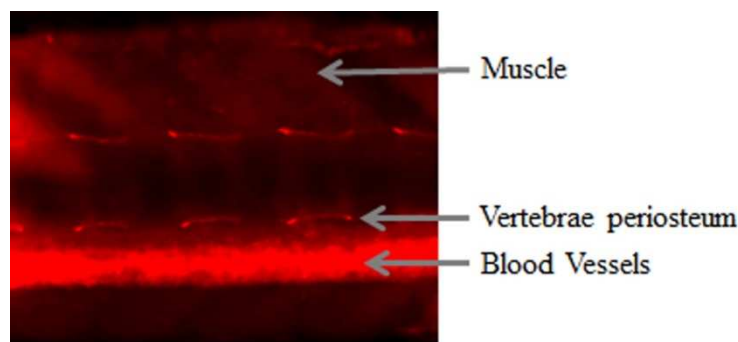


Figure 3.5 zTG Catalytic Activity in Zebrafish Larvae. *Ex Vivo* incorporation of synthetic rhodamine-labeled synthetic TG peptide substrate Pro-Val-Lys-Gly, SY2011. SY2011 was incorporated into zebrafish ossifying vertebrae, blood vessels and muscle.

4. KCC-009 is a Potent Inhibitor of zTG Cross-Linking Activity in Zebrafish Tissues

To analyze the role for TG-mediated cross-linking in bone formation, we employed a pharmacologic approach to inhibit total catalytic activity of TGs with a small molecule inhibitor KCC-009 which inhibits the deamidation step of the cross-linking reaction (Choi et al., 2005;Poster et al., 1981). Using a pentylamine-based activity assay, we tested KCC-009's potency for inhibiting total TG cross-linking activity in total tissue lysates from 19dpf zebrafish. Purified guinea pig liver TG2 was used as a control in these studies, which demonstrated the complete inhibition of the TG-mediated cross-linking in zebrafish tissues (Fig. 3.6). We also found that KCC-009 was able to inhibit protein cross-linking in adult tissue extracts (data not shown), indicating that it can be used to study the role of TGs both in fish development and adult tissue homeostasis.

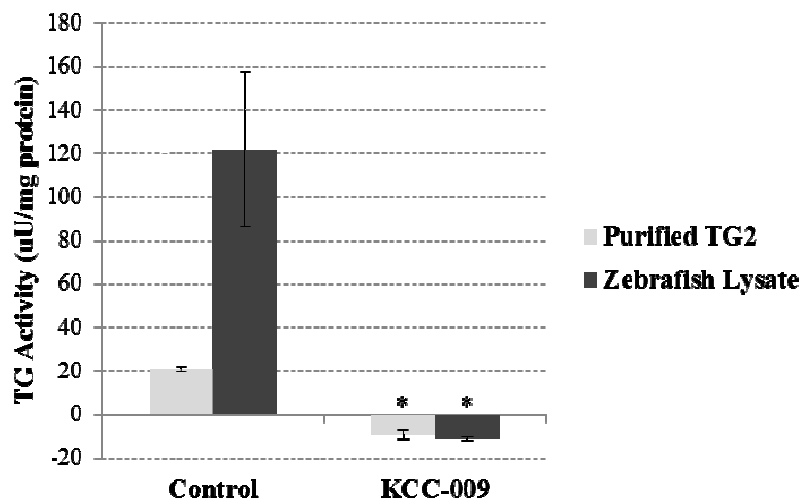


Figure 3.6 KCC-009 Inhibits Total TG Activity in Zebrafish. *In vitro* TG cross-linking activity assayed by pentylamine-biotin incorporation into *N,N'*-dimethylcasein. Total protein lysates from 14dpf zebrafish were used. To inhibit TG activity, samples were pre-incubated for 1 hour at 28°C with KCC-009. Purified guinea pig liver TG2 (Sigma) was used as positive control (* $P \leq 0.05$).

In vivo, KCC-009 showed low toxicity in mice and cancer xenografts (Choi et al., 2005; Yuan et al., 2007; Satpathy et al., 2009). Similarly, KCC-009 had no toxic effects on zebrafish as evident by unaffected viability (Fig. 3.7A), total vertebrae number (Fig 3.7B) and standard length (SL) as a reflection of development (Parichy et al., 2009) (Fig. 3.7C) in zebrafish treated with 30 μ M KCC-009 for 5-6 days when treatment was initiated before 6dpf.

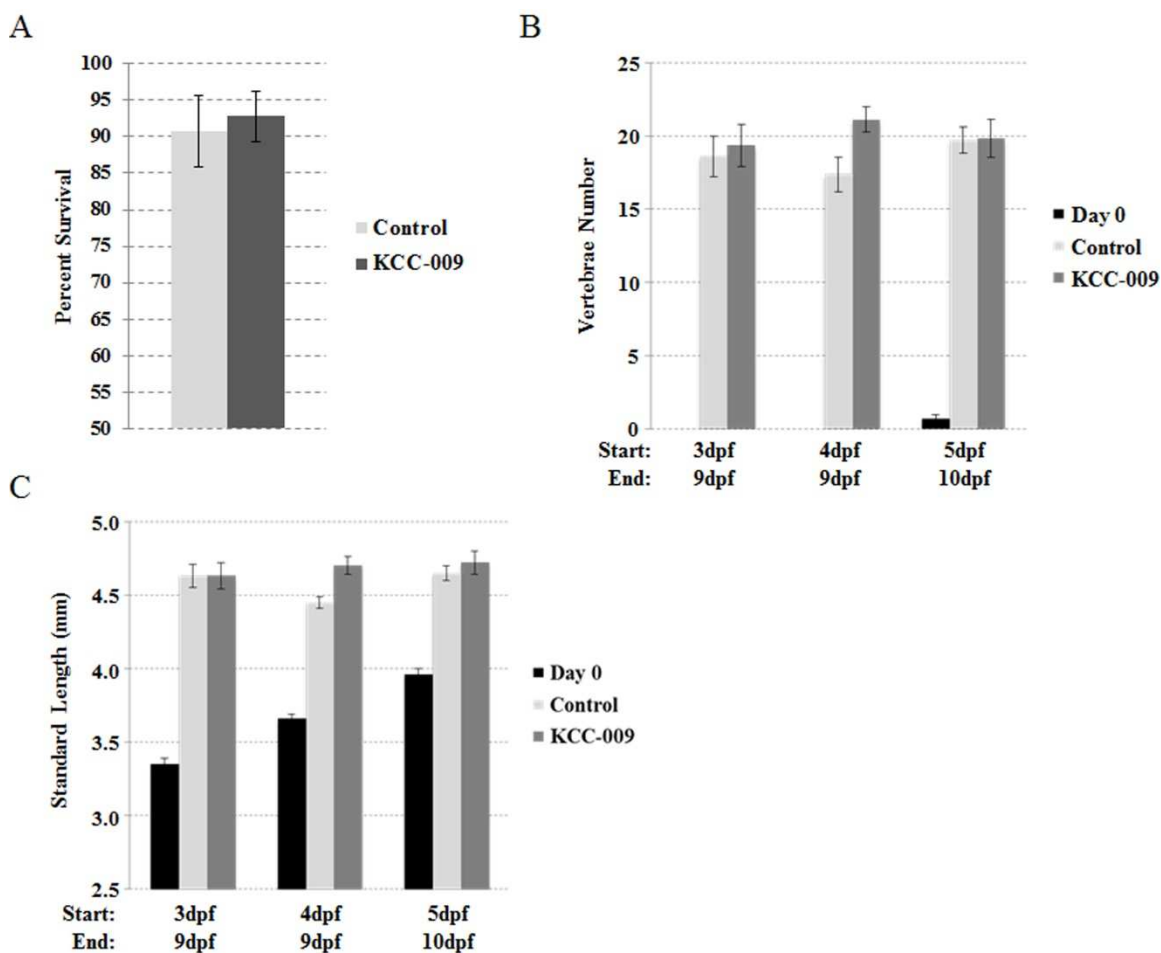


Figure 3.7 KCC-009 Shows No Toxicity in Zebrafish. Toxicity of KCC-009 treatment was analyzed by comparing the (A) average survival percent, (B) average total vertebrae number and (C) standard length in millimeters (Day 0 black bar, Control at 9/10dpf light grey bar and KCC-009 treated at 9/10dpf dark grey bar in b and c) for the untreated control zebrafish and fish grown for 5-6 days in the presence of 30 μ M KCC-009. N=9-16 per time point (*P \leq 0.05).

5. *In Vivo* Inhibition of zTG Activity with KCC-009 Hinders Bone Formation

In order to analyze the role of TGs in bone formation, we grew zebrafish in the continuous presence of 30 μ M KCC-009 over 5 days starting at 3-5dpf. Control fish were grown in the presence of 0.3% DMSO which served as the vehicle for KCC-009. Bone mineralization was analyzed by *in vivo* calcein staining (Du et al., 2001). A representative pair of calcein stained vertebrae for both the control and KCC-009 treated

zebrafish is shown in Fig. 3.8A, demonstrating the dramatic decrease in vertebrae mineralization for the KCC-009 treated group. Quantitative analysis of calcein staining intensity of mineralized vertebrae revealed a significant average decrease of 30% in mineralization for KCC-009-treated fish (Fig 3.8B; * $p < 0.05$, $n = 45$), although there was a high variation in the degree of KCC-009 induced reduction in vertebrae calcification. Due to KCC-009's potent ability to inhibit the cross-linking activity of all zTGs (Fig 3.6), these results suggest that TG-mediated cross-linking plays a critical role in vertebrae ossification.

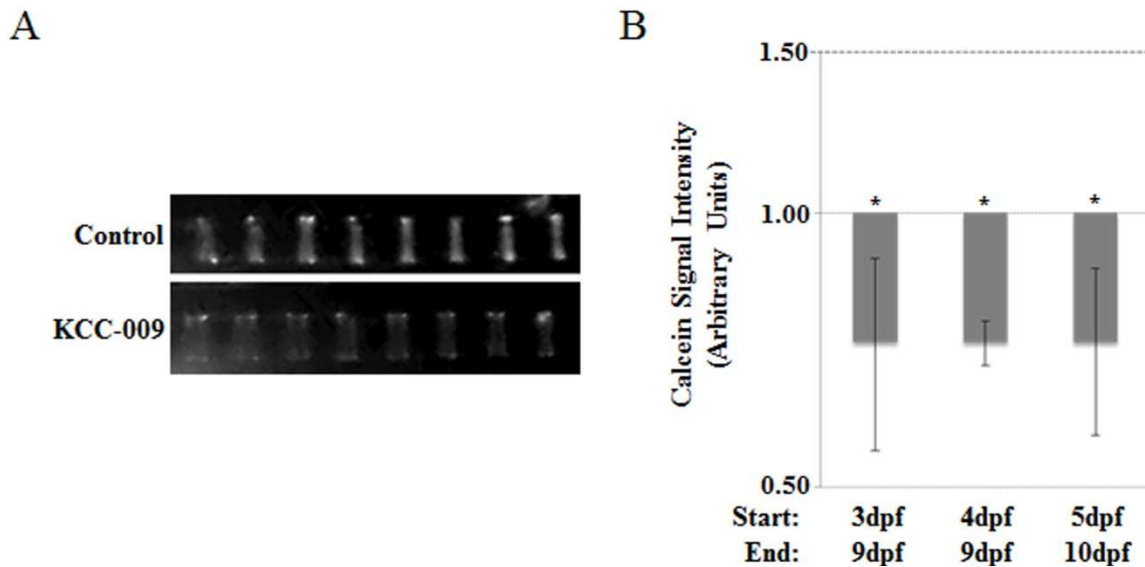


Figure 3.8 Inhibition of TGs Reduces Vertebrae Mineralization. Zebrafish were grown for 5-6 days starting at 3-5dpf in the presence of 30 μ M KCC-009. (A) Representative calcein stained images of zebrafish, Control (top) and KCC-009 (bottom) treated fish, KCC-009 treatment started at 3dpf and images taken at 9dpf, shown in grayscale. (B) Average change in calcein staining intensity per vertebra in the presence of KCC-009. Intensity of calcein staining for each vertebra was determined with Photoshop. $N = 16$ fish for 5dpf treatment, 9 for 4dpf treatment and 20 for 3dpf experiment. (* $P \leq 0.05$)

E. DISCUSSION

In this study, we characterized the zebrafish family of TG genes, *Danio rerio*. We identified thirteen zTG genes homologous to mammalian TGs, of which five are homologous to hTG1, three are homologous to hTG2 and three show homology to hFXIIIa, as revealed by phylogenetic analysis. Two zebrafish TGs show little similarity to any hTGs and have therefore been classified as novel TGs with the names zTG-84 and zTG-91, in spite of previous annotations for these genes as homologues of hTG5 and hTG2.

The expression pattern of zTGs analyzed at 4dpf, 13dpf and in adult fish by real-time PCR shows ubiquitous expression of zTG-84, zTG-91 and zTG2b genes, resembling the ubiquitous expression of mammalian TG2 enzyme, which is implicated in many biological processes including bone formation. In addition, zFXIIIa-87, zTG2c, zTG1-81, zTG1-73, and zTG2-12 are up-regulated during stages of development that are significant to bone mineralization, implicating a potential role in bone development. Our data from *in situ* hybridization further supports this hypothesis by demonstrating the notochord-specific expression of zTGb, restricted expression of zFXIIIa-87 to the pectoral fins and presence of zTG1-81 RNA in the notochord. In contrast, mRNA for zTG2c was identified only in skeletal muscle in agreement with earlier studies (Thisse et al., 2004) and supporting specificity of this analysis. Although RNAs for several zTGs were not detected by *in situ* hybridization in this study, likely due to low levels of their expression, the data obtained clearly demonstrates expression of TG2 and FXIIIa genes in the skeletal tissues. Mammalian homologues of these genes have been implicated as

potent regulators of osteoblast differentiation *in vitro* (Nurminskaya et al., 2003;Becker et al., 2008), supporting a notion that TGs may also regulate bone development *in vivo*.

The original finding of this study is the demonstrated reduction in vertebrae mineralization in zebrafish grown in the presence of KCC-009, a TG-specific irreversible acivicin-derived inhibitor. No signs of general toxicity were observed in zebrafish grown from 3-4dpf until 9-10dpf in KCC-009-treated water, suggesting that tissue-specific inhibition of TG-mediated cross-linking in the skeleton underlies this effect. Our initial *in situ* hybridization analysis on 2-3dpf fish identified expression of three zTG genes in skeletal tissues - zTG2b, zFXIIIa-87 and zTG1-81. However, other zTGs may also be expressed in mineralizing bone later in development, and this should be studied in more detail for comprehensive understanding of the molecular control of tissue calcification. Although the demonstrated importance of zTG activity in vertebrae mineralization is an important contribution towards this goal, the weak selectivity of KCC-009 toward individual zTGs is a limitation of this study. The KCC-009 compound efficiently inhibits total TG activity in zebrafish lysates in which expression of at least nine isogenes have been identified at each analyzed stage of growth. This precludes identification of individual zTG roles in the regulation of bone calcification. Further genetic studies could prove advantageous as they may allow for identification of individual zTG roles in this process; however, it is possible that a compensation mechanism may occur in zebrafish similarly to mice making genetic studies impracticable.

Comprehensive understanding of the molecular mechanisms that govern osteoblast maturation and calcification of bone matrix is crucial to develop novel therapeutics for bone disease. Bone tissue homeostasis requires a delicate balance

between bone formation by osteoblasts and bone resorption by osteoclasts, which is disrupted in osteoporosis. The current approach to treatment for osteoporosis relies on anti-resorptive agents to inhibit osteoclast function but do not restore bone mass (Rawadi, 2008). This study provides *in vivo* evidence for the critical role of TG-mediated cross-linking in bone mineralization, which could lead to a new therapeutic target in osteoporosis and other bone diseases. Furthermore, this study demonstrates the value of the zebrafish model for *in vivo* analysis of the multiple biological roles of transglutaminases proposed by *in vitro* or correlative studies, including various developmental processes and disorders such as neurodegenerative, skin and ocular pathologies as well as cancer (Mione and Trede, 2010).

CHAPTER IV: TRANSGLUTAMINASE ACTIVITY IN THE REGENERATIVE BLASTEMA CONTRIBUTES TO BONE REGENERATION IN THE ZEBRAFISH CAUDAL FIN

A. ABSTACT

Examination of bone regeneration in model organisms may unveil underlying mechanisms to target and stimulate regeneration of human bone. Lower vertebrate models, such as zebrafish, are able to regenerate numerous tissues, including bone. In this study we utilized the zebrafish model of caudal fin regeneration to examine the role of enzyme transglutaminases, which have been shown to regulate osteogenesis *in vitro*. TG-mediated cross-linking activity continuously associates with regenerative blastema. Upon treatment of regenerating zebrafish with a competitive TG inhibitor, cystamine, a significant 60% reduction in the formation of regenerated mineralized bone rays was observed that associated with reduced deposition of collagen type I. In addition, TG inhibition attenuated activation of the canonical β -catenin signaling axis in the regenerative blastema. Through real-time PCR analysis, we identified two zTGs that are dramatically induced in a subset of mesenchymal-like precursor cells during fin regeneration, zTG2b and zFXIIIa-87 (showing 11- and 28-fold induction respectively). These data identify TGs as novel regulators of bone regeneration in addition to their evolutionary conservative role in matrix mineralization.

B. INTRODUCTION

Upon injury mammalian tissues respond by one of two mechanisms, repair or regeneration. Select human tissues maintain a regenerative capability (e.g. Liver); however the majority of tissues lack this ability and heal via repair, resulting in tissue scarring (Poss et al., 2003). Due to this less than ideal repair process, interest in understanding tissue regeneration has arisen in the hope of unveiling mechanisms to target and stimulate regeneration in human tissues. Interestingly, lower vertebrate animal models have a remarkable regenerative capacity of various tissues such as the heart, appendages and eyes and have therefore been utilized for studies examining regenerative mechanisms (Brookes and Kumar, 2005; Brookes et al., 2001; Sanchez, 2000; Poss et al., 2003).

In this study we examined bone regeneration in the caudal fin of zebrafish, *Danio rerio*, the most commonly studied regenerative tissue due to its easy access for amputation, relatively simple and symmetric structure and amputation having little to no effect on zebrafish survival (Poss et al., 2003). The caudal fin is composed of blood vessels, nerves, pigment cells, mesenchymal-like cells that reside in the intra-ray area of the bony fin rays, referred to as lepidotrichia; all of which are encased by a typical epidermis (Becerra et al., 1983). Lepidotrichia lack skeletal muscle and form via intramembranous ossification in which bone forms by direct mineralization of the matrix (Landis and Geraudie, 1990). Regeneration of the caudal fin occurs via three major phases: wound healing, blastema formation that involves disorganization and migration of mesenchymal tissue, and lastly regenerative outgrowth.

The blastema, a mass of proliferative undifferentiated cells, provides progenitor cells for newly regenerating tissues in the fin. Two cell types contribute to the formation of newly regenerated bone including the intra-ray mesenchymal-like cells and differentiated osteoblasts of the mature bone, which undergo de-differentiation and migrate to the amputation site (Knopf et al., 2011; Sousa et al., 2011). Remarkably, ablation of osteoblasts from caudal fins prior-to amputation has no detrimental effects on regeneration demonstrating that intra-ray mesenchymal-like cells, which re-enter the cell cycle and migrate towards the regeneration area upon amputation, contain precursors required to maintain proper bone formation during fin regeneration (Singh et al., 2012). However, the precise molecular mechanisms supporting bone regeneration in caudal fins remains largely unknown.

Diverse factors regulate osteogenic cell differentiation. Among these are enzymes from the TG which are Ca^{2+} dependent proteins frequently associated with numerous biological processes and diseases (Lorand and Graham, 2003; Nurminskaya and Belkin, 2012). Two mammalian TGs, TG2 and FXIIIa, are linked to bone formation due to their expression pattern in osteo-chondrogenic tissues (Aeschlimann et al., 1993; Nurminskaya and Linsenmayer, 1996; Nurminskaya et al., 2002; Summey, Jr. et al., 2002; Al-Jallad et al., 2006) and ability to promote osteoblast differentiation *in vitro* (Nurminskaya et al., 2003; Becker et al., 2008). In a previous study, we characterized zTGs and identified significant homology of eleven zTG genes with three mammalian TGs, TG1, TG2 or FXIIIa (Deasey et al., 2011). Expression of zTG2b, zFXIIIa-87, and zTG1-81 was shown to localize to skeletal progenitors at 2dpf suggesting their role in bone formation. Since many genes are similarly involved in development and regeneration (Poleo et al.,

2001), we postulate that zTGs may also have a role in bone regeneration. Further, we investigated whether zTGs regulate bone regeneration via activation of β -catenin and/or hedgehog signaling pathways, which have been implicated in zebrafish caudal fin regeneration (Stoick-Cooper et al., 2007; Quint et al., 2002) and shown to be regulated by TG2 in mammalian cells (Deasey et al., 2013a).

C. MATERIALS AND METHODS

1. Zebrafish Caudal Fin Amputation

WT zebrafish were maintained in fish water (distilled water supplemented with 0.03% Instant Ocean Sea Salts) at 28°C at the Aquaculture Research Center, Center of Marine Biotechnology University of Maryland. Adult zebrafish were anesthetized with a 150mg/L Tricaine solution as previously described (ZFIN (<http://zfin.org/cgi-bin/webdriver?MIval=aa-xpatselect.app>)). The caudal fin was amputated at a point half way between the end of the scales and the tip of the fin. Post-amputation the fish were returned to tanks with plain fish water or supplemented with 178 μ M Cystamine (Sigma) where they regenerated at 28°C for the indicated period of time. The therapeutically relevant dosage of cystamine in humans is from 10^{mg/kg} - 70^{mg/kg} with the optimal dosage being from 20^{mg/kg} - 40^{mg/kg} (Dubinsky and Gray, 2006). As the average adult weighs approximately 70kg, the average adult is receiving 1400mg of cystamine/treatment. To apply this clinical dosage to zebrafish, we found that the average 70kg adult's volume is approximately 70L and indicating that the therapeutic range is 20^{mg/L} - 40^{mg/L} and we chose to treat the zebrafish at 40^{mg/L}. They were then left to regenerate at 28°C for the indicated period of time.

2. Real-Time PCR

Total RNA was isolated from mature fins and the regenerating area of amputated zebrafish fins with Trizol reagent (Invitrogen) (Detailed description of RNA isolation in Appendix A.1-2) and used for first-strand cDNA synthesis (Detailed description of reverse transcription in Appendix A.3). Primers for zTGs were designed using NCBI primer design software (Table of primers in Appendix B.2). Real-time PCR was run on a BioRad CFX96 Thermal Cycler following the manufactures instructions for heat activation, amplification and melting curves for 45 cycles (Detailed description in Appendix A.4). Expression levels were normalized to the average of two housekeeping genes, β -actin and EF α 1.

3. *In Situ* Hybridization

Tissue was fixed in RNase free 4% paraformaldehyde overnight at 4°C, cryo-protected in 30% sucrose and frozen in OCT (Tissue-Tek). Tissue was cut on a cryostat, 10 μ m thick sections were air-dried at 37°C for 30mins and then rehydrated in PBS and incubated in PBS-T for 4 minutes. This was followed by Proteinase K (Novagen) digestion (0.05mg/ml) in PK Buffer (50mM Tris-HCl, pH 8.0, 10mM NaCl, 10mM EDTA) for 4 minutes followed by two washes in PBS and DEPC-water. DIG-labeled antisense RNA probes (Detailed description of probe preparation in Appendix A.7) were applied to the slides at 1 μ g/mL concentration in hybridization buffer (50% formamide, 5X SSC buffer, 0.1% Tween-20, 50 μ g/mL heparin and 500 μ g/mL tRNA; pH 6.0 with citric acid) and left overnight at 55°C; the next day non-specific staining was blocked with 1% DIG blocking solution (Roche) in Tris buffer (0.1M Tris-HCl pH7.5, 0.15M NaCl) for 30 minutes at 37°C. Hybridized DIG-RNA was detected with an anti-DIG fab fragments antibody

fused to alkaline phosphatase (Roche) at a 1:1000 dilution followed by colorimetric assay with NBT/BCIP solution (Roche) in the dark for 48-72 hours until color developed. Staining progression was monitored with a Leica DMIL FLUO microscope equipped with a SPOT RT slider real-time CCD camera (Diagnostic Instruments, Inc.). To identify tissue morphology, slides were counterstained with nuclear fast red for 5min, washed with distilled water for 5min and cover-slipped with permount (Ameresco). A detailed description of *in situ* hybridization and nuclear fast red counterstaining protocols is in Appendix A.9.

4. *In Vivo* Detection of TG Cross-Linking Activity in Zebrafish

Transglutaminase cross-linking activity in zebrafish fins was visualized by incubating live fish in 5mM rhodamine-conjugated synthetic substrate Pro-Val-Lys-Gly, SY2011 (Kim et al., 1997) for four hours at 28°C. Fish were then washed in fish water for one hour, to allow all unincorporated substrate to diffuse out. Fish were anesthetized by 150mg/L Tricaine and SY2011 incorporation was visualized in live fish on a Leica DMIL FLUO microscope equipped with a SPOT RT slider real-time CCD camera (Diagnostic Instruments, Inc.).

Tissue was fixed in 4% PFA for 2 hours at RT and cryo-protected in 20% sucrose-PBS solution at 4°C overnight. Tissue was then embedded in OCT freezing medium (TissueTek) and frozen in liquid nitrogen and stored at -80°C. Sections of tissue were cut at -22°C into 10µm sections with a cryostat on SuperFrost Plus slides, images were acquired by a Leica DMIL FLUO microscope equipped with a SPOT RT slider real-time CCD camera (Diagnostic Instruments, Inc.).

5. Histological Analysis

Bone formation in regenerating fins was analyzed by Alizarin Red and Von Kossa Staining. Caudal fins were fixed in 4% PFA for 2 hours at RT. For alizarin red staining fins were incubated in 70% EtOH for 24 hours at RT, followed by staining with Alizarin Red S dye (Ameresco) solution (12mg/L in 1% Potassium Hydroxide) for 24 hours at RT. Fins were cleared in a 70% EtOH/Glycerol solution (1:1) until the desired level of clearing was achieved. For von kossa staining, sections of tissue were cut at -22°C into 10µm sections with a cryostat on SuperFrost Plus slides and stored at -80°C. Sections were warmed to RT and re-hydrated in distilled water. They were then moved into a coplin jar containing 5% silver solution (2g silver nitrate in 40mL distilled water) and placed under a strong desk lamp for 20min. They were then rinsed 3x's in distilled water and silver was precipitated with 5% sodium thiosulfate (2g sodium thiosulfate in 40mL distilled water) for 5 minutes. Slides were washed in tap water for 5 minutes and rinsed quickly in distilled water. Sections were counterstained with nuclear fast red for 5 minutes and this was followed with a 5 minute wash in distilled water. Slides were cover-slipped with permount (Ameresco). Images were captured with a Leica DMIL FLUO microscope equipped with a SPOT RT slider real-time CCD camera (Diagnostic Instruments, Inc.)

6. Immunocytochemistry

Cryostat sections of caudal fins were rehydrated in PBS, permeabilized with methanol at -20°C for 10 minutes and quenched with 50mM Glycine in PBS for 10 minutes at RT. Non-specific binding was blocked with 5% goat serum (β -catenin) or 5% BSA (Collagen I and Zns5) for one hour at RT, followed by incubation with primary antibody (rabbit

anti- β -catenin 1:80 (Santa Cruz Biotechnology); rabbit anti-Collagen I 1:300 (Abcam); mouse anti-Zns5 1:200 (ZIRC)) overnight at 4°C in 1% goat serum (β -catenin) or 1% BSA (Collagen I and Zns5) in PBS. Secondary antibody (Dylight-549-Conjugated goat anti-rabbit, 1:400 (Jackson ImmunoResearch); Alexaflour-555-Conjugated goat anti-mouse (Invitrogen)) was incubated for 1 ½ hours at RT; nuclei were stained with TO-PRO3 Iodide (Invitrogen) or DAPI Fluoromount-G (SouthernBiotech). β -catenin staining was examined via confocal microscopy using a Leica LM50 laser scanning microscope and detector. Collagen I and Zns5 staining were visualized Leica DMIL FLUO microscope equipped with a SPOT RT slider real-time CCD camera (Diagnostic Instruments, Inc.).

7. Data and Statistical Analysis

Data was collected and analyzed by both Microsoft Excel and Photoshop. Statistical significance was calculated by the student's t-test and the error bars demonstrate the standard error mean. Localization of β -catenin protein was scored by a count of one intra-ray field per fin (at least 20 cells per field) for each treatment condition. Photoshop was used to quantify the level of β -catenin staining per each cell in no amputation control fins (baseline of β -catenin activity), untreated and cystamine treated 5dpf fins.

D. RESULTS

1. zTG Expression During Fin Regeneration

zTG expression was analyzed by real-time PCR of fin tissue collected from both control fish that did not undergo amputation (0dpa), and the three phases of fin regeneration: mesenchymal disorganization and migration (1dpa), blastema formation (2dpa), and regenerative outgrowth (4dpa). At 1dpa, expression of zTG1-18, zTG-91,

zTG-84, and zTG1-81 were significantly induced by approximately 15- ($p \leq 0.05$), 9- ($p \leq 0.00005$), 3- ($p \leq 0.0005$), and 2.5-fold ($p \leq 0.0005$) respectively (Table 4.1). Expression of zTG-84 and zTG1-18 remained elevated at 4dpa compared to mRNA levels at 1dpa (with no significant changes detected), while zTG-91 and zTG-81 were rapidly down-regulated at 2dpa and even further at 4dpa (Figure 4.1A). Expression of zTG1-62, zTG2-12 and zTG1-73 did not significantly change at 1 dpa (Table 4.1) but showed a modest induction of zTG1-62 and zTG2-12 and a slight down-regulation of zTG1-73 by 4dpa (Fig. 4.1B).

In contrast, expression of zFXIIIa-87 and zTG2b mRNAs was dramatically reduced during mesenchymal disorganization and migration (about 10 and 5-fold respectively, $p \leq 0.00005$) (Table 4.1). However, both genes were significantly induced by approximately 28- and 11-fold respectively ($p \leq 0.05$) during the regenerative outgrowth phase (4dpa) (Fig. 4.1C). This pattern of expression suggests an association with osteoblast maturation and bone mineralization in analogy with the reported *in vitro* activities of mammalian homologues, TG2 and FXIIIa (Nurminskaya et al., 2003; Al-Jallad et al., 2011), prompting further analysis on their potential role(s) in bone regeneration.

Gene	Fold Change Expression at 1dpa Compared to No Amputation Control (0dpa)	P Value
zTG1-18	14.782	0.041
zTG-84	3.168	0.00031
zTG-91	9.228	2.9×10^{-11}
zTG1-81	2.505	0.00038
zTG1-62	1.501	0.23
zTG2-12	0.786	0.027
zTG1-73	1.712	1.2×10^{-5}
zFXIIIa-87	0.141	6.8×10^{-16}
zTG2b	0.233	4.1×10^{-7}

Table 4.1 zTG Expression at 1dpa Compared to a No Amputation Control. Real-time PCR analysis was used to determine the zTG expression levels at 1dpa. RNA was extracted from fins at 0dpa and 1dpa. Data was normalized to the average of two housekeeping genes, β -actin and EF α -1 and is presented as a fold change in expression compared to expression in no amputation control (0dpa). N=3.

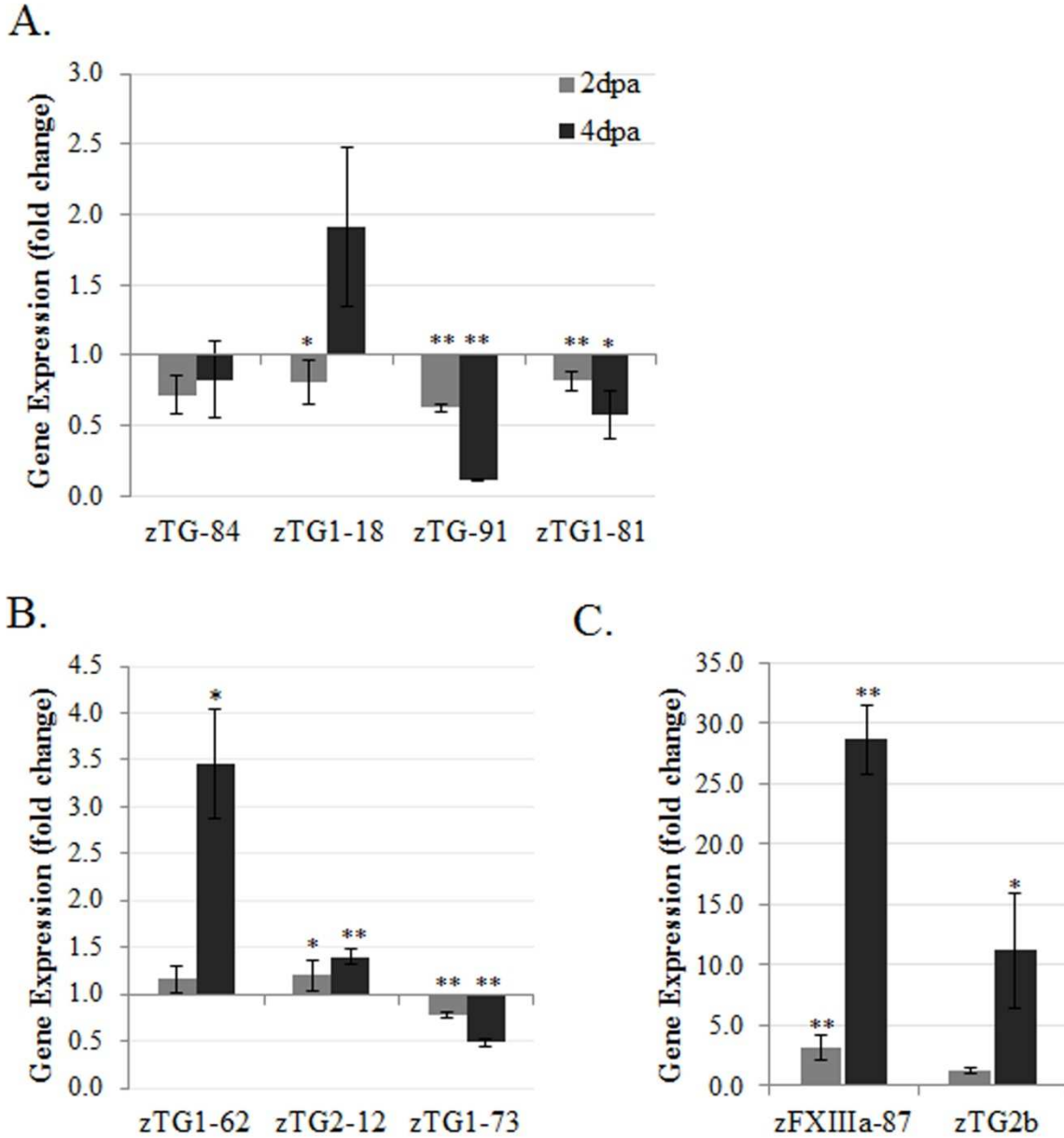


Figure 4.1 zTG Expression Pattern During Zebrafish Fin Regeneration. Real-time PCR analysis was used to determine the expression pattern of zTGs during fin regeneration. RNA was extracted from the regeneration area of fins at three time-points: 1dpa, 2dpa, and 4dpa. Data was normalized to the average of two housekeeping genes, β -actin and EF α -1 and is presented as a fold change in expression compared to expression at 1dpa. (A) zTGs that are down-regulated or are un-changed at 2dpa and 4dpa, (B) zTGs that show no substantial change at 2dpa and 4dpa and (C) zTGs that are substantially up-regulated at 4dpa (n=3, *p \leq 0.05, **p \leq 0.005).

2. Localization of zFXIIIa-87 and zTG2b mRNA in Mature and Regenerating Caudal Fins

The proliferative intra-ray blastema in the outgrowth region is believed to support bone regeneration (Smith et al., 2006). To determine whether expression of zFXIIIa-87 and zTG2b corresponds to this tissue we employed *in situ* hybridization. Localization of zFXIIIa-87 and zTG2b mRNAs was examined on longitudinal sections from three different fin areas (diagramed in Fig. 4.2A): mineralized bone rays in no-amputation control fish (section 1) and 4dpa regenerating fins in the newly formed bone rays above the amputation plane (section 2) and mineralized bone below the amputation plane (section 3). Low intensity staining for zFXIIIa-87 mRNA was observed in cells of the intra-ray area of no-amputation control fish (Fig. 4.2B, section 1, black arrow). In contrast, a significant induction of zFXIIIa-87 expression was observed in the intra-ray mesenchyme both above and below the amputation plane in 4dpa regenerating fins (Fig. 4.2B, section 2-3, black arrows). A similar pattern of gene expression was also detected for zTG2b, although its induction was more restricted to the proliferative blastema of the newly regenerating bony rays (Fig. 4.2C, section 2, black arrow).

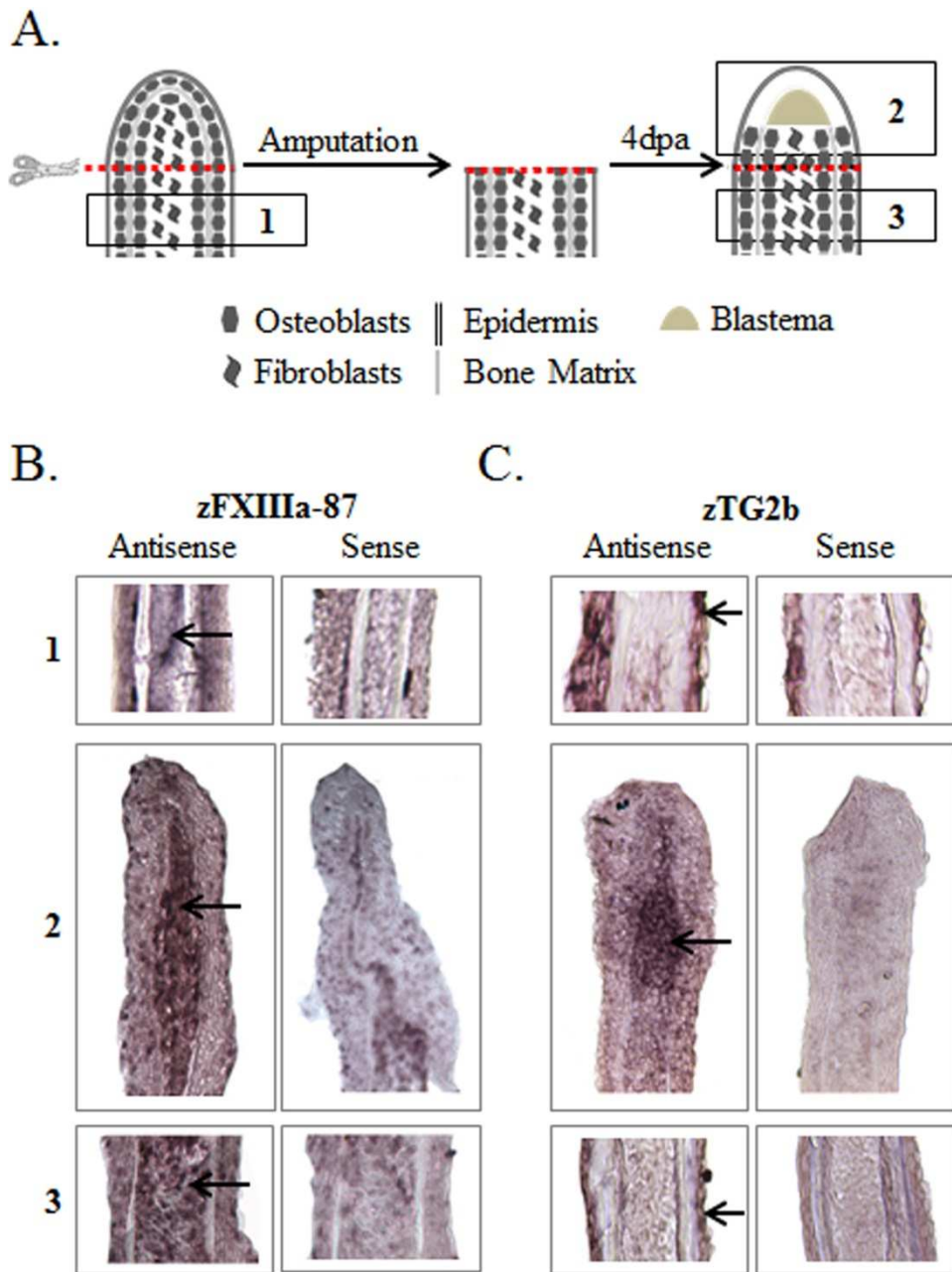


Figure 4.2 Expression of zFXIIIa-87 and zTG2b Localizes to the Regenerative Blastema in Zebrafish Fins. (A) Schematic outlining the process of fin regeneration and cellular composition of fins at 0dpa and 4dpa. Representative (B) zFXIIIa-87 and (C) zTG2b *in situ* hybridization for both antisense and sense probes as indicated in figure on longitudinal sections. Three fin zones were examined: (1) no-amputation control, (2) above the amputation plane at 4dpa and (3) below the amputation plane at 4dpa. Black arrows highlight the area of positive and specific staining.

Increased expression of zFXIIIa-87 and zTG2b in the intra-ray proliferative blastema (Fig. 4.2B-C, section 2) compared to the mesenchyme of mature bone below the amputation plane (Fig. 4.2B-C, section 3) was further confirmed by *in situ* hybridization on tissue cross-sections from above and below the amputation plane (Fig. 4.3A). Interestingly, only a subset of the mesenchymal cells are zTG-positive and these cells are mixed with zTG-negative cells in the intra-ray space of the bones as revealed by counterstaining with nuclear fast red (Fig. 4.3B).

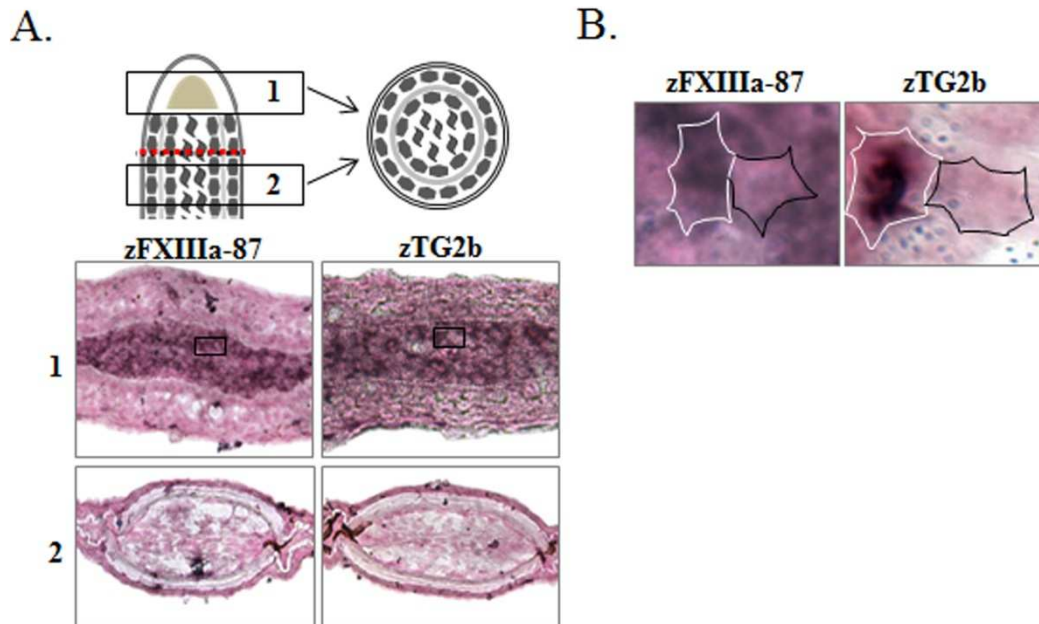


Figure 4.3 Expression of zFXIIIa-87 and zTG2b Localizes to the Regenerative Blastema in Zebrafish Fins. (A) Diagram of fin cross-sections (top panel). Representative zFXIIIa-87 and zTG2b *in situ* hybridization on cross-sections of 4dpa fins above the amputation plane (section 1) and below the amputation plane (section 2) (bottom panel). Black squares highlighting area examined by higher magnification in B. (B) Nuclear fast red counterstaining shows expression of either zFXIIIa-87 or zTG2b (white outline) in a subset of regenerative mesenchymal cells interspersed with cells not expressing TGs (black outline).

3. *In Vivo* zTG Activity in the Regenerating Caudal Fin

To examine whether increased gene expression of zTG2b and zFXIIIa-87 associates with elevated cross-linking activity in the intra-ray zone of regenerating bone rays, zTG activity was visualized by *in vivo* incorporation of a rhodamine labeled TG-peptide substrate, SY2011 (Kim et al., 1997). Regenerating zebrafish were incubated with SY2011 for 4 hours and incubated in fresh water for 1 hour to wash out the non-incorporated peptide, followed by fluorescent imaging at 1dpa, 2dpa, 3dpa, and 5dpa. The zone of zTG activity identified by incorporation of the rhodamine label into fin tissue corresponded to the newly forming blastema at 1dpa (Fig. 4.4A, left panel, black arrow), and remained associated with the regenerative blastema during the progression of fin regeneration (Fig. 4.4A). At 5dpa, substantial zTG activity was detected in the blastema of the regenerating fin and also in some cells of the epidermis (Fig. 4.4B, top panel, black arrows). In the newly regenerated bones visually identified by the thick layers of extracellular matrix, the major zTG activity was detected in the intra-ray mesenchyme with limited SY2011 incorporation in the area between the rays (Fig. 4.4B, middle panel, black arrows), likely corresponding to blood vessels as erythrocytes have high levels of TG activity (Lorand *et al.*, 1976). Lastly, in fin tissue below the amputation plane, limited SY2011 incorporation was detected outside the bone rays likely in the blood vessels (Fig. 4.4B, bottom panel, black arrows). Together these results demonstrate localization of zTG activity to the proliferative blastema of regenerating fins and suggest a role for zTGs in both formation and function of the blastema.

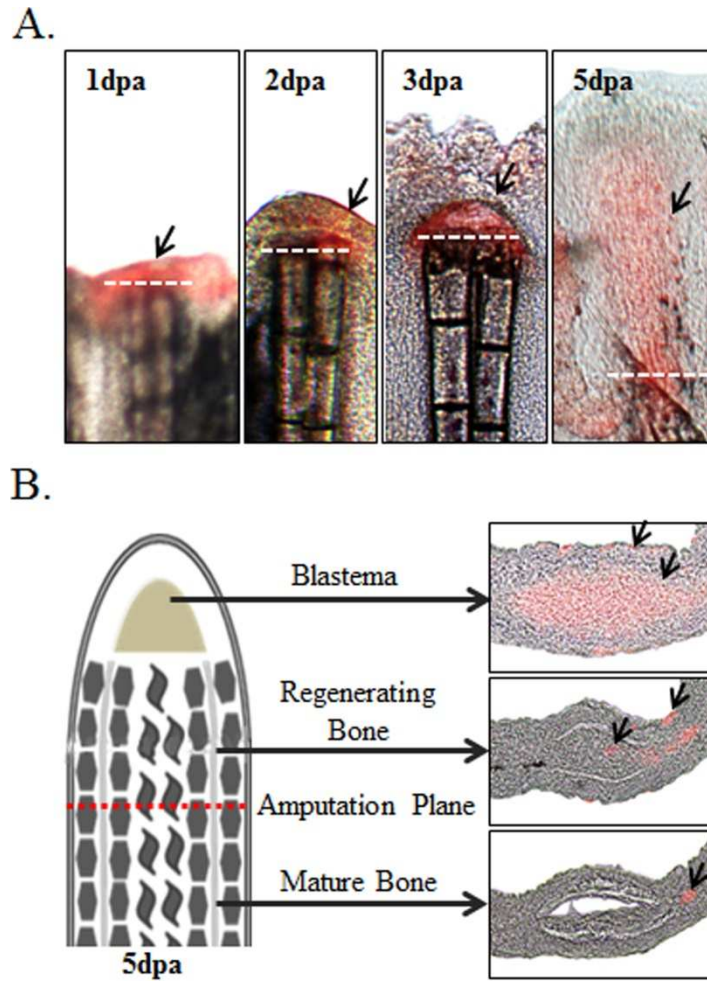


Figure 4.4 zTG Activity in Regenerating Zebrafish Fins. (A) *In vivo* labeling of regenerating zebrafish fins with rhodamine-labeled TG substrate (SY2011) imaged with fluorescent Leica microscope at 1dpa, 2dpa, 3dpa, and 5dpa. (B) Schematic of cross-sections taken from 5dpa regenerating adult zebrafish fins (left) and fluorescent images of a representative cross-sectioned 4dpa ray labeled with SY2011 (right).

4. Cystamine Treatment Impedes Bone Regeneration

To determine whether enzymatically active zTGs contribute to bone regeneration, zebrafish were treated from 0dpa-5dpa with a general competitive inhibitor of transglutaminase-mediated cross-linking, cystamine. At 5dpa regeneration is approximately 50% complete and sufficient bone regeneration has occurred to allow for visualization and quantification of a potential effect of zTG inhibition on this process.

We first examined the effect of this treatment on SY2011 incorporation as a measure of zTG inhibition and found that cystamine treated fish showed an almost complete inhibition of zTG activity in regenerating 5dpa fins (Fig. 4.5A).

To examine how zTG inhibition affects bone regeneration we examined the progression of bone mineralization, an end marker for bone formation/regeneration. Specifically, control and cystamine treated fins were stained with alizarin red, which binds calcium and is commonly used to identify mineralizing bone. Inhibition of zTG with a clinically-relevant dose of cystamine caused a noticeable decrease in bone regeneration (Fig. 4.5B). Quantitative comparison of the distance from the amputation plane (dashed line in Fig. 4.5B) to the end of Alizarin-stained mineralized bone in untreated (solid line in Fig. 4.5B) and cystamine treated fish (dotted line in Fig. 4.5B) revealed an approximate 60% reduction in regenerative bone outgrowth in zTG inhibited fish (Fig. 4.5C, $p \leq 0.005$, $n=12$). However, overall regenerative outgrowth of the fins was not affected by zTG inhibition (Fig. 4.5D), suggesting a specific role for zTG activity in bone regeneration.

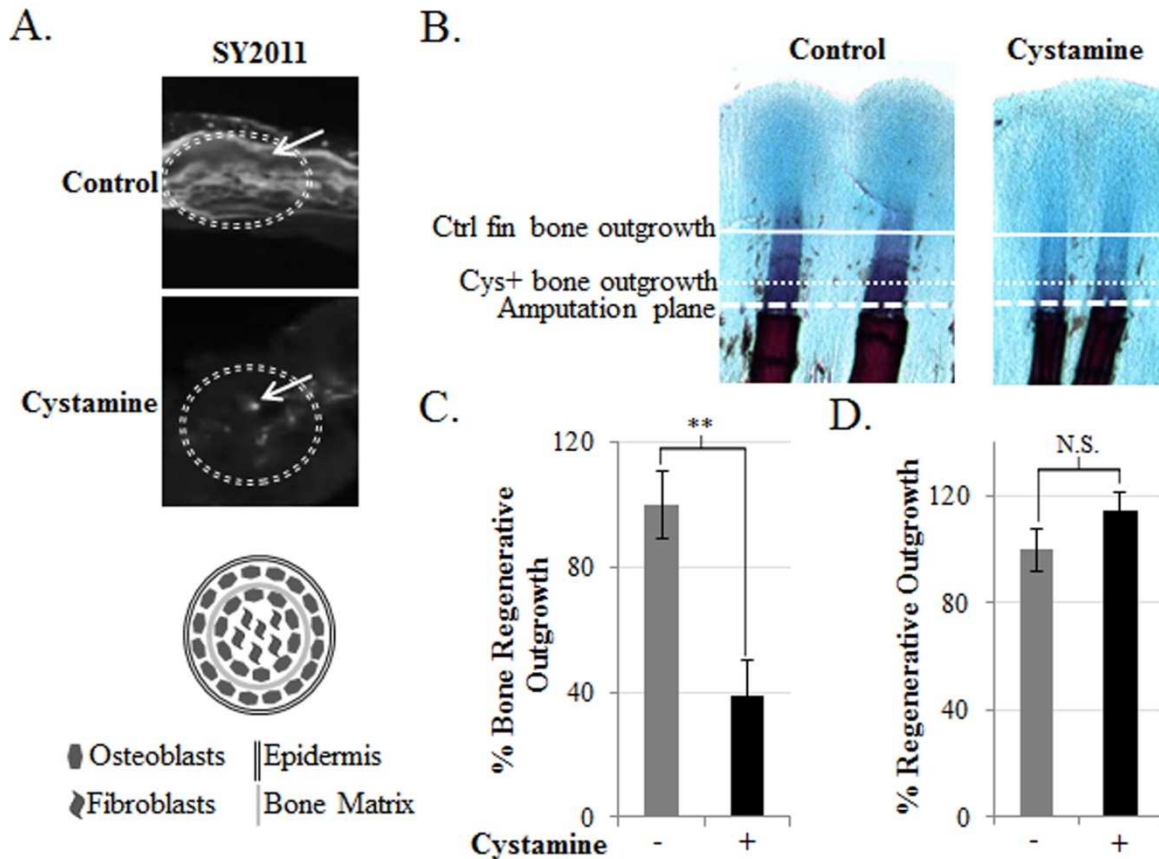


Figure 4.5 Cystamine Treatment Impedes Bone Formation in Regenerating Fins. (A) Cystamine treatment inhibits zTG catalytic activity as demonstrated by reduced SY2011 incorporation. (B) Representative image of regenerating fins stained with Alizarin red. Dashed line indicates the plane of amputation, dotted line indicates the bone outgrowth for cystamine treated fins and solid line indicates the bone outgrowth for control fins. (C-D) The length of regenerated bone (C), measured from the amputation plane to the end of the zone of Alizarin red staining, and total regenerative outgrowth (D), measured from the amputation plane to the top of the fin, were measured in untreated control and cystamine-treated fish. Control fins were set to 100% (n=12, **p≤0.005, N.S.= not significant).

Alizarin red is commonly used as a bone stain due to its ability to bind the intra- and extracellular calcium that is high in mature bone; however, detection of calcium phosphate characteristic for the extracellular bone matrix requires Von Kossa stain. Histological analysis with Von Kossa stain revealed an almost complete prevention of

calcium phosphate deposition in fish regenerating in the presence of TG inhibitor (Fig. 4.6A, left panel, black arrows point to calcified bone tissue in the newly-regenerated fin).

We next examined the expression of osteoblast markers *Zns5* and type I Collagen (Col I) by immunohistochemistry. No change in expression of *Zns5*, an osteoblast-specific marker (Johnson and Weston, 1995), was detected between control untreated and cystamine-treated fish (Fig. 4.6A, middle panel, white arrows), indicating that zTG inhibition has no effect on osteoblast commitment and early differentiation. On the contrary, there was a dramatic decrease in Col I staining in cystamine treated fins above the amputation plane compared to control untreated fish (Fig. 4.6A, right panel, white arrows). This observed decrease indicates that zTG inhibition affects the ability of osteoblasts to lay down Col I - the major extracellular bone protein (McKee et al., 2006). To determine whether zTG inhibition affected Col I deposition by inhibiting Col I gene expression, we performed real-time PCR for both control untreated and cystamine treated fins and found that cystamine treatment has no effect on Col I mRNA expression (Fig. 4.6B).

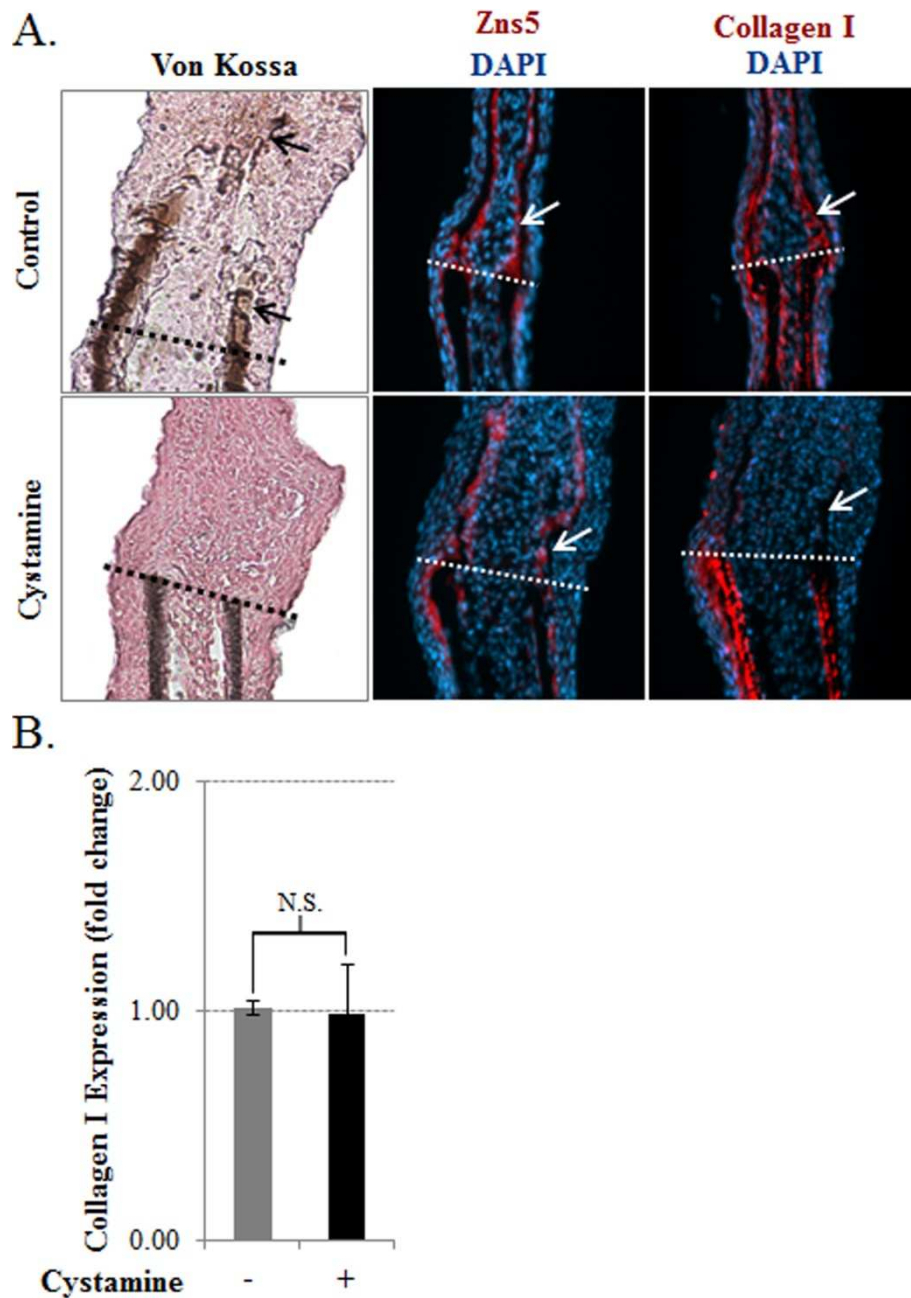


Figure 4.6 Cystamine Treatment Impedes Bone Formation and Type-I Collagen Deposition in Regenerating Caudal Fins. (A) Representative images of longitudinal sections of 5dpa fins stained with Von Kossa (left panel), Zns5 (middle panel) antibody or Col I (right panel) antibody to monitor the effect on bone regeneration. Arrows highlight areas of positive staining above the amputation plane (dotted line). (B) Real-time PCR performed on RNA extracted from 5dpa fins \pm Cystamine for Col I expression. Data was compared to untreated control fins and normalized to the average of two house-keeping genes, β -actin and EF α -1 (n=3, N.S. = not significant).

5. zTG Inhibition Effects Canonical β -Catenin Signaling in Regenerating Fins

To further understand the role of zTGs in bone regeneration we investigated their potential molecular mechanism of action. Previous studies have shown that TGs activate various signaling pathways (Nurminskaya and Belkin, 2012) including hedgehog and canonical β -catenin pathways (Beazley et al., 2012b;Faverman et al., 2008;Dierker et al., 2009), which are both necessary for bone formation and homeostasis (Chen et al., 2007;Kim et al., 2007;Mak et al., 2008;St-Jacques et al., 1999). Further, activation of these signaling pathways has been associated with proper zebrafish fin regeneration (Stoick-Cooper et al., 2007;Quint et al., 2002). Therefore, we examined markers of both pathways by real-time PCR in control untreated and cystamine treated fins at 5dpa. A significant down-regulation was detected for markers of β -catenin signaling, MMP7 and TCF1 (Fig. 4.7), while none of the analyzed Hedgehog markers, including Gli1, Gli3 and Patched, were affected by cystamine treatment (Table 4.2).

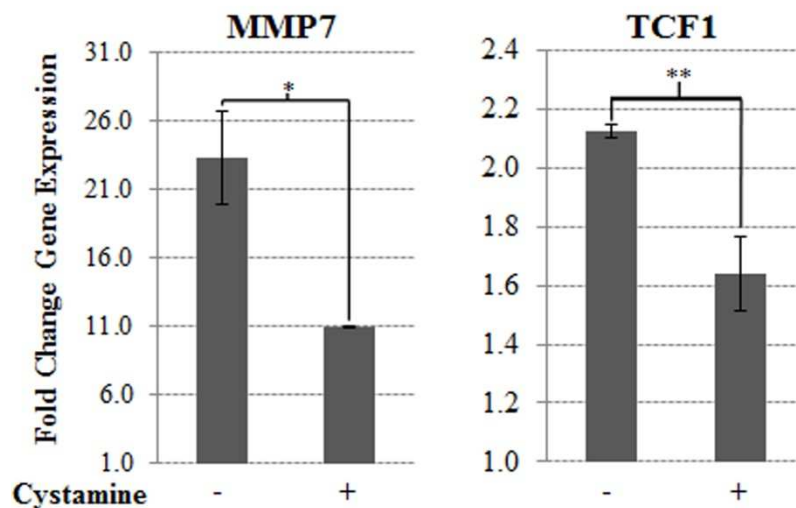


Figure 4.7 Cystamine Treatment Affects Activation of Canonical β -Catenin Signaling in Regenerating Caudal Fins. Real-time PCR performed on RNA extracted from 5dpa fins \pm Cystamine for two markers of β -catenin signaling, MMP7 and TCF1. Data was compared to 0dpa and normalized to the average of two house-keeping genes, β -actin and EF α 1. (n=3, *P \leq 0.05, **P \leq 0.005).

Hedgehog Signaling	
Gene	Cystamine Treatment
Gli1	No Change
Gli3	No Change
Patched	No Change

Table 4.2 Cystamine Treatment has No Effect on Hedgehog Activation. Examination of three markers of Hedgehog signaling showed no significant reduction in expression with Cystamine treatment. Data was normalized to β -actin and compared to a no-amputation control.

Inactive β -catenin is targeted for degradation, however upon activation it accumulates in the cytoplasm and translocates to the nucleus (Huang and He, 2008). Therefore, to confirm the effect of zTG inhibition on β -catenin activation, we utilized immunohistochemistry to examine the subcellular localization of β -catenin. In 5dpa control regenerating fish, accumulation of cytoplasmic and nuclear β -catenin was observed in many cells of the intra-ray regenerative area (Fig. 4.8A, middle panel) compared to uninjured fin tissue (Fig. 4.8A, top panel). Conversely, in 5dpa fins treated with cystamine, we saw a significant reduction of both cytoplasmic and nuclear β -catenin staining compared to 5dpa untreated regenerating fins (Fig. 4.8A, bottom panel). To quantify the reduction in nuclear β -catenin staining associated with inhibition of zTG activity, the intensity of nuclear β -catenin staining was measured in the intra-ray/blastema area as diagramed in Fig. 4.8B (orange box) in regenerated 5dpa fins from untreated and cystamine-treated fish. We found that in untreated fins approximately 85% of the nuclei showed positive nuclear β -catenin staining whereas in cystamine treated fins approximately 7% of the cells showed positive nuclear β -catenin staining (Fig. 4.8B). These results demonstrate that zTG inhibition impedes β -catenin signaling activation and thereby provides a potential mechanism of action for zTGs in bone regeneration.

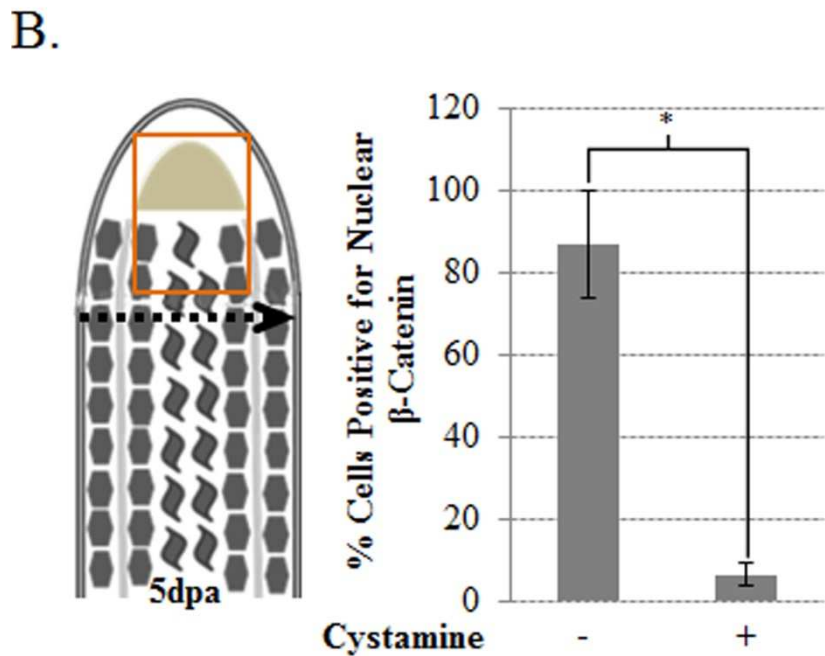
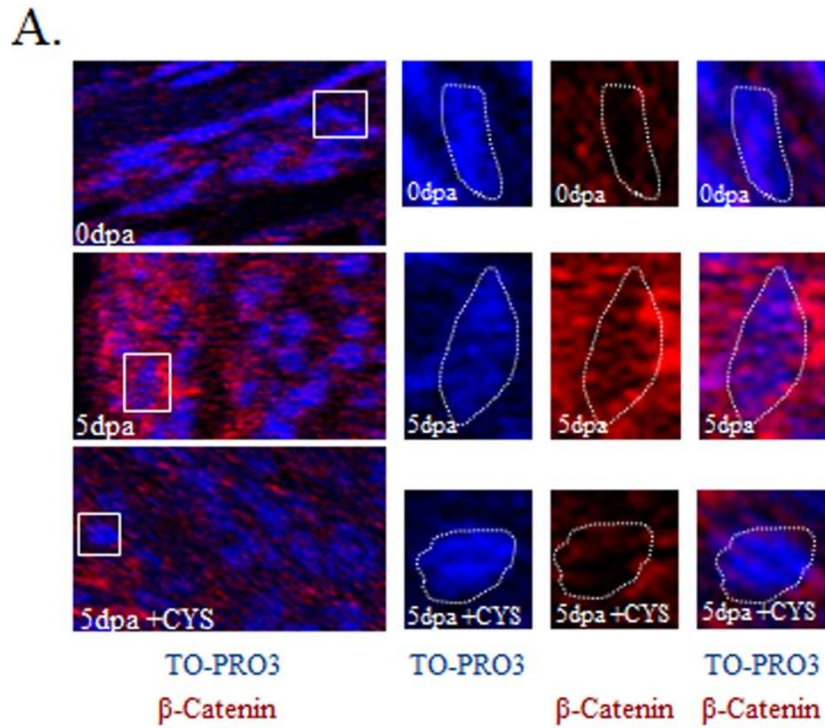


Figure 4.8 Cystamine Treatment Affects Activation of Canonical β -Catenin Signaling in Regenerating Caudal Fins. (A) Longitudinal sections of 5 dpa fins \pm Cystamine immunostained for β -catenin (red) and nuclei counterstained with TOPRO Red (blue). (B) Schematic of area of regenerating fin used for quantification of effect of Cystamine treatment on β -catenin activation (left panel). Quantification of nuclear localization (right panel) displayed as the percent of nuclei positive for β -catenin staining ($n=3$, $*p \leq 0.05$).

E. DISCUSSION

In this study we examined mechanisms of early bone regeneration employing the zebrafish model of caudal fin regeneration. We demonstrate for the first time an association between zTG expression in the proliferative intra-ray blastema and proper bone regeneration during the first 5dpa. Our data suggests that enzymatically active TGs support formation of mineralized bones via β -catenin signaling and deposition of Col I matrix.

The observed expression pattern of zTGs suggests specific roles in fin regeneration. Examination of the wound healing phase of regeneration at 1dpa revealed expression of four zTG homologues to mammalian TG1, which is associated with mature keratinocytes and regulates formation of the cornified layer of the epidermis (Candi et al., 2005). This observed induction of zTG1-81, zTG1-62, zTG1-73, and zTG1-18 genes at 1dpa suggests a role in wound healing and epidermal closure. The continuous increase in expression of zTG1-62 through 4dpa and the presence of epidermal cells that actively incorporate the TG substrate SY2011 suggests a role for this enzyme in regeneration of the epidermis. Further studies examining the role of zTG1 isozymes could be informative for understanding the mechanisms of scarless skin regeneration versus scar formation. In addition, two zebrafish-specific TG genes, zTG-91 and zTG-84 may also contribute to tissue disorganization and migration as suggested by their rapid induction at 1dpa; further, the continuous expression of zTG-84 through 4dpa indicates a role for this enzyme in the later phases of regeneration.

In contrast to TG1 homologues, zTG2b and zFXIIIa-87 are dramatically down-regulated at 1dpa indicating low (if any) levels of expression in epithelial or other cells

during wound healing. However, these two genes are significantly induced in the intra-ray proliferative mesenchymal cells that reportedly contribute to the formation of mineralized bone rays at 4-5dpa (Singh et al., 2012). Further, our inhibitory study has shown that these enzymes specifically regulate bone regeneration but not general outgrowth of the amputated fin. Previous studies have associated TG-mediated cross-linking with enhanced stability and mechanical strength of Col I-based matrices and the ability to support cell adhesion, proliferation and viability (Chau et al., 2005; Ciardelli et al., 2010; Garcia et al., 2009). Inhibition of zTGs with cystamine prevented Col I deposition, a major extracellular bone protein, necessary for bone mineralization. This study is the first, to the best of our knowledge, to demonstrate an *in vivo* role for TG activity in Col I deposition in bone formation, and inspires further inquiry into the mechanisms of this regulation. Our data indicates that Col I expression is independent of zTG activity and is not affected by cystamine treatment. Therefore, it seems reasonable to suggest that zTGs regulate either protein synthesis, secretion/deposition or matrix stability of Col I. Previous *in vitro* studies indicated a role for active mammalian FXIIIa in microtubule stabilization and thus Col I secretion in osteogenic cells (Al-Jallad et al., 2011), suggesting that cystamine treatment affects a similar activity of zFXIIIa-87 in regenerating fin bone. In addition, mammalian TG2 has been implicated in the regulation of collagen deposition by the reduced Col I content of atherosclerotic plaques in TG2^{-/-} mice (Van Herck et al., 2010). Further studies will determine whether one or both zTGs regulate deposition of the Col I-rich bone matrix to support tissue mineralization in regenerating fin bony rays.

In addition, our results demonstrate that zTGs act as agonists of the β -catenin signaling pathway in the blastema of regenerating fins. This pathway has been found to be critical to fin regeneration (Stoick-Cooper et al., 2007; Poss et al., 2003), bone formation/healing (Westendorf et al., 2004; Chen et al., 2007; Kim et al., 2007) and osteoblast maturation (Day et al., 2005). Inhibition of the β -catenin signaling axis which is activated in the blastema by 2dpa correlates with inhibition of fin regeneration (Stoick-Cooper et al., 2007). Here, we demonstrate that the TG inhibitor cystamine attenuates activation of this signaling at 5dpa and may thus inhibit bone regeneration. Our data warrant further inquiry into the possibility of β -catenin signaling regulating deposition of the Col I-rich bone extracellular matrix. Alternatively, impaired bone matrix formation may affect β -catenin signaling via insufficient retention and/or localization of activating extracellular ligands. In addition, zTG activity may regulate these processes independently, and zTG2b and zFXIIIa-87 may be working synergistically or individually in activation of β -catenin signaling and Col I deposition during bone regeneration. An additional question for future study is whether there is a specific subset of intra-ray mesenchymal cells expressing both zTGs or if these two enzymes are expressed by different intra-ray cellular subpopulations. If different cellular populations exist, it would be interesting to investigate whether both zTG2b and zFXIIIa-87 are required for bone regeneration. Of note, no FXIIIa expression has been detected in mammalian bone-marrow mesenchymal cells (our unpublished data) allowing speculation on the possible stimulation of mammalian bone regeneration via introduction of FXIIIa.

This study demonstrated the ability of clinically relevant doses of cystamine to attenuate bone formation *in vivo*, which is important for developing therapeutic strategies in pathogenic heterotopic ossification, seen in musculoskeletal trauma, spinal cord injury, central nervous system injury, and combat wounds (Shehab et al., 2002). The benefits to using cystamine in our studies include its low toxicity and the rapid clinical transition of the reported findings due to the approved use of the reduced form of cystamine, cysteamine, as an orphan drug (Sooahoo et al., 1997). Cystamine is commonly used as an inhibitor of TGs (Elli et al., 2011; Jeon et al., 2004; Alcock et al., 2011), however its potential side effects via inhibition of other thiol-containing enzymes should be acknowledged (Lesort et al., 2003). Nevertheless, we have also shown reduced bone mineralization in the developing fish treated with a TG2-specific inhibitor KCC-009, indicating that zTG activity is similarly involved in bone formation and regeneration.

In conclusion, we have identified a new population of fibroblast-like zTG-positive cells in the proliferating mesenchymal blastema and demonstrate a role for zTG activity in bone regeneration. Our data support a role for mesenchymal-like cells (Singh et al., 2012) in bone regeneration, which likely work alongside de-differentiating osteoblasts (Sousa et al., 2011; Knopf et al., 2011) in the zebrafish caudal fin.

CHAPTER V: TRANSGLUTAMINASE 2 AS A NOVEL ACTIVATOR OF LRP6/ β -CATENIN SIGNALING³

A. ABSTRACT

The β -catenin signaling axis is critical for normal embryonic development and tissue homeostasis in adults. We have previously shown that extracellular enzyme TG2 activates β -catenin signaling in vascular smooth muscle cells (VSMCs). Further, we have shown that inhibition of zTG activity by cystamine results in reduced β -catenin activation. In this study, we provide several lines of evidence that TG2 functions as an activating ligand of the LRP5/6 receptors. Specifically, we show that TG2 activates β -catenin-dependent gene expression and that interfering with the LRP5/6 receptors attenuates TG2-induced activation of β -catenin in Cos-7 cells. Further, we show that TG2 binds directly to the extracellular domain of LRP6, which is also able to act as a substrate for TG2-mediated protein cross-linking. Together, our findings identify and characterize a new activating ligand of the LRP5/6 receptors and uncover a novel activity of TG2 as an agonist of β -catenin signaling, contributing to the understanding of diverse developmental events and pathological conditions in which TG and β -catenin signaling are implicated.

³ Deasey SC, Nurminsky D, Shanmugasundaram S, Lima F, Nurminskaya M *Cellular Signaling* 2013 [In Press]

B. INTRODUCTION

Wnt/ β -catenin signaling is a key signal transduction pathway in normal development and disease (Nusse, 2005). The “canonical” pathway is activated by the binding of a secreted lipid-modified glycoprotein from the Wnt protein family (Tamai et al., 2000) to a cell surface receptor complex, consisting of a serpentine receptor from the Fzd family and a low-density-lipoprotein-related protein co-receptor LRP5/6. Binding of a Wnt ligand leads to LRP5/6 oligomerization and phosphorylation of its cytoplasmic tail (Cong and Varmus, 2004; Bilic et al., 2007; Tamai et al., 2004). This results in disruption of the destruction complex containing Axin, APC and GSK3, which targets β -catenin for proteasomal degradation. Stabilized β -catenin can then translocate to the nucleus, where it forms a complex with transcription factors of the TCF/LEF family and activates expression of target genes (Kikuchi et al., 2007).

Mutations in LRP5/6 signaling are associated with bone disorders, abnormal ocular vascularization, early onset cardiovascular disease and metabolic syndromes (Tamai et al., 2004; Mani et al., 2007; Fujino et al., 2003). However, not all of these phenotypes may be attributable to altered activation by ligands of the Wnt family. For instance, during ocular vascularization activation of canonical β -catenin signaling is mediated by a Norrin-LRP5-Fzd interaction (Xu et al., 2004b). Activation by Norrin utilizes both the LRP5/6 and Fzd-4 co-receptors, similar to Wnt ligands; however, Fzd-independent mechanisms of β -catenin activation have also been reported. For instance, PTH activates β -catenin through the LRP6/PTH1R complex (Wan et al., 2008), while cysteine knot proteins SOST/Sclerostin and WISE bind directly to LRP5/6 to either inhibit or activate signaling in a context-dependent manner (Semenov and He,

2006;Itasaki et al., 2003;Ellies et al., 2006). Similarly, Dkk1, a protein of the Dickkopf family, binds to LRP6 and antagonizes signaling by preventing ligand binding (Semenov et al., 2008). The multiplicity of LRP5/6-regulated biological processes suggests that identification of novel interacting ligands will advance understanding of diverse and significant aspects of normal development and its pathological disruptions.

Previously, we have shown that extracellular enzyme TG2 activates β -catenin signaling in primary mouse VSMCs and interacts with the LRP5 receptor on the cell surface (Faverman et al., 2008). In mammals, eight Ca^{2+} -dependent TGs have been identified, comprising a family of enzymes that catalyze formation of intra- or intermolecular glutamyl-lysine-protein cross-links. TG2 is unique owing to its ability to catalyze more than one enzymatic reaction and interact with a number of cell-surface receptors upon externalization into the extracellular matrix (ECM) (Nurminskaya and Belkin, 2012). Inside the cell, TG2 is able to act as a deaminase, GTPase, protein kinase and protein disulphide isomerase (Lorand and Graham, 2003). While in the ECM TG2 can interact with β 1 and β 3 integrins (Akimov et al., 2000), the atypical G-protein-coupled receptor GPR56 (Xu et al., 2006), VEGF receptor 2 (Dardik and Inbal, 2006) and LRP5 (Faverman et al., 2008). Further, we have recently shown that the protein cross-linking catalytic activity of TG2 is critical for warfarin-induced activation of β -catenin signaling in VSMCs (Beazley et al., 2012b). Taking into consideration that TG2 is often externalized and activated in response to tissue insult (Siegel et al., 2008) and that this often correlates with activation of β -catenin signaling in disease, further identification and characterization of biologically relevant TG2-receptor interactions is important for a better understanding of cardiovascular disease and other conditions.

The previously reported interaction of TG2 with LRP5 on the cell surface of osteogenic cells (Faverman et al., 2008) supports the hypothesis that induction of the β -catenin signaling pathway by TG2 is mediated by the homologous LRP5 and LRP6 receptors. However, recent findings implied that TG2 activates β -catenin signaling through a c-Src-dependent mechanism (Condello et al., 2013), thus putting the role of LRP5/6 into question. In this study we found that TG2 binds directly to and cross-links the LRP5/6 receptor. Moreover, we found that LRP5/6 is required for TG2-induced activation of β -catenin. These results may help us to understand the intertwined diversity of the biological functions of LRP5/6 and TG2 and suggest oligomerization of the LRP receptor by cross-linking as a mechanism of activation.

C. MATERIALS AND METHODS

1. Cell Culture, Plasmid constructs, DNA Transfection and Luciferase Assay

Cos-7 cells (Gluzman, 1981) obtained from ATCC and were maintained in Dulbecco's modified Eagle's medium supplemented with 100 U/mL of penicillin G, 100 μ g/mL of streptomycin, and 10% fetal bovine serum (complete DMEM) in 5% CO₂ at 37°C. Cells stably carrying TCF/LEF firefly luciferase reporter and constitutively active renilla luciferase reporter were established using lentivirus-based constructs, according to the manufacturer's instructions (SABiosciences). Puromycin-resistant colonies were expanded and maintained in complete DMEM supplemented with 1 μ g/mL puromycin. For assays cells were seeded at 5x10³ cells/well in 96-well plates and transiently transfected with plasmids for expression of LRP5, LRP6, TG2, and Wnt3a, using FuGene 6 (Roche). Dual luciferase assay was performed two days post-transfection to measure the luciferase activity. Renilla activity was used as the internal normalization control. In

separate experiments, Cos-7 cells were transiently transfected with TCF/LEF luciferase reporter construct TOP-FLASH and a β -galactosidase expression plasmid (Upstate) together with other expression constructs. In this case the β -galactosidase activity, measured using specific substrate (Promega), was used as the reference to normalize for transfection efficiency. When medium was supplemented with TG2 protein, the medium was changed to 1% serum 24hr post-transfection, and supplemented with purified gpITG2 (Sigma) (0.01U/mL, unless indicated otherwise) or purified recombinant human TG2 (N-zyme, 300 ng/mL) (N-Zyme), and cells cultured for 48hrs. The plasmid for transient expression of secreted human TG2 was previously described (Nurminsky et al., 2011). Expression constructs for GST-TG2 fusion proteins were kindly provided by Dr. A Belkin (University of Maryland). Plasmids for transient expression of human LRP6 and Wnt3a were kindly provided by Dr. X He (Harvard Medical School).

2. Western Blot Analysis and Immunoprecipitation

For Western blotting, antibodies against LRP6 (clone C-10, Santa Cruz), and phospho-LRP6 (Ser1490) (Antibody #2568, Cell Signaling) were used at a 1:1000 dilution. Secondary anti-mouse or anti-rabbit HRP-conjugated antibodies (Pierce) were used at a 1:10,000 dilution. The presence of His-tagged proteins was detected using the HRP-conjugated His probe (Pierce) at a 1:10,000 dilution. HRP-conjugated proteins were detected by the chemiluminescence method (Pierce). For immunoprecipitation, antibodies against GST (clone GST-2, Sigma) or TG2 (Abcam) were utilized and protein A/G-Sepharose (Pierce) beads were used to purify the protein complexes.

3. TG2 Over-Expression in Zebrafish Larvae

Expression construct encoding externalized human TG2 in RCASBP(A) vector was used (Nurminsky et al., 2011). The TG2 open reading frame was excised from the RCAS-TG2 vector with ClaI restriction digest and inserted into the ClaI site of the pCS2+ vector. For RNA synthetic reaction pCS2+-TG2 was linearized with NSII and mMessage mMachine (Ambion) was used to synthesize RNA as directed by the manufacturer. RNA was cleaned with MEGAclear kit (Ambion). RNA was dissolved in water and a final concentration of 0.1% phenol red was added to allow for visualization during injections. Approximately, 1nL of the 60µg/mL RNA was injected via a pressure injection apparatus into zebrafish embryos at the 2-8 cell stage. Embryos were fixed in 4% PFA 24 hours after injection and analyzed by microscopy with a Nikon T-80 microscope equipped with SPOT RT slider real-time CCD camera. 83 embryos were analyzed.

4. TG Activity Assay

TG cross-linking activity was assayed as previously described (Trigwell et al., 2004). 96-well microtiter plates (Maxisorp NUNC) were incubated overnight with 250µL of 1mg/mL *N,N'*-Dimethylcasein (Sigma-Aldrich) in 5mM Sodium Carbonate pH 9.8, and blocked with 200µL of 0.1% BSA (HyClone) in 5mM Sodium Carbonate pH 9.8 for 1hr at 37°C. LRPΔC (R & D Systems), purified gpITG2 (80ng) (Sigma-Aldrich) and Ez-link Pentylamine-Biotin (2.5mM) (Pierce) were incubated at 37°C for 1hr in reaction buffer (100mM Tris-HCl pH 8.5, 6.7mM CaCl₂, 13.3mM DTT) with increasing molar concentrations of LRPΔC. Incorporated Ez-link Pentylamine-Biotin was detected with 1:5000 ExtrAvidin-Peroxidase (Sigma) and Super AquaBlue ELISA Substrate

(eBioscience) followed by reading the absorbance at 405nm on a Polarstar Optima plate reader.

5. Data and Statistical Analysis

For all figures, error bars represent Standard Errors and P values were calculated by a one-tailed student's T test (*p<0.05, **p<0.01). At least three independent replicates were performed for each experiment.

D. RESULTS

1. Extracellular TG2 Activates β -Catenin Signaling in Cos-7 cells

Previously, we have shown that exogenously purified TG2 activates β -catenin signaling in mouse VSMCs (Faverman et al., 2008). In this study, we sought to identify the target position for TG2 activity in the β -catenin signaling pathway. For this, we monitored activation of this pathway using a luciferase reporter driven by TCF/LEF-binding promoter (TOP-FLASH) in Cos-7 cells, which are conventionally used for the analysis of β -catenin signaling. Similar to its effect on mouse VSMCs, extracellular gpITG2 induced activation of β -catenin in Cos-7 cells in a dose-dependent manner (Fig. 5.1A). We examined levels of gpITG2 ranging from 1.5×10^{-4} to 1×10^{-2} U/mL as this is within the range of endogenous TG2 levels in smooth muscle cells (Ou et al., 2000). To confirm that this effect was specific to TG2 and not due to possible contaminants from the liver tissue, we showed a similar induction of the TOP-FLASH reporter with recombinant human TG2 purified from *E coli* (Fig. 5.1B, hTG2). In addition, over-expression of human TG2, fused to a secretory peptide to assure its externalization, also activated the TOP-FLASH reporter in Cos-7 cells (Fig. 5.1B, sTG2). In aggregate, these observations strongly indicate that extracellular TG2 can

serve as an activator of β -catenin signaling.

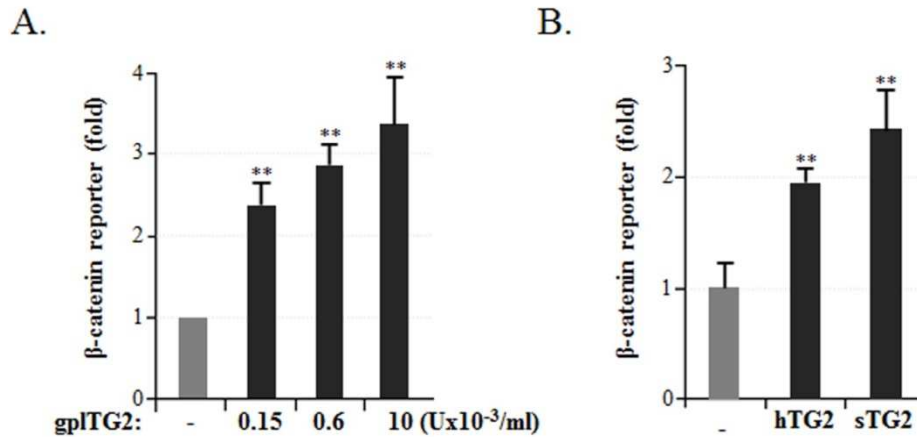


Figure 5.1 Extracellular TG2 Activates β -Catenin Signaling in Cos-7 Cells. (A) Dose-dependent activation of TOP-FLASH expression by purified gpITG2. (B) Exogenous recombinant human TG2 (hTG2) and overexpression of secreted human TG2 (sTG2) activate TOP-FLASH expression in Cos-7 cells. Figure credit to D Nurminsky, S Shanmugasundaram, and F Lima.

Activation of canonical β -catenin signaling by Wnt ligands results in phosphorylation of the serine residue in the NPPSPATE motif of the intracellular LRP6 domain (Tamai et al., 2004). Similar to the canonical ligand Wnt3a, extracellular gpITG2 strongly induces phosphorylation of LRP6 expressed in Cos-7 cells (Fig. 5.2). These observations provide evidence that TG2 utilizes the canonical intracellular components to activate β -catenin signaling.

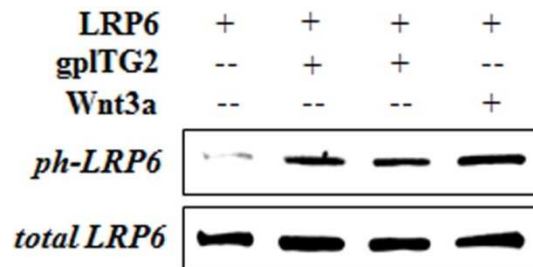


Figure 5.2 Extracellular TG2 Stimulates LRP6 Phosphorylation in Cos-7 Cells. LRP6-Overexpressing Cos-7 Cells were treated for 4 hours in serum-free medium with 0.01U /mL purified gpITG2 or with 200 ng/mL canonical Wnt3a (Positive Control). Figure credit to D Nurminsky, S Shanmugasundaram, and F Lima.

2. TG2-induced activation of β -Catenin is mediated by LRP6

Previous studies have shown that purified TG2 binds to the LRP5 receptor on the cell surface of VSMCs (Faverman et al., 2008). Since both LRP5 and its homologue LRP6 play a key role in canonical Wnt/ β -catenin signaling, we hypothesized that these receptors also mediate activation of β -catenin by TG2. To test this we analyzed the synergistic effects of TG2 and LRP6. Singular over-expression of LRP6 in Cos-7 cells did not affect the baseline level of β -catenin activity, but it significantly augmented gpITG2-mediated induction of β -catenin activity as shown by the TOP-FLASH reporter (Fig. 5.3A).

To complement this gain-of-function approach we performed loss-of-function studies, in which we employed a monoclonal anti-LRP5/6 antibody 1A12 to block LRP6 receptor overexpressed in Cos-7 cells (Ellies et al., 2006). As expected, blocking the LRP5/6 receptor with this antibody quenched the responsiveness of β -catenin signaling to exogenous gpITG2 (Fig. 5.3B). These observations suggest that LRP6 is a mediator of TG2-induced β -catenin signaling.

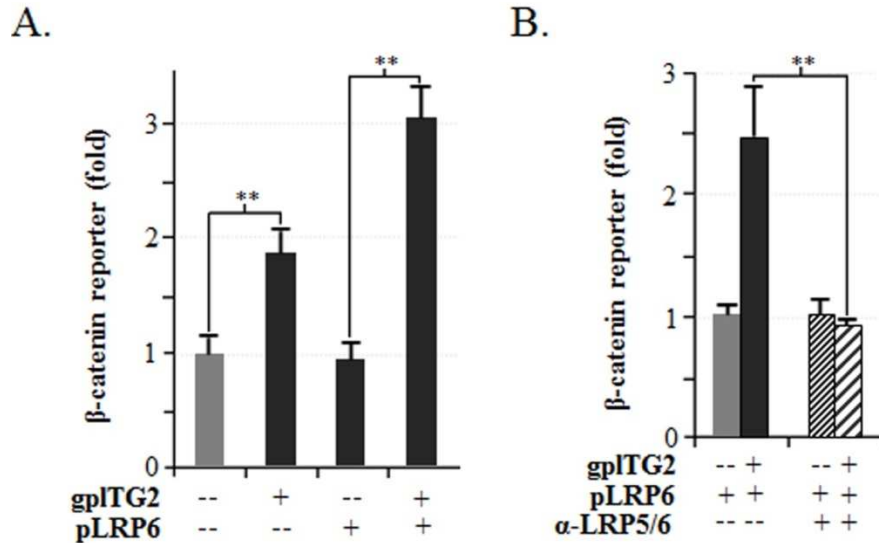


Figure 5.3 TG2-Induced Activation of β -Catenin is Mediated by LRP6. (A) Addition of exogenous purified gpITG2 activates β -catenin as shown by TOP-FLASH expression, which is augmented by overexpression of LRP6 in Cos-7 cells. (B) LRP6 augmentation of gpITG2-induced β -catenin activation is inhibited by a monoclonal anti-LRP5/6 antibody 1A12, which blocks LRP6 receptor binding. Figure credit to D Nurminsky, S Shanmugasundaram, and F Lima.

3. TG2 Over-Expression Mirrors β -Catenin Over-Activation Phenotype in Zebrafish

Previous studies have observed that over-activation of β -catenin signaling in zebrafish larvae results in a ventral phenotype of small or no eyes (van de Water et al., 2001). Here we tested whether the demonstrated TG2-mediated activation of β -catenin signaling has similar biological effects. Zebrafish embryos were injected with GFP (negative control) or hTG2 RNA before they reached the 8-cell stage and the resulting phenotype was analyzed at 1dpf, paying particular attention to the eyes. Upon injection of hTG2 we observed two phenotypes: the Wnt-like phenotype of small or no eyes (Fig 5.4A, middle-right panels) and an additional phenotype of curled tails (Fig 5.4A, top-right panel). Interestingly, a small population of hTG2 injected larvae showed both phenotypes (Fig 5.4A, bottom-right panel). Using a chi squared statistical analysis we were able to determine that these two phenotypes were statistically independent events,

indicating that TG2 is affecting other developmental pathways in addition to β -catenin signaling and that the curled tail phenotype is independent of the Wnt-like phenotype of small/no eyes. Quantification of these injected larvae showed that approximately 50% of TG2 injected embryos showed a mutated phenotype (Fig 5.4B), and of these embryos approximately 15% demonstrated a non-Wnt-like phenotype whereas approximately 85% showed a no/small eyes phenotype (Wnt-like phenotype) (Fig 5.4C). Importantly, these results demonstrate the *in vivo* activation of β -catenin signaling through TG2.

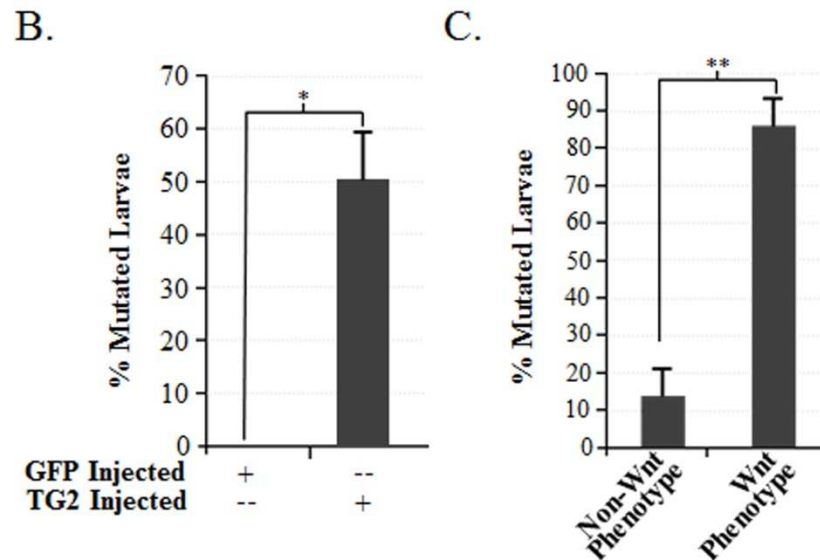
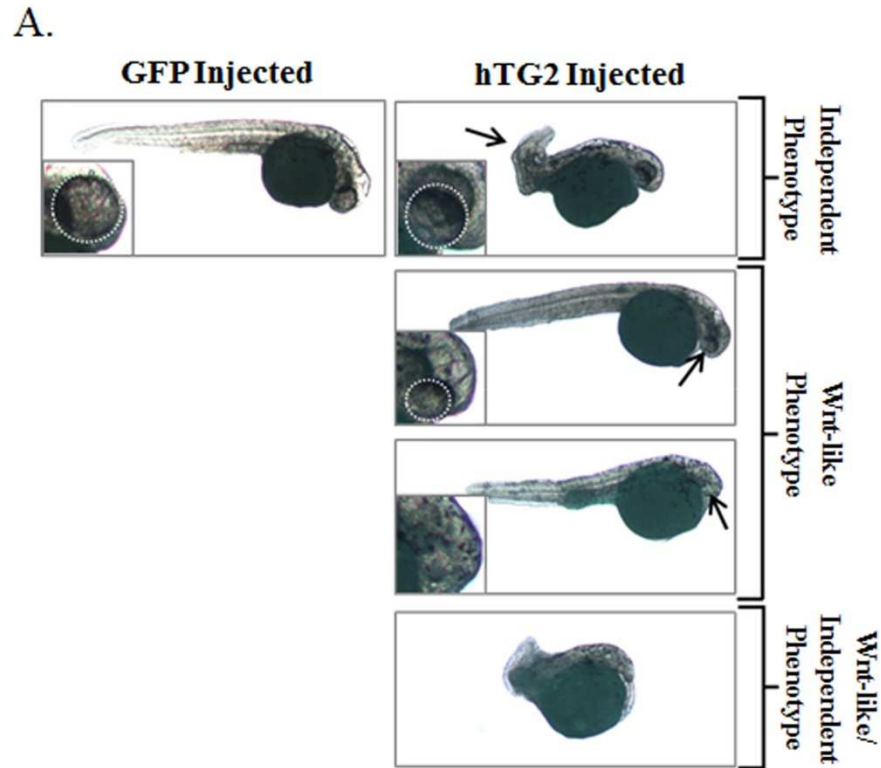
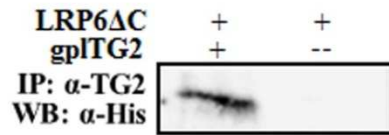


Figure 5.4 TG2 Over-Expression Mirrors β -Catenin Over-Activation Phenotype in Zebrafish. (A) Representative images of GFP (negative control) and hTG2 RNA injected larvae 1dpf with arrows highlighting resulting phenotypes. Quantitation of mutant phenotype occurrence in GFP and TG2 injected embryos. (B) 50% of TG2 injected embryos show a mutated phenotype compared to the 0% in GFP injected embryos. (C) Of the 50% mutated TG2 injected embryos, ~85% showed a no/small eye phenotype (Wnt Phenotype), while ~15% showed non-Wnt-like phenotype.

4. TG2 binds to the extracellular domain of LRP6 *in vitro*

Our data suggest that extracellular TG2 acts as an agonist of β -catenin signaling through an interaction with the LRP6 receptors. To determine whether TG2 binds directly to LRP6 or regulates signaling through other LRP5/6-interacting protein(s), we employed a co-immunoprecipitation analysis using purified gpITG2 and purified recombinant extracellular domain of human LRP6 (LRP6 Δ C) carrying a His-tag. We found that incubation of LRP6 Δ C and gpITG2 resulted in LRP6 Δ C specifically co-precipitating with an anti-TG2 antibody while no precipitation occurred in the absence of gpITG2 (Fig. 5.5A), thus demonstrating that TG2 directly binds to the extracellular domain of LRP6. To further investigate which domain of TG2 is involved in these interactions, we analyzed binding of the LRP6 Δ C protein to two truncated TG2 mutants along with full-sized TG2 (Fig 5.5B, upper panel, (Belkin et al., 2005)). TG2 variants were expressed as GST fusions in *E.coli* and purified by affinity chromatography. These proteins were incubated with purified LRP6 Δ C and co-immunoprecipitated with an anti-GST antibody. Co-immunoprecipitation of LRP6 Δ C and TG2 was observed for full-size TG2-GST and for the truncated mutant lacking the two C-terminal β -barrel domains (Fig. 5.5B, bottom panel). However, the TG2N-GST mutant protein lacking both the β -barrel domains and the catalytic core domain failed to co-precipitate LRP6 Δ C. Thus, the central catalytic core domain of TG2 is essential for binding of this protein to the extracellular domain of LRP6 raising the question of whether LRP6 is able to act as a substrate for TG2 cross-linking.

A.



B.

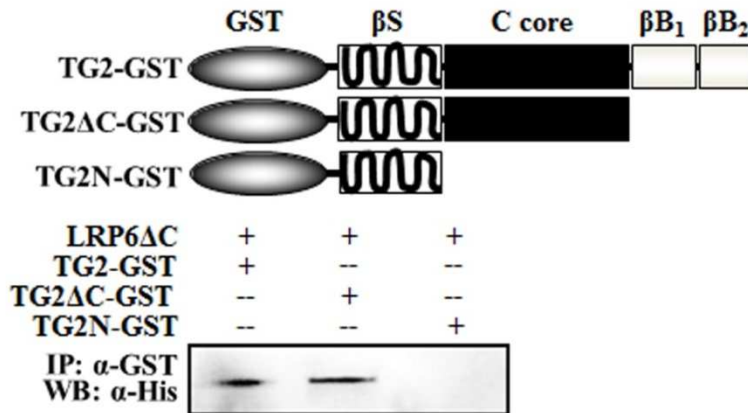


Figure 5.5 TG2 Binds to the Extracellular Domain of LRP6 *In Vitro*. (A) Purified, recombinant His-tagged extracellular LRP6 domain (LRP Δ C) was incubated with purified gpITG2. Precipitation with anti-TG2 antibody and detection by western blot with anti-His antibody showed an interaction between TG2 and LRP Δ C. (B) Two truncated forms of TG2, TG2 Δ C-GST and TGN-GST, or full length TG2 were incubated with LRP Δ C. Precipitation with anti-GST antibody and detection by western blot with anti-His antibody revealed that TG2 core domain is necessary for this interaction. Figure credit to D Nurminsky, S Shanmugasundaram, and F Lima.

5. Extracellular domain of LRP6 is cross-linked by TG2

TG2 was originally characterized as a protein cross-linking enzyme, in which it catalyzes the formation of an isopeptide bond between lysine and glutamine residues (Iismaa et al., 2009). To examine whether LRP6 is a substrate for TG2-mediated cross-linking we performed a competition assay with LRP6. For this we tested whether purified LRP6 Δ C acts as a competitive inhibitor of TG2 enzymatic activity using an ELISA-based assay of pentylamine cross-linking to casein by purified gpITG2. This assay showed that irreversible cross-linking of biotin-labeled EZ-link pentylamine to

casein-coated plates was reduced in a dose-dependent manner by the addition of purified recombinant LRP6 Δ C (Fig. 5.6A). The addition of LRP6 Δ C to the EZ-link substrate mixture at 2:1 ratio caused an approximately 50% reduction in incorporation of EZ-link amide and increasing this ratio to 4:1 almost completely inhibited incorporation of EZ-link pentylamine. These data suggest that LRP6 Δ C acts as a competitive inhibitor to the pentylamine substrate and is likely cross-linked by TG2. This was confirmed by Western blot analysis, in which high molecular weight-complexes of LRP6 Δ C formed in the presence of purified gpITG2 (Fig. 5.5B, arrows). Together these results suggest that LRP6 is a substrate for TG2-mediated cross-linking.

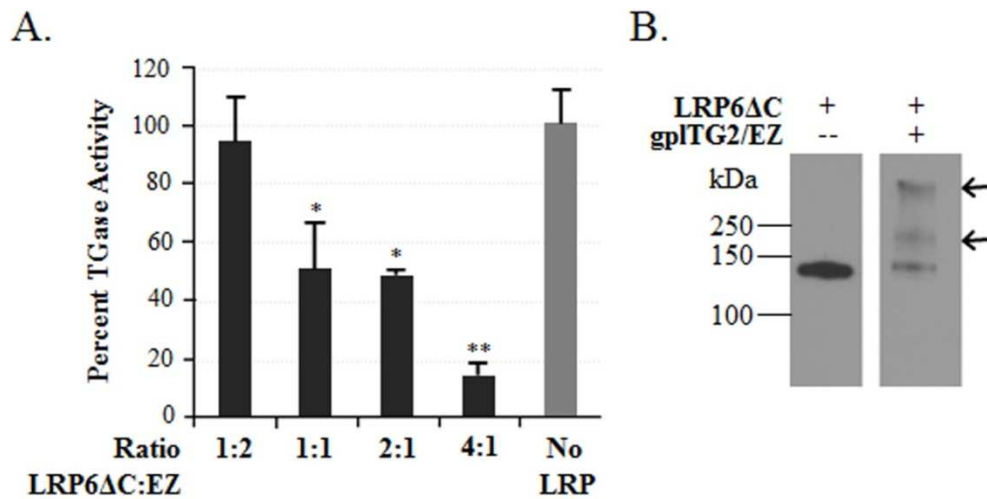


Figure 5.6 Extracellular Domain of LRP6 is Cross-Linked by TG2. (A) TG2 activity assay performed using stable levels of gpITG2 and Ez-link pentylamine with increasing doses of LRP6 shows that LRP6 inhibits TG2 cross-linking activity. (B) Western blot analysis of LRP6 Δ C alone (left panel) or an LRP6 Δ C/gpITG2 mixture (right panel) reveals formation of LRP6 complexes in the presence of gpITG2.

E. DISCUSSION

Our previous finding that extracellular TG2 activates canonical β -catenin signaling in VSMCs (Faverman et al., 2008) suggested that TG2 is able to bind to a

receptor pertinent to β -catenin signaling. The receptors and corresponding ligands that regulate the molecular pathways of β -catenin activation and signaling are diverse (MacDonald et al., 2007); however, our studies strongly indicate that TG2 acts through the canonical LRP5/6 receptors. TG2 shows synergy with LRP6 in activation of β -catenin-dependent gene expression in the Cos-7 model system. Blocking LRP5/6 receptors by antibody incubation quenches the effect of TG2 on β -catenin activity. Similarly, in VSMCs blocking LRP5/6 receptors with an antibody or inhibition of LRP5/6-mediated signaling with the soluble extracellular domain of LRP6 attenuates TG2-induced mineralization, which is associated with β -catenin activation in these cells (Faverman et al., 2008). These observations are consistent with LRP5/6 being the major receptors for TG2-regulated β -catenin activation. Indeed, our results demonstrate direct binding of TG2 to the extracellular domain of LRP6 *in vitro* and indicate that this binding requires the TG2 catalytic core domain. Intriguingly, the catalytic domain of TG2 has also been implicated in binding to LRP1, another member of the LRP family (Zemskov et al., 2007). While LRP1 has rather weak sequence similarity with LRP5/6, 35% identity in the most conserved regions, the organization of the extracellular domains of these receptors shows similar structural motifs including β -propeller/EGF repeat modules and LDLR repeats (Brown et al., 1998). Even though the LRP1 domain capable of TG2 binding has not been defined (Zemskov et al., 2007), our finding that TG2 directly interacts with the extracellular domain of LRP6 in combination with previous observations of a LRP1-TG2 interaction suggests that TG2 interacts with the structurally similar extracellular domains of the LRP family and thus has the potential to regulate the diverse biological activities of these receptors.

We observed that binding of TG2 to the extracellular domain of LRP6 results in phosphorylation of its intracellular domain suggesting that the mechanism of LRP5/6-mediated signaling by TG2 is similar to that of the canonical ligands (e.g. canonical Wnts). Binding of the TG2 catalytic domain to other proteins can lead to TG2-mediated cross-linking of the binding partners, as indicated by studies on human papillomavirus protein E7 (Jeon et al., 2003). We found that LRP6 is also a substrate for TG2-mediated cross-linking. Incubation of the extracellular domain of LRP6 with TG2 resulted in two bands of higher molecular weight and one band at the correct size for LRP6. It is probable that the band around 200 kDa is TG2 cross-linked to LRP6, based on the molecular weight, while the highest band is likely to be a multimer of LRP6. Moreover, in an artificial model system oligomerization of LRP6 can activate β -catenin signaling and bypass the requirement for the Fzd co-receptors (Cong and Varmus, 2004; Bilic et al., 2007). While further experiments will determine whether this mechanism is indeed in place for TG2-induced β -catenin activation, our studies identify extracellular TG2 as an activating ligand of the LRP5/6 receptors. This finding has broad significance for the understanding of diverse developmental processes and pathological conditions where both transglutaminase and β -catenin signaling have been implicated, including vascular calcification (Faverman et al., 2008), osteogenesis (Nurminskaya et al., 2003; Baron et al., 2006), neurodegeneration (Muma, 2007; Inestrosa et al., 2002) and cancers such as melanoma (Fok et al., 2006; Larue and Delmas, 2006), prostate cancer (Davies et al., 2007; Verras and Sun, 2006) and breast cancer (Mangala et al., 2007; Lindvall et al., 2007). Specifically, the identification of a novel activator for β -catenin signaling presents a new target for pharmacological treatment of such ailments. This is particularly

advantageous as identification of specific biological inhibitors for Wnt-mediated β -catenin signaling have yet to be identified (Voronkov and Krauss, 2013).

CHAPTER VI: CONCLUSIONS AND FUTURE DIRECTIONS

A. CONCLUSIONS

1. TG Compensation Mechanism in the Mouse Model

Development of TG2 null mice, which showed no skeletal phenotype, raised the question of whether a compensation mechanism was occurring. We examined tissues in which TG2 had previously been identified and investigated whether transamidating activity was affected in TG2 null mice. This examination showed transcriptional compensation in the liver, heart and kidney and functional compensation in the non-hypertrophic cartilage and aorta. Further, we proposed the presence of both transcriptional compensation by TG1 and TG3 and functional compensation by FXIIIa in the joint/ossifying cartilage. Lastly, we did not observe compensation for loss of TG2 in the skeletal muscle, suggesting that in this tissue TG2 is in an inactive form. Importantly for our studies, we observed compensation in the skeletal tissue by TG1, TG3 and FXIIIa indicating that generation of TG2/FXIIIa knockout mice may not reveal the *in vivo* role of TGs in skeletal elements as previously believed. It is important to note that this observed compensation mechanism also has implications for examining other systems in TG2 knockout mice and demonstrates the deep complexity that is involved in this enzyme family's regulation.

2. Zebrafish Transglutaminases

In this study, we sought to identify the *in vivo* role of TGs in bone mineralization; however, the use of a genetic mouse model was complicated by a complex system of compensation mechanisms (Deasey et al., 2013b). We therefore sought an alternative model to examine the *in vivo* role of TGs in bone mineralization. Zebrafish have become an invaluable model for the study of developmental processes due to characteristics such as transparency during early development, availability of both pharmacologic and genetic approaches, and a remarkable regenerative capability. However, enzyme TGs had not been characterized in this model, so we first sought to identify and characterize this multifunctional family of enzymes.

We identified thirteen TG genes in zebrafish; eleven of which are homologous to one of three mammalian TGs, TG1, TG2 and FXIIIa, and the remaining two were termed novel or zebrafish-specific TGs. Our studies identified expression of five zTGs, zFXIIIa-87, zTG2c, zTG2-12, zTG1-81, and zTG1-73, with developmental processes and two zTGs, zFXIIIa-53 and zFXIIIa-42, with adult homeostasis. Lastly expression of three zTGs, zTG2b, zTG-91 and zTG-84, were identified with both development and adult homeostasis. Further, two of these enzymes, zTG2b and zFXIIIa-87, were localized to areas skeletal formation. In-line with this, during bone regeneration zTG2b and zFXIIIa-87 were up-regulated and expressed in the skeletal precursors. This expression pattern of zTG2b and zFXIIIa-87 during development and regeneration in addition to their homology to the two mammalian TGs associated with bone mineralization *in vitro* led us to further investigate their role in bone formation.

3. TGs in Bone Formation/Regeneration

In these studies we show that TG transamidating activity is required for the proper progression of bone mineralization via a pharmacological approach. We utilized two different inhibitors, KCC-009 and cystamine, with KCC-009 being a TG-specific inhibitor and cystamine being a broad-spectrum inhibitor. Cystamine inhibits thiol-containing enzymes (Jeon et al., 2004;Elli et al., 2011;Alcock et al., 2011) and its reduced form, cysteamine, is approved for use as an orphan drug (Soohoo et al., 1997). The use of these two inhibitors allowed for us to determine that this was a TG-specific effect and that this could be translated into a clinically relevant study, as cysteamine is approved for clinical use. Further, we found that TG inhibition during bone regeneration impeded Col I deposition and β -catenin activation. Interestingly, *in vitro* studies have associated mammalian FXIIIa with Col I secretion (Al-Jallad et al., 2011) and mammalian TG2 with β -catenin activation (Faverman et al., 2008;Beazley et al., 2012b).

Our observed role of TGs in bone mineralization *in vivo* creates a new target for treatment of various bone pathologies. Specifically, our finding that a clinically relevant dose of cystamine is able to effectively inhibit bone mineralization is particularly applicable to pathologies involving over-mineralization of bone.

4. TG2 as a Regulator of β -Catenin Signaling

Studies performed by previous lab members showed the ability of TG2 to activate β -catenin signaling in Cos 7 cells through the LRP5/6 receptors. These studies also found that TG2 binds to the extracellular domain of LRP5/6 through its core domain. To better understand the activation of β -catenin signaling via TG2 we investigated whether

LRP5/6 was able to act as a substrate for TG2's transamidating activity and whether this activation had a biological relevance. We found that LRP6 was able to competitively inhibit TG2-mediated cross-linking of a biotin labeled substrate to casein. Further we found that TG2 was able to cross-link the extracellular domain of LRP6 into LRP6 multimers and TG2-LRP6 dimers, demonstrating that LRP6 is able to act as a substrate for TG2-mediated cross-linking. We therefore proposed that TG2-mediated activation of β -catenin signaling occurred via TG2-mediated dimerization of LRP receptors.

Previous studies showed that over-activation of β -catenin signaling in developing zebrafish results in a small eye/eyeless phenotype (van de Water et al., 2001). We sought to determine whether over-expression of TG2 would result in over-activation of β -catenin signaling *in vivo* and therefore result in a similar phenotype in zebrafish. We found that over-expression of TG2 resulted two independent phenotypes one mirroring β -catenin over-activation and resulting in a small eye/eyeless phenotype and a second resulting in a mutated . Enzyme TG2 acts in a vast number of biological processes in the body as evident from previous studies (reviewed in (Nurminskaya and Belkin, 2012;Iismaa et al., 2009)), therefore induction of two independent phenotypes from TG2 over-expression was not surprising.

B. FUTURE DIRECTIONS

These studies have provided an enhanced understanding of the role of enzyme TGs in bone mineralization; however with this increase in knowledge several questions arose. We first demonstrated the presence of compensation mechanisms in the TG2 null

mouse model. Particularly, we showed the presence of both functional and transcriptional compensation mechanisms; however further studies are necessary to understand the underlying mechanisms of this compensation. Specifically, what triggers the increase in activation of certain TGs and what determines the type of compensation observed in each tissue.

This study settled the observed discrepancy between *in vitro* studies from several groups demonstrating a role for TGs in osteo-chondrogenic differentiation and *in vivo* studies in which single knock-out mice lacked a skeletal phenotype by suggesting a complex compensatory mechanism in mammalian tissue. We showed that zTG2b and zFXIIIa-87 are expressed by mesenchymal-like cells that function in caudal fin regeneration and more specifically bone regeneration. Further, we have shown that inhibition of zTGs during regeneration leads to reduced bone regeneration likely via inhibiting Col I deposition and β -catenin activation. However, further studies are necessary to understand whether zTG2b and zFXIIIa-87 work cooperatively or individually in promoting Col I deposition and β -catenin activation. Additionally, it remains unclear whether β -catenin signaling and Col I deposition are directly linked or if they are two independent processes in regeneration. Further, we found that not all the intra-ray mesenchymal cells expressed zFXIIIa-87 or zTG2b, indicating the presence of at least two cellular populations. It would therefore, be interesting to determine whether the cells that do express zTGs, express both zTG2b and zFXIIIa-87 or whether they only express one of these zTGs. If they only express a singular zTG it would be interesting to determine if they then differentiate into different fates.

This study utilized a pharmacologic approach to examine TGs in bone mineralization. While this showed a role for TGs in bone mineralization, it did not allow for examination of individual roles of TGs in bone mineralization. Therefore, future genetic studies in zebrafish could prove very useful as this may allow for examination of individual roles. It would also be interesting to examine whether zebrafish TGs adopt a similar compensation mechanism as that seen in mammalian systems. If they do this would again complicate the examination of individual roles by a genetic approach.

Through the use of the zebrafish model we were able to identify an *in vivo* role for TGs in bone mineralization. While this model facilitated this examination it would be extremely interesting to examine this in higher vertebrates. It would be especially interesting to examine whether TGs have the same role in mammalian regeneration, by examining the expression of TGs during the limited toe regeneration that can be seen in young mice (Rinkevich et al., 2011). It would also be interesting to examine the expression of TGs in mammalian mesenchymal cells and to examine whether induction of any TGs results in improved differentiation into fates such as osteoblasts.

Lastly the focus of this study was on bone and bone mineralization. However, we did observe expression of other TGs during regeneration and further examination of these TGs could prove to be very interesting. For example, a deeper examination of zebrafish TG1 homologues that were up-regulated during regeneration could reveal insight into epidermis regeneration and improve scar-less skin healing.

APPENDIX

A. EXPANDED MATERIALS AND METHODS

1. RNA Isolation

Tissue was homogenized by (1) freezing with liquid nitrogen and crushing with mortar and pestle for the heart, kidney, skeletal muscle, sternum, liver and zebrafish embryos and fins or (2) by using a Mini-BeadBeater 16 (BioSpec) for the aorta and RNA was isolated by Trizol. Once tissues were homogenized in 1mL of Trizol, they were incubated for 5mins at RT, after which 0.2mL of chloroform was added and the samples were vigorously shaken for 15secs by hand. Samples were then incubated at RT for 3mins and then centrifuged at 12,000 x g for 15min at 4°C. The aqueous phase was then transferred into a fresh tube and 0.5mL of isopropyl alcohol was added and incubated for 10min at RT. This was followed by centrifuging at 12,000 x g for 10mins at 4°C. All supernatant was then removed and to wash the RNA, 1mL of 75% EtOH was added and the sample was mixed by vortexing. This was followed by centrifuging at 7,500 x g for 5min at 4°C and then removing the supernatant and allowing the pellet to air dry for approximately 5min. The pellet was then dissolved in DEPC-water and concentration and purity was measured by nano-drop.

2. RNA DNase Digestion and Clean-up

The RNeasy micro kit (Qiagen) was used for digestion of genomic DNA and RNA clean-up. 10µL of buffer RDD and 2.5uL DNase stock (2.73Kunitz units/µL) was added to the RNA sample and the volume was brought-up to 100uL with DEPC-water. This mixture

was incubated for 10min at RT. This DNase digested mixture was then added to 350 μ L Buffer RLT and mixed well. 250 μ L of 100% EtOH was then added to this mixture and mixed by pipetting and transferred to an RNeasy Mini spin column and centrifuged at 8,000 x g for 15sec. The flow-through was discarded and 700 μ L of Buffer RW1 was added to the column and centrifuged at 8,000 x g for 15sec. Again flow-through was discarded and 500 μ L of Buffer RPE was added to the column and centrifuged again at 8,000 x g for 15sec, again the flow-through was discarded. Next 500 μ L of 80% EtOH was added to the column and centrifuged at 8,000 x g for 2min. The column was then placed into a new collection tube and was centrifuged at full speed for 5min. The RNeasy spin column was then placed in a clean 1.5mL centrifuge tube and 14 μ L RNase-free water was added to the spin column membrane and the tube was centrifuged for 1min at full speed. The RNA concentration and purity was read by nanodrop.

3. Reverse Transcription of RNA

The Maxima First Strand cDNA Synthesis Kit (ThermoScientific) was used to reverse transcribe the cDNA for real-time PCR. In an RNase-free tube 4 μ L of the 5X Reaction Mix, 2 μ L of the Maxima Enzyme Mix, 0.4 μ g RNA was combined and brought up to 20 μ L. The kit utilizes oligo (dT)₁₈ and random hexamer primers, which are in the 5X reaction mix. This mixture was then mixed gently and centrifuged and incubated for 10min at 25°C, followed by 30min at 50°C and the reaction was terminated by incubating for 5min at 85°C.

4. Real-time PCR

cDNA was diluted 20X's in DEPC-water and used as a template for real-time PCR on a BIO RAD CFX96 Real-Time System. SsoFast EvaGreen Supermix and 0.3 μ M Primers

were used. The heat activation, amplification and melting curve cycles were set as follows: 95°C for 30sec, then 45 cycles of 95°C for 5sec followed by 58°C for 20sec, after completion of 45 cycles the samples were incubated at 65°C for 5sec.

5. Total Protein Isolation

Tissue was frozen by liquid nitrogen and ground into powder by mortar and pestle and transferred to an eppendorf tube. This was followed by addition of 500µL of lysis buffer (5mM Tris-HCl pH 7.5, 0.25M Sucrose, 0.2mM MgSO₄, 2mM DTT, 0.4mM PMSF, 5µg/mL Leupeptine and 0.4% Triton X-100), solution and was then mixed and left on ice for 30min. Samples were then centrifuged and protein containing supernatant was removed. Protein concentration was read by BCA Protein Assay (ThermoScientific).

6. Whole-Mount *In Situ* Hybridization

2dpf embryos were fixed overnight at 4°C in 4% PFA, washed 2X's in PBS and stored at -20°C in methanol. Embryos were rehydrated with series of EtOH washes: 75% EtOH/25% PBS + 0.1% Tween-20 (PBT), 50% EtOH/50% PBT, 25% EtOH/75% PBT. The embryos were then washed in PBT 4X's for 5min each at RT. They were then bleached in 3% Hydrogen Peroxide in 0.5% Potassium Hydroxide in PBT for 15min, followed by Proteinase K (Novagen) digestion (10µg/mL) for 30min at RT. This was followed by a second fixation in 4% PFA and acetone treatment for 8min at -20°C. Embryos were prehybridized for 1hr at 65°C in Pre-hybridization solution: 50% formamide, 5X SSC Buffer, 0.1% Tween-20, 50µg/mL heparin and 500µg/mL tRNA, brought to pH 6.0 with citric acid. This was followed by hybridization overnight at 65°C in pre-hybridization solution + 2ng/µL DIG-labeled antisense RNA probes. The next day, embryos were washed for 10min each at 65°C in 75% Pre-hybridization solution (no

tRNA or Heparin)/25% 2X SSC Buffer, 50% Pre-hybridization solution (no tRNA or Heparin)/50% 2X SSC Buffer and 25% Pre-hybridization solution (no tRNA or Heparin)/75% 2X SSC Buffer. This was followed by washing 2X's in 0.2X SSC buffer for 30min at 65°C. The embryos were then washed for 5min each at RT in 75% 0.2X SSC/25% PBT, 50% 0.2X SSC/50% PBT and 25% 0.2X SSC/75% PBT. The embryos were then blocked in 1X blocking solution (2mg/mL BSA and 2% Sheep serum) at RT. The anti-DIG antibody fused to alkaline phosphatase (Roche) was pre-absorbed in at a 1:400 dilution in blocking solution for 2hr at RT. The insoluble materials were removed by centrifugation at 12,000 rpm for 5min, the pre-absorbed anti-body was further diluted by 1:15 in blocking solution and added to the fish embryos and left overnight at 4°C with gentle agitation. This was followed by washing for 2hr at RT in PBT, changing the PBT 4-5 times, followed by 3 washes with 1X AP Buffer (0.1M Tris pH 9.5, 50mM MgCl₂, 0.1M NaCl and 0.1% Tween-20). Signal was detected calorimetrically by incubating in developing solution (1mL AP Buffer + 20uL stock NBT/BCIP solution (Roche)) in the dark for 24-72hrs until color developed. Staining progression was monitored with a Nikon AZ100 microscope and analyzed with Nikon Elements software.

7. DIG-RNA Probe Preparation

cDNA was inserted into the pGEM-T Easy Vector System 1 (Promega). Plasmid-cDNA was linearized by restriction digest and this was followed by purification. Purified plamid-cDNA was used for *in vitro* transcription using SP6 or T7 RNA Polymerases (Roche) for sense and antisense probes respectively. During *in vitro* transcription RNA was DIG labeled with the DIG RNA labeling kit (Roche). Transcribed RNA was then made to the correct size for *in situ* hybridization by alkaline hydrolysis. The digestion

time was calculated by the following formula: $\text{Time} = (\text{Initial length of RNA transcript (kb)} - \text{Final RNA probe length (kb)}) / 0.11(\text{Initial length of RNA transcript (kb)} \times \text{Final RNA probe length (kb)})$. The hydrolyzed probe was then stored at -80°C .

8. Real-time PCR

cDNA was diluted 20X's in DEPC-water and used as a template for real-time PCR on a BIO RAD CFX96 Real-Time System. LightCycler 480 SYBR Green I Master Mix and $0.3\mu\text{M}$ Primers were used. The heat activation and amplification cycles were set as follows: 95°C for 5min, then 45 cycles of 95°C for 10sec followed by 58°C for 20sec followed by 72°C for 30sec, after completion of 45 cycles the samples were incubated at 72°C for 5sec.

9. Tissue Section *In Situ* Hybridization

Amputated fins were fixed in 4% PFA overnight at 4°C , followed by 3 washes in PBS and transferred into 30% Sucrose in PBS overnight at 4°C . Tissue was blocked in OCT and cryo-sectioned, sections were stored at -20°C .

For Hybridization sections were removed from -20°C and air-dried at 37°C for 30min. The following steps were performed at RT unless stated otherwise. Sections were re-hydrated in DEPC-PBS for 4min and then incubated in 1% Triton X-100 in DEPC-PBS (PBT) for 4min. Tissue was digested with a fresh 0.05mg/mL Protease K solution for 4min. Slides were then rinsed twice in DEPC-PBS for 2min/wash and then briefly washed in DEPC-water. Slides air-dried for 30min and then $1\mu\text{g/mL}$ of DIG-labeled RNA probe was added to Hybridization solution (50% formamide, 5X SSC Buffer, 0.1% Tween-20, $50\mu\text{g/mL}$ heparin and $500\mu\text{g/mL}$ tRNA, brought to pH 6.0 with citric acid) and heated to 65°C for 5min. $80\mu\text{L}$ of pre-heated probe/hybridization solution was then

added to the slides which were then covered with individual parafilm pieces. They were then put in a sealed humid box and incubated at 55°C overnight. The next day parafilm pieces were soaked off by washing the slides in 2X SSC buffer. Once the parafilm pieces were removed, the slides were washed twice in 2X SSC for 30min/wash and then twice in pre-warmed 0.1X SSC at 60°C for 30min/wash. Slides were then equilibrated in Tris Buffer (0.1M Tris-HCl, pH 7.5, 0.15M NaCl) for 2min and blocked in 1% blocking reagent in Tris buffer for 30min at 37°C in a humid box. This was followed by incubation with an anti-DIG-AP antibody (Roche, CA) at a 1:1000 dilution in blocking solution for 2hr in a humid box. Sections were then washed 3X's in Tris buffer for 10min/wash on a shaker and then equilibrated in AP buffer (0.1M Tris, pH 9.5, 0.1M NaCl, 0.05M MgCl₂) for 2min. Signal was then detected by incubation with NBT-BCIP solution (10mL AP Buffer + 200uL stock NBT/BCIP solution (Roche, CA)) in the dark for 48hrs. Once signal was developed to the desired level, the sections were washed once in AP buffer and then three times in distilled water for 10min/wash. Slides were stored dry, for imaging the slides were rehydrated and coverslipped with 50% glycerol in PBS. Nuclear fast red counter-stain was done by incubating slides in nuclear fast red for 5min and then washing in distilled water for 5min. Slides were then coverslipped with permount for imaging.

B. SUPPLEMENTARY TABLES AND FIGURES

Target	Forward Primer (5'→3')	Reverse Primer (5'→3')	Accession Number
RPL19	aagaggaagggtactgccatgct	tgacctcaggtacaggctgtgat	NM_009078
TG1	tcaactctgcacacgacacagaca	tcttcatccagcagtcgtccaca	NM_019984
TG2	aggtgtccctgaagaaccacttt	ttccacagacttctgctccttgg	NM_009374
TG3	ttcaactcggctcagacacagat	tccacacgctatcaactgcctttct	NM_009374
TG4	tgctgaggcgtggacagatattca	tgctactggatcaagctccaccat	NM_177911
TG5	tgcagaagctacaggctacaaggt	acatcactgggtgaagggaaggt	NM_028799
TG6	tgtggccatcctacagaagtgggt	tgagttgaagttggacaccacct	NM_177726
TG7	agatcctggcccataacaccagtt	aatgaatgcagaccgctcctcaga	NM_001160424
FXIIIa	ttacttctcgcccacgacaatga	agcagtggtagtccacaccgaat	NM_028784

Table B.1 Primer sequences for mouse genes analyzed by real-time PCR

Target	Forward Primer (5'→3')	Reverse Primer (5'→3')	Accession Number
zFXIIIa-87	gttcggcccaaacagcgggt	cctgcggatgccgtacgggtg	NM_001077154
zTG2c	acgcactctgaacgggtgtggaca	aaggcagatgtccagtattccgtgc	NM_001004647
zTG2b	ggcaagtgatccaacgccgc	ggcgtctctgggtgctgtagtca	NM_212656
zTG-91	tgctgatgacggacgggtcc	gatcctctgtcccgggccga	XP_688146.5
zTG-84	tgaacgcagacgtgcggacc	tggcggccgtcatctgagga	XM_689249
zTG1-81	atcgcgggtggaacggcctg	cgcagagtgcagggcagagg	XM_689658
zTG1-48	ctccggagcaagaactgcgaa	ctgtagcgtccgatgcacgc	XM_001331878
zTG1-96	tcatgcctttctcatgcagccca	cagtgcgtcacaacgctgagc	XM_001332039
zTG1-73	atatccatcgaactgaagcta	agccttcaactctttaccaac	XP_002665624
zFXIIIa-53	atcaatctccaacttcccgaac	tccatcaaggcgaagctca	XP_686649
zFXIIIa-42	gaatttaaagcgacagtcacc	tgagcattaaagccatacaca	NP_001070179
zTG1-18	agcacgtcaaaaccatccac	agcacctccaaaatcagatcg	XP_003201279
zTG2-12	aagcctctgtcattgttcg	gctgtcattgagtatatcgc	XP_687398.2
Cyclin-D1	aacagatcgagtcctgctggaat	taatgtctctgacgtctgtgggagtg	NM_131025.4
Gli3	ggacagactcacctttaaccctt	ggctgcagaaacctggacaaaga	NM_205728
MMP7	tttggcctggaagagagtggagaa	ttccgaaccgctcgacatgagaa	XM_685884
Patched1	attcccacatctctgtccaaccct	ttccgaaccgctcgacatgagaa	XM_001922126
TCF1	tcccgaatccaaacagacctccat	agctgtctgtaactgtcatggga	NM_200814
cMyc	aagtggtttcagagagactggcgt	tcagatcctgcaaatagctcgcgt	XM_005162561

Table B.2 Primer sequences for zebrafish genes analyzed by real-time PCR

Reference List

Achyuthan KE, Greenberg CS (1987) Identification of a guanosine triphosphate-binding site on guinea pig liver transglutaminase. Role of GTP and calcium ions in modulating activity. *J Biol Chem* 262:1901-1906

Achyuthan KE, Rowland TC, Birckbichler PJ, Lee KN, Bishop PD, Achyuthan AM (1996) Hierarchies in the binding of human factor XIII, factor XIIIa, and endothelial cell transglutaminase to human plasma fibrinogen, fibrin, and fibronectin. *Mol Cell Biochem* 162:43-49

Aeschlimann D, Wetterwald A, Fleisch H, Paulsson M (1993) Expression of tissue transglutaminase in skeletal tissues correlates with events of terminal differentiation of chondrocytes. *J Cell Biol* 120:1461-1470

Akimov SS, Krylov D, Fleischman LF, Belkin AM (2000) Tissue transglutaminase is an integrin-binding adhesion coreceptor for fibronectin. *J Cell Biol* 148:825-838

Al-Jallad HF, Myneni VD, Piercy-Kotb SA, Chabot N, Mulani A, Keillor JW, Kaartinen MT (2011) Plasma membrane factor XIIIa transglutaminase activity regulates osteoblast matrix secretion and deposition by affecting microtubule dynamics. *PLoS One* 6:e15893

Al-Jallad HF, Nakano Y, Chen JL, McMillan E, Lefebvre C, Kaartinen MT (2006) Transglutaminase activity regulates osteoblast differentiation and matrix mineralization in MC3T3-E1 osteoblast cultures. *Matrix Biol* 25:135-148

Alcock J, Warren AY, Goodson YJ, Hill SJ, Khan RN, Lymn JS (2011) Inhibition of tissue transglutaminase 2 attenuates contractility of pregnant human myometrium. *Biol Reprod* 84:646-653

Ameye L, Young MF (2002) Mice deficient in small leucine-rich proteoglycans: novel in vivo models for osteoporosis, osteoarthritis, Ehlers-Danlos syndrome, muscular dystrophy, and corneal diseases. *Glycobiology* 12:107R-116R

Bakker EN, Pistea A, VanBavel E (2008) Transglutaminases in vascular biology: relevance for vascular remodeling and atherosclerosis. *J Vasc Res* 45:271-278

Baron R, Rawadi G, Roman-Roman S (2006) Wnt signaling: a key regulator of bone mass. *Curr Top Dev Biol* 76:103-27.:103-127

Baumgartner W, Golenhofen N, Weth A, Hiiragi T, Saint R, Griffin M, Drenckhahn D (2004) Role of transglutaminase 1 in stabilisation of intercellular junctions of the vascular endothelium. *Histochem Cell Biol* 122:17-25

Beazley KE, Banyard D, Lima F, Deasey SC, Nurminsky DI, Konoplyannikov M, Nurminskaya MV (2012a) Transglutaminase Inhibitors Attenuate Vascular Calcification in a Preclinical Model. *Arterioscler Thromb Vasc Biol*

Beazley KE, Deasey S, Lima F, Nurminskaya MV (2012b) Transglutaminase 2-Mediated Activation of beta-Catenin Signaling Has a Critical Role in Warfarin-Induced Vascular Calcification. *Arterioscler Thromb Vasc Biol* 32:123-130

Becerra J, Montes GS, Bexiga SR, Junqueira LC (1983) Structure of the tail fin in teleosts. *Cell Tissue Res* 230:127-137

Becker S, Maissen O, Ponomarev I, Stoll T, Meury T, Sprecher C, Alini M, Wilke I (2008) Osteopromotion with a plasmatransglutaminase on a beta-TCP ceramic. *J Mater Sci Mater Med* 19:659-665

Begg GE, Carrington L, Stokes PH, Matthews JM, Wouters MA, Husain A, Lorand L, Iismaa SE, Graham RM (2006) Mechanism of allosteric regulation of transglutaminase 2 by GTP. *Proc Natl Acad Sci U S A* 103:19683-19688

Belkin AM, Tsurupa G, Zemskov E, Veklich Y, Weisel JW, Medved L (2005) Transglutaminase-mediated oligomerization of the fibrin(ogen) alphaC domains promotes integrin-dependent cell adhesion and signaling. *Blood* 105:3561-3568

Bianco P, Cancedda FD, Riminucci M, Cancedda R (1998) Bone formation via cartilage models: the "borderline" chondrocyte. *Matrix Biol* 17:185-192

Bilic J, Huang YL, Davidson G, Zimmermann T, Cruciat CM, Bienz M, Niehrs C (2007) Wnt induces LRP6 signalosomes and promotes dishevelled-dependent LRP6 phosphorylation. *Science* 316:1619-1622

Bird NC, Mabee PM (2003) Developmental morphology of the axial skeleton of the zebrafish, *Danio rerio* (Ostariophysi: Cyprinidae). *Dev Dyn* 228:337-357

Borge L, Demignot S, Adolphe M (1996) Type II transglutaminase expression in rabbit articular chondrocytes in culture: relation with cell differentiation, cell growth, cell adhesion and cell apoptosis. *Biochim Biophys Acta* 1312:117-124

Boudin E, Fijalkowski I, Piters E, Van HW (2013) The role of extracellular modulators of canonical Wnt signaling in bone metabolism and diseases. *Semin Arthritis Rheum* %20. pii: S0049-0172:10

Brittijn SA, Duivesteijn SJ, Belmamoune M, Bertens LF, Bitter W, de Bruijn JD, Champagne DL, Cuppen E, Flik G, Vandenbroucke-Grauls CM, Janssen RA, de Jong IM, de Kloet ER, Kros A, Meijer AH, Metz JR, van der Sar AM, Schaaf MJ, Schulte-Merker S, Spaank HP, Tak PP, Verbeek FJ, Vervoordeldonk MJ, Vonk FJ, Witte F, Yuan H, Richardson MK (2009) Zebrafish development and regeneration: new tools for biomedical research. *Int J Dev Biol* 53:835-850

- Brockes JP, Kumar A (2005) Appendage regeneration in adult vertebrates and implications for regenerative medicine. *Science* 310:1919-1923
- Brockes JP, Kumar A, Velloso CP (2001) Regeneration as an evolutionary variable. *J Anat* 199:3-11
- Brown SD, Twells RC, Hey PJ, Cox RD, Levy ER, Soderman AR, Metzker ML, Caskey CT, Todd JA, Hess JF (1998) Isolation and characterization of LRP6, a novel member of the low density lipoprotein receptor gene family. *Biochem Biophys Res Commun* 248:879-888
- Candi E, Oddi S, Paradisi A, Terrinoni A, Ranalli M, Teofoli P, Citro G, Scarpato S, Puddu P, Melino G (2002) Expression of transglutaminase 5 in normal and pathologic human epidermis. *J Invest Dermatol* 119:670-677
- Candi E, Paradisi A, Terrinoni A, Pietroni V, Oddi S, Cadot B, Jogini V, Meiyappan M, Clardy J, Finazzi-Agro A, Melino G (2004) Transglutaminase 5 is regulated by guanine-adenine nucleotides. *Biochem J* 381:313-319
- Candi E, Schmidt R, Melino G (2005) The cornified envelope: a model of cell death in the skin. *Nat Rev Mol Cell Biol* 6:328-340
- Chau DY, Collighan RJ, Verderio EA, Addy VL, Griffin M (2005) The cellular response to transglutaminase-cross-linked collagen. *Biomaterials* 26:6518-6529
- Chen Y, Whetstone HC, Lin AC, Nadesan P, Wei Q, Poon R, Alman BA (2007) Beta-catenin signaling plays a disparate role in different phases of fracture repair: implications for therapy to improve bone healing. *PLoS Med* 4:e249
- Chhabra A, Verma A, Mehta K (2009) Tissue transglutaminase promotes or suppresses tumors depending on cell context. *Anticancer Res* 29:1909-1919
- Choi K, Siegel M, Piper JL, Yuan L, Cho E, Strnad P, Omary B, Rich KM, Khosla C (2005) Chemistry and biology of dihydroisoxazole derivatives: selective inhibitors of human transglutaminase 2. *Chem Biol* 12:469-475
- Ciardelli G, Gentile P, Chiono V, Mattioli-Belmonte M, Vozzi G, Barbani N, Giusti P (2010) Enzymatically crosslinked porous composite matrices for bone tissue regeneration. *J Biomed Mater Res A* 92:137-151
- Condello S, Cao L, Matei D (2013) Tissue transglutaminase regulates beta-catenin signaling through a c-Src-dependent mechanism. *FASEB J*
- Cong F, Varmus H (2004) Nuclear-cytoplasmic shuttling of Axin regulates subcellular localization of beta-catenin. *Proc Natl Acad Sci U S A* 101:2882-2887

- Dardik R, Inbal A (2006) Complex formation between tissue transglutaminase II (tTG) and vascular endothelial growth factor receptor 2 (VEGFR-2): proposed mechanism for modulation of endothelial cell response to VEGF. *Exp Cell Res* 312:2973-2982
- Davies G, Ablin RJ, Mason MD, Jiang WG (2007) Expression of the prostate transglutaminase (TGase-4) in prostate cancer cells and its impact on the invasiveness of prostate cancer. *J Exp Ther Oncol* 6:257-264
- Day TF, Guo X, Garrett-Beal L, Yang Y (2005) Wnt/beta-catenin signaling in mesenchymal progenitors controls osteoblast and chondrocyte differentiation during vertebrate skeletogenesis. *Dev Cell* 8:739-750
- De L, V, Melino G (2001) Gene disruption of tissue transglutaminase. *Mol Cell Biol* 21:148-155
- Deasey S, Grichenko O, Du S, Nurminskaya M (2011) Characterization of the transglutaminase gene family in zebrafish and in vivo analysis of transglutaminase-dependent bone mineralization. *Amino Acids*
- Deasey S, Nurminsky D, Shanmugasundaram S, Lima F, Nurminskaya M (2013a) Transglutaminase 2 as a novel activator of LRP6/beta-catenin signaling. *Cell Signal* 10
- Deasey S, Shanmugasundaram S, Nurminskaya M (2013b) Tissue-specific responses to loss of transglutaminase 2. *Amino Acids* 44:179-187
- Demignot S, Borge L, Adolphe M (1995) Transglutaminase activity in rabbit articular chondrocytes in culture. *Biochim Biophys Acta* 1266:163-170
- Dierker T, Dreier R, Migone M, Hamer S, Grobe K (2009) Heparan sulfate and transglutaminase activity are required for the formation of covalently cross-linked hedgehog oligomers. *J Biol Chem* 284:32562-32571
- Du SJ, Frenkel V, Kindschi G, Zohar Y (2001) Visualizing normal and defective bone development in zebrafish embryos using the fluorescent chromophore calcein. *Dev Biol* 238:239-246
- Dubinsky R, Gray C (2006) CYTE-I-HD: phase I dose finding and tolerability study of cysteamine (Cystagon) in Huntington's disease. *Mov Disord* 21:530-533
- Elli L, Ciulla MM, Busca G, Roncoroni L, Maioli C, Ferrero S, Bardella MT, Bonura A, Paliotti R, Terrani C, Braidotti P (2011) Beneficial effects of treatment with transglutaminase inhibitor cystamine on the severity of inflammation in a rat model of inflammatory bowel disease. *Lab Invest* 91:452-461
- Ellies DL, Viviano B, McCarthy J, Rey JP, Itasaki N, Saunders S, Krumlauf R (2006) Bone density ligand, Sclerostin, directly interacts with LRP5 but not LRP5G171V to modulate Wnt activity. *J Bone Miner Res* 21:1738-1749

Faverman L, Mikhaylova L, Malmquist J, Nurminskaya M (2008) Extracellular transglutaminase 2 activates beta-catenin signaling in calcifying vascular smooth muscle cells. *FEBS Lett* 582:1552-1557

Fesus L, Szondy Z (2005) Transglutaminase 2 in the balance of cell death and survival. *FEBS Lett* 579:3297-3302

Fisher M, Jones RA, Huang L, Haylor JL, El NM, Griffin M, Johnson TS (2009) Modulation of tissue transglutaminase in tubular epithelial cells alters extracellular matrix levels: a potential mechanism of tissue scarring. *Matrix Biol* 28:20-31

Fok JY, Ekmekcioglu S, Mehta K (2006) Implications of tissue transglutaminase expression in malignant melanoma. *Mol Cancer Ther* 5:1493-1503

Fujino T, Asaba H, Kang MJ, Ikeda Y, Sone H, Takada S, Kim DH, Ioka RX, Ono M, Tomoyori H, Okubo M, Murase T, Kamataki A, Yamamoto J, Magoori K, Takahashi S, Miyamoto Y, Oishi H, Nose M, Okazaki M, Usui S, Imaizumi K, Yanagisawa M, Sakai J, Yamamoto TT (2003) Low-density lipoprotein receptor-related protein 5 (LRP5) is essential for normal cholesterol metabolism and glucose-induced insulin secretion. *Proc Natl Acad Sci U S A* 100:229-234

Garcia Y, Hemantkumar N, Collighan R, Griffin M, Rodriguez-Cabello JC, Pandit A (2009) In vitro characterization of a collagen scaffold enzymatically cross-linked with a tailored elastin-like polymer. *Tissue Eng Part A* 15:887-899

Gluzman Y (1981) SV40-transformed simian cells support the replication of early SV40 mutants. *Cell* 23:175-182

Greenberg CS, Birckbichler PJ, Rice RH (1991) Transglutaminases: multifunctional cross-linking enzymes that stabilize tissues. *FASEB J* 5:3071-3077

Grenard P, Bates MK, Aeschlimann D (2001) Evolution of transglutaminase genes: identification of a transglutaminase gene cluster on human chromosome 15q15. Structure of the gene encoding transglutaminase X and a novel gene family member, transglutaminase Z. *J Biol Chem* 276:33066-33078

Griffin M, Casadio R, Bergamini CM (2002) Transglutaminases: nature's biological glues. *Biochem J* 368:377-396

Gundemir S, Colak G, Tucholski J, Johnson GV (2012) Transglutaminase 2: a molecular Swiss army knife. *Biochim Biophys Acta* 1823:406-419

Han XH, Jin YR, Seto M, Yoon JK (2011) A WNT/beta-catenin signaling activator, R-spondin, plays positive regulatory roles during skeletal myogenesis. *J Biol Chem* 286:10649-10659

- Hasegawa G, Suwa M, Ichikawa Y, Ohtsuka T, Kumagai S, Kikuchi M, Sato Y, Saito Y (2003) A novel function of tissue-type transglutaminase: protein disulphide isomerase. *Biochem J* 373:793-803
- Heath DJ, Downes S, Verderio E, Griffin M (2001) Characterization of tissue transglutaminase in human osteoblast-like cells. *J Bone Miner Res* 16:1477-1485
- Hiiragi T, Sasaki H, Nagafuchi A, Sabe H, Shen SC, Matsuki M, Yamanishi K, Tsukita S (1999) Transglutaminase type 1 and its cross-linking activity are concentrated at adherens junctions in simple epithelial cells. *J Biol Chem* 274:34148-34154
- Ho KC, Quarmby VE, French FS, Wilson EM (1992) Molecular cloning of rat prostate transglutaminase complementary DNA. The major androgen-regulated protein DPI of rat dorsal prostate and coagulating gland. *J Biol Chem* 267:12660-12667
- Huang H, He X (2008) Wnt/beta-catenin signaling: new (and old) players and new insights. *Curr Opin Cell Biol* 20:119-125
- Hwang KC, Gray CD, Sweet WE, Moravec CS, Im MJ (1996) Alpha 1-adrenergic receptor coupling with Gh in the failing human heart. *Circulation* 94:718-726
- Iismaa SE, Mearns BM, Lorand L, Graham RM (2009) Transglutaminases and disease: lessons from genetically engineered mouse models and inherited disorders. *Physiol Rev* 89:991-1023
- Inestrosa N, De Ferrari GV, Garrido JL, Alvarez A, Olivares GH, Barria MI, Bronfman M, Chacon MA (2002) Wnt signaling involvement in beta-amyloid-dependent neurodegeneration. *Neurochem Int* 41:341-344
- Itasaki N, Jones CM, Mercurio S, Rowe A, Domingos PM, Smith JC, Krumlauf R (2003) Wise, a context-dependent activator and inhibitor of Wnt signalling. *Development* 130:4295-4305
- Jayo A, Conde I, Lastres P, Jimenez-Yuste V, Gonzalez-Manchon C (2009a) New insights into the expression and role of platelet factor XIII-A. *J Thromb Haemost* 7:1184-1191
- Jayo A, Conde I, Lastres P, Jimenez-Yuste V, Gonzalez-Manchon C (2009b) Possible role for cellular FXIII in monocyte-derived dendritic cell motility. *Eur J Cell Biol* 88:423-431
- Jeon JH, Choi KH, Cho SY, Kim CW, Shin DM, Kwon JC, Song KY, Park SC, Kim IG (2003) Transglutaminase 2 inhibits Rb binding of human papillomavirus E7 by incorporating polyamine. *EMBO J* 22:5273-5282
- Jeon JH, Lee HJ, Jang GY, Kim CW, Shim DM, Cho SY, Yeo EJ, Park SC, Kim IG (2004) Different inhibition characteristics of intracellular transglutaminase activity by cystamine and cysteamine. *Exp Mol Med* 36:576-581

- Johnson GV, Cox TM, Lockhart JP, Zinnerman MD, Miller ML, Powers RE (1997) Transglutaminase activity is increased in Alzheimer's disease brain. *Brain Res* 751:323-329
- Johnson KA, Polewski M, Terkeltaub RA (2008) Transglutaminase 2 is central to induction of the arterial calcification program by smooth muscle cells. *Circ Res* 102:529-537
- Johnson SL, Weston JA (1995) Temperature-sensitive mutations that cause stage-specific defects in Zebrafish fin regeneration. *Genetics* 141:1583-1595
- Karsenty G, Wagner EF (2002) Reaching a genetic and molecular understanding of skeletal development. *Dev Cell* 2:389-406
- Kiesselbach TH, Wagner RH (1972) Demonstration of factor XIII in human megakaryocytes by a fluorescent antibody technique. *Ann N Y Acad Sci* 202:318-328
- Kikuchi A, Yamamoto H, Kishida S (2007) Multiplicity of the interactions of Wnt proteins and their receptors. *Cell Signal* 19:659-671
- Kim JB, Leucht P, Lam K, Luppen C, Ten BD, Nusse R, Helms JA (2007) Bone regeneration is regulated by wnt signaling. *J Bone Miner Res* 22:1913-1923
- Kim SY, Park WM, Jung SW, Lee J (1997) Novel transglutaminase inhibitors reduce the cornified cell envelope formation. *Biochem Biophys Res Commun* 233:39-44
- Knopf F, Hammond C, Chekuru A, Kurth T, Hans S, Weber CW, Mahatma G, Fisher S, Brand M, Schulte-Merker S, Weidinger G (2011) Bone regenerates via dedifferentiation of osteoblasts in the zebrafish fin. *Dev Cell* 20:713-724
- Komaromi I, Bagoly Z, Muszbek L (2011) Factor XIII: novel structural and functional aspects. *J Thromb Haemost* 9:9-20
- Koseki-Kuno S, Yamakawa M, Dickneite G, Ichinose A (2003) Factor XIII A subunit-deficient mice developed severe uterine bleeding events and subsequent spontaneous miscarriages. *Blood* 102:4410-4412
- Kristiansen GK, Andersen MD (2011) Reversible activation of cellular factor XIII by calcium. *J Biol Chem* 286:9833-9839
- Kuramoto N, Takizawa T, Takizawa T, Matsuki M, Morioka H, Robinson JM, Yamanishi K (2002) Development of ichthyosiform skin compensates for defective permeability barrier function in mice lacking transglutaminase 1. *J Clin Invest* 109:243-250

- Landis WJ, Geraudie J (1990) Organization and development of the mineral phase during early ontogenesis of the bony fin rays of the trout *Oncorhynchus mykiss*. *Anat Rec* 228:383-391
- Larue L, Delmas V (2006) The WNT/Beta-catenin pathway in melanoma. *Front Biosci* 11:733-42.:733-742
- Lauer P, Metzner HJ, Zettlmeissl G, Li M, Smith AG, Lathe R, Dickneite G (2002) Targeted inactivation of the mouse locus encoding coagulation factor XIII-A: hemostatic abnormalities in mutant mice and characterization of the coagulation deficit. *Thromb Haemost* 88:967-974
- Lesort M, Lee M, Tucholski J, Johnson GV (2003) Cystamine inhibits caspase activity. Implications for the treatment of polyglutamine disorders. *J Biol Chem* 278:3825-3830
- Li X, Zhang Y, Kang H, Liu W, Liu P, Zhang J, Harris SE, Wu D (2005) Sclerostin binds to LRP5/6 and antagonizes canonical Wnt signaling. *J Biol Chem* 280:19883-19887
- Lieschke GJ, Currie PD (2007) Animal models of human disease: zebrafish swim into view. *Nat Rev Genet* 8:353-367
- Lindvall C, Bu W, Williams BO, Li Y (2007) Wnt signaling, stem cells, and the cellular origin of breast cancer. *Stem Cell Rev* 3:157-168
- Lorand L, Graham RM (2003) Transglutaminases: crosslinking enzymes with pleiotropic functions. *Nat Rev Mol Cell Biol* 4:140-156
- MacDonald BT, Semenov MV, He X (2007) SnapShot: Wnt/beta-catenin signaling. *Cell* 131:1204
- Mak KK, Bi Y, Wan C, Chuang PT, Clemens T, Young M, Yang Y (2008) Hedgehog signaling in mature osteoblasts regulates bone formation and resorption by controlling PTHrP and RANKL expression. *Dev Cell* 14:674-688
- Mangala LS, Fok JY, Zorrilla-Calancha IR, Verma A, Mehta K (2007) Tissue transglutaminase expression promotes cell attachment, invasion and survival in breast cancer cells. *Oncogene* 26:2459-2470
- Mani A, Radhakrishnan J, Wang H, Mani A, Mani MA, Nelson-Williams C, Carew KS, Mane S, Najmabadi H, Wu D, Lifton RP (2007) LRP6 mutation in a family with early coronary disease and metabolic risk factors. *Science* 315:1278-1282
- McKee TD, Grandi P, Mok W, Alexandrakis G, Insin N, Zimmer JP, Bawendi MG, Boucher Y, Breakefield XO, Jain RK (2006) Degradation of fibrillar collagen in a human melanoma xenograft improves the efficacy of an oncolytic herpes simplex virus vector. *Cancer Res* 66:2509-2513

- Mione MC, Trede NS (2010) The zebrafish as a model for cancer. *Dis Model Mech* 3:517-523
- Mishra S, Murphy LJ (2004) Tissue transglutaminase has intrinsic kinase activity: identification of transglutaminase 2 as an insulin-like growth factor-binding protein-3 kinase. *J Biol Chem* 279:23863-23868
- Muma NA (2007) Transglutaminase is linked to neurodegenerative diseases. *J Neuropathol Exp Neurol* 66:258-263
- Muszbek L, Adany R, Szegedi G, Polgar J, Kawai M (1985) Factor XIII of blood coagulation in human monocytes. *Thromb Res* 37:401-410
- Muszbek L, Bereczky Z, Bagoly Z, Komaromi I, Katona E (2011) Factor XIII: a coagulation factor with multiple plasmatic and cellular functions. *Physiol Rev* 91:931-972
- Nadalutti C, Viiri KM, Kaukinen K, Maki M, Lindfors K (2011) Extracellular transglutaminase 2 has a role in cell adhesion, whereas intracellular transglutaminase 2 is involved in regulation of endothelial cell proliferation and apoptosis. *Cell Prolif* 44:49-58
- Nakaoka H, Perez DM, Baek KJ, Das T, Husain A, Misono K, Im MJ, Graham RM (1994) Gh: a GTP-binding protein with transglutaminase activity and receptor signaling function. *Science* 264:1593-1596
- Nanda N, Iismaa SE, Owens WA, Husain A, Mackay F, Graham RM (2001) Targeted inactivation of Gh/tissue transglutaminase II. *J Biol Chem* 276:20673-20678
- Nurminskaya M, Kaartinen MT (2006) Transglutaminases in mineralized tissues. *Front Biosci* 11:1591-606.:1591-1606
- Nurminskaya M, Linsenmayer TF (1996) Identification and characterization of up-regulated genes during chondrocyte hypertrophy. *Dev Dyn* 206:260-271
- Nurminskaya M, Magee C, Faverman L, Linsenmayer TF (2003) Chondrocyte-derived transglutaminase promotes maturation of preosteoblasts in periosteal bone. *Dev Biol* 263:139-152
- Nurminskaya M, Magee C, Nurminsky D, Linsenmayer TF (1998) Plasma transglutaminase in hypertrophic chondrocytes: expression and cell-specific intracellular activation produce cell death and externalization. *J Cell Biol* 142:1135-1144
- Nurminskaya MV, Belkin AM (2012) Cellular functions of tissue transglutaminase. *Int Rev Cell Mol Biol* 294:1-97.:1-97
- Nurminskaya MV, Recheis B, Nimpf J, Magee C, Linsenmayer TF (2002) Transglutaminase factor XIIIa in the cartilage of developing avian long bones. *Dev Dyn* 223:24-32

- Nurminsky D, Shanmugasundaram S, Deasey S, Michaud C, Allen S, Hendig D, Dastjerdi A, Francis-West P, Nurminskaya M (2011) Transglutaminase 2 regulates early chondrogenesis and glycosaminoglycan synthesis. *Mech Dev* 128:234-245
- Nusse R (2005) Wnt signaling in disease and in development. *Cell Res* 15:28-32
- Ou H, Haendeler J, Aebly MR, Kelly LA, Cholewa BC, Koike G, Kwitek-Black A, Jacob HJ, Berk BC, Miano JM (2000) Retinoic acid-induced tissue transglutaminase and apoptosis in vascular smooth muscle cells. *Circ Res* 87:881-887
- Parichy DM, Elizondo MR, Mills MG, Gordon TN, Engeszer RE (2009) Normal table of postembryonic zebrafish development: staging by externally visible anatomy of the living fish. *Dev Dyn* 238:2975-3015
- Pistea A, Bakker EN, Spaan JA, Hardeman MR, van RN, VanBavel E (2008) Small artery remodeling and erythrocyte deformability in L-NAME-induced hypertension: role of transglutaminases. *J Vasc Res* 45:10-18
- Poleo G, Brown CW, Laforest L, Akimenko MA (2001) Cell proliferation and movement during early fin regeneration in zebrafish. *Dev Dyn* 221:380-390
- Poss KD, Keating MT, Nechiporuk A (2003) Tales of regeneration in zebrafish. *Dev Dyn* 226:202-210
- Poster DS, Bruno S, Penta J, Neil GL, McGovren JP (1981) Acivicin. An antitumor antibiotic. *Cancer Clin Trials* 4:327-330
- Quint E, Smith A, Avaron F, Laforest L, Miles J, Gaffield W, Akimenko MA (2002) Bone patterning is altered in the regenerating zebrafish caudal fin after ectopic expression of sonic hedgehog and *bmp2b* or exposure to cyclopamine. *Proc Natl Acad Sci U S A* 99:8713-8718
- Rawadi G (2008) Wnt signaling and potential applications in bone diseases. *Curr Drug Targets* 9:581-590
- Rinkevich Y, Lindau P, Ueno H, Longaker MT, Weissman IL (2011) Germ-layer and lineage-restricted stem/progenitors regenerate the mouse digit tip. *Nature* 476:409-413
- Rosenthal AK, Derfus BA, Henry LA (1997) Transglutaminase activity in aging articular chondrocytes and articular cartilage vesicles. *Arthritis Rheum* 40:966-970
- Sanchez AA (2000) Regeneration in the metazoans: why does it happen? *Bioessays* 22:578-590
- Satpathy M, Shao M, Emerson R, Donner DB, Matei D (2009) Tissue transglutaminase regulates matrix metalloproteinase-2 in ovarian cancer by modulating cAMP-response element-binding protein activity. *J Biol Chem* 284:15390-15399

- Semenov MV, He X (2006) LRP5 mutations linked to high bone mass diseases cause reduced LRP5 binding and inhibition by SOST. *J Biol Chem* 281:38276-38284
- Semenov MV, Zhang X, He X (2008) DKK1 antagonizes Wnt signaling without promotion of LRP6 internalization and degradation. *J Biol Chem* 283:21427-21432
- Shehab D, Elgazzar AH, Collier BD (2002) Heterotopic ossification. *J Nucl Med* 43:346-353
- Siegel M, Strnad P, Watts RE, Choi K, Jabri B, Omary MB, Khosla C (2008) Extracellular transglutaminase 2 is catalytically inactive, but is transiently activated upon tissue injury. *PLoS One* 3:e1861
- Singh SP, Holdway JE, Poss KD (2012) Regeneration of amputated zebrafish fin rays from de novo osteoblasts. *Dev Cell* 22:879-886
- Small K, Feng JF, Lorenz J, Donnelly ET, Yu A, Im MJ, Dorn GW, Liggett SB (1999) Cardiac specific overexpression of transglutaminase II (G(h)) results in a unique hypertrophy phenotype independent of phospholipase C activation. *J Biol Chem* 274:21291-21296
- Smith A, Avaron F, Guay D, Padhi BK, Akimenko MA (2006) Inhibition of BMP signaling during zebrafish fin regeneration disrupts fin growth and scleroblasts differentiation and function. *Dev Biol* 299:438-454
- Sooahoo N, Schneider JA, Kaplan RM (1997) A cost-effectiveness analysis of the orphan drug cysteamine in the treatment of infantile cystinosis. *Med Decis Making* 17:193-198
- Sousa S, Afonso N, Bensimon-Brito A, Fonseca M, Simoes M, Leon J, Roehl H, Cancela ML, Jacinto A (2011) Differentiated skeletal cells contribute to blastema formation during zebrafish fin regeneration. *Development* 138:3897-3905
- Spina AM, Esposito C, Pagano M, Chiosi E, Mariniello L, Cozzolino A, Porta R, Illiano G (1999) GTPase and transglutaminase are associated in the secretion of the rat anterior prostate. *Biochem Biophys Res Commun* 260:351-356
- St-Jacques B, Hammerschmidt M, McMahon AP (1999) Indian hedgehog signaling regulates proliferation and differentiation of chondrocytes and is essential for bone formation. *Genes Dev* 13:2072-2086
- Stenberg P, Roth EB, Sjoberg K (2008) Transglutaminase and the pathogenesis of coeliac disease. *Eur J Intern Med* 19:83-91
- Stoick-Cooper CL, Weidinger G, Riehle KJ, Hubbert C, Major MB, Fausto N, Moon RT (2007) Distinct Wnt signaling pathways have opposing roles in appendage regeneration. *Development* 134:479-489

- Summey BT, Jr., Graff RD, Lai TS, Greenberg CS, Lee GM (2002) Tissue transglutaminase localization and activity regulation in the extracellular matrix of articular cartilage. *J Orthop Res* 20:76-82
- Tamai K, Semenov M, Kato Y, Spokony R, Liu C, Katsuyama Y, Hess F, Saint-Jeannet JP, He X (2000) LDL-receptor-related proteins in Wnt signal transduction. *Nature* 407:530-535
- Tamai K, Zeng X, Liu C, Zhang X, Harada Y, Chang Z, He X (2004) A mechanism for Wnt coreceptor activation. *Mol Cell* 13:149-156
- Tanaka K, Yokosaki Y, Higashikawa F, Saito Y, Eboshida A, Ochi M (2007) The integrin alpha5beta1 regulates chondrocyte hypertrophic differentiation induced by GTP-bound transglutaminase 2. *Matrix Biol* 26:409-418
- Thisse B, Heyer V, Lux A, Alunni V, Degraeve A, Seiliez I, Kirchner J, Parkhill JP, Thisse C (2004) Spatial and temporal expression of the zebrafish genome by large-scale in situ hybridization screening. *Methods Cell Biol* 77:505-19.:505-519
- Thomazy V, Fesus L (1989) Differential expression of tissue transglutaminase in human cells. An immunohistochemical study. *Cell Tissue Res* 255:215-224
- Thomazy VA, Davies PJ (1999) Expression of tissue transglutaminase in the developing chicken limb is associated both with apoptosis and endochondral ossification. *Cell Death Differ* 6:146-154
- Trigwell SM, Lynch PT, Griffin M, Hargreaves AJ, Bonner PL (2004) An improved colorimetric assay for the measurement of transglutaminase (type II) -(gamma-glutamyl) lysine cross-linking activity. *Anal Biochem* 330:164-166
- van de Water S, van de Wetering M, Joore J, Esseling J, Bink R, Clevers H, Zivkovic D (2001) Ectopic Wnt signal determines the eyeless phenotype of zebrafish masterblind mutant. *Development* 128:3877-3888
- Van Herck JL, Schrijvers DM, De Meyer GR, Martinet W, Van Hove CE, Bult H, Vrints CJ, Herman AG (2010) Transglutaminase 2 deficiency decreases plaque fibrosis and increases plaque inflammation in apolipoprotein-E-deficient mice. *J Vasc Res* 47:231-240
- Verras M, Sun Z (2006) Roles and regulation of Wnt signaling and beta-catenin in prostate cancer. *Cancer Lett* 237:22-32
- Voronkov A, Krauss S (2013) Wnt/beta-catenin signaling and small molecule inhibitors. *Curr Pharm Des* 19:634-664
- Wan M, Yang C, Li J, Wu X, Yuan H, Ma H, He X, Nie S, Chang C, Cao X (2008) Parathyroid hormone signaling through low-density lipoprotein-related protein 6. *Genes Dev* 22:2968-2979

Westendorf JJ, Kahler RA, Schroeder TM (2004) Wnt signaling in osteoblasts and bone diseases. *Gene* 341:19-39.:19-39

Xu L, Begum S, Hearn JD, Hynes RO (2006) GPR56, an atypical G protein-coupled receptor, binds tissue transglutaminase, TG2, and inhibits melanoma tumor growth and metastasis. *Proc Natl Acad Sci U S A* 103:9023-9028

Xu Q, Wang Y, Dabdoub A, Smallwood PM, Williams J, Woods C, Kelley MW, Jiang L, Tasman W, Zhang K, Nathans J (2004a) Vascular development in the retina and inner ear: control by Norrin and Frizzled-4, a high-affinity ligand-receptor pair. *Cell* %19;116:883-895

Xu Q, Wang Y, Dabdoub A, Smallwood PM, Williams J, Woods C, Kelley MW, Jiang L, Tasman W, Zhang K, Nathans J (2004b) Vascular development in the retina and inner ear: control by Norrin and Frizzled-4, a high-affinity ligand-receptor pair. *Cell* %19;116:883-895

Xu W, Kimelman D (2007) Mechanistic insights from structural studies of beta-catenin and its binding partners. *J Cell Sci* 120:3337-3344

Yin X, Chen Z, Liu Z, Song C (2012) Tissue transglutaminase (TG2) activity regulates osteoblast differentiation and mineralization in the SAOS-2 cell line. *Braz J Med Biol Res* 45:693-700

Yuan L, Siegel M, Choi K, Khosla C, Miller CR, Jackson EN, Piwnica-Worms D, Rich KM (2007) Transglutaminase 2 inhibitor, KCC009, disrupts fibronectin assembly in the extracellular matrix and sensitizes orthotopic glioblastomas to chemotherapy. *Oncogene* %19;26:2563-2573

Zemskov EA, Mikhailenko I, Strickland DK, Belkin AM (2007) Cell-surface transglutaminase undergoes internalization and lysosomal degradation: an essential role for LRP1. *J Cell Sci* 120:3188-3199